BELGIAN RESEARCH PROGRAMME ON THE ANTARCTIC

SCIENTIFIC RESULTS OF PHASE III (1992-1996)

VOLUME II

Part A: HYDRODYNAMICS
Part B: MARINE GEOPHYSICS

EDITED BY S. CASCHETTO

FEDERAL OFFICE FOR SCIENTIFIC, TECHNICAL AND CULTURAL AFFAIRS

BELGIAN RESEARCH PROGRAMME ON THE ANTARCTIC

SCIENTIFIC RESULTS OF PHASE III (1992-1996)

VOLUME II

Part A: HYDRODYNAMICS
Part B: MARINE GEOPHYSICS

EDITED BY S. CASCHETTO

FEDERAL OFFICE FOR SCIENTIFIC, TECHNICAL AND CULTURAL AFFAIRS

1997

LEGAL NOTICE

Additional information on the Belgian Research Programme on the Antarctic is available on Internet (http://www.belspo.be/antar)

D/1997/1191/22

Published by the Federal Office for Scientific, Technical and Cultural Affairs (OSTC)
Brussels, Belgium

Cover photograph : Dr J.-L. Tison

Serial number ANTAR/97/4

FOREWORD

This volume presents the scientific results of research projects in the areas of Hydrodynamics (Part A) and of Marine Geophysics (Part B) funded under the Third Phase of the Belgian Research Programme on the Antarctic (1992-1996). Achievements of research projects in the other areas of the Programme form the subject of two separate volumes (Volume I : Marine Biogeochemistry and Ecodynamics; Volume III : Glaciology and Climatology)

The Programme, which was initiated by the Belgian Government in 1985, is funded, managed and co-ordinated by the Federal Office for Scientific, Technical and Cultural Affairs (OSTC). The money allocated to the Third Phase was 160 MBEF. Research-work was implemented by means of 3-years projects undertaken by university- or federal scientific institute-based scientists.

All research costs (personnel, equipment, travel, working and overheads) were financed by the OSTC.

Such research effort aimed at contributing to the development of the knowledge required for a science-based conservation and management of the Antarctic environment and to the assessment of the mechanisms through which the Antarctic and the global climate interact. Emphasis was given on a multi-disciplinary approach of the dynamics of the global functioning of Antarctic main natural systems and of their evolution and interactions. Seven research lines were selected under three priority areas :

- ECODYNAMICS OF THE SOUTHERN OCEAN AND INTERACTIONS WITH THE CLIMATE :
  - Biogeochemical fluxes and cycles in the main trophic compartments
  - Modelling the global dynamics of ecosystems
  - Assessment of the role of " new production " in the burial of atmospheric CO_2 by the Southern Ocean

- EVOLUTION AND PROTECTION OF MARINE ECOSYSTEMS :
  - Application of predictive ecological models to simulate ecosystem responses to man-made climatic disturbances
  - Study of hydrocarbons spills dispersion

- ROLE OF THE ANTARCTIC IN GLOBAL CHANGES :
  - Ocean-Cryosphere-Atmosphere interactions.
  - Sedimentary palaeoenvironment.

Belgium's commitment in scientific research on the Antarctic is currently covered by the Fourth Phase of the Programme (1997-2000). The overall budget of this new phase amounts to 236 MBEF. In addition the OSTC contributes a sum of 20 MBEF to the operational costs of the European Project for Ice Coring in Antarctica (EPICA).

CONTENTS

Part A : HYDRODYNAMICS

Part B : MARINE GEOPHYSICS

Contents of VOLUME I

MARINE BIOGEOCHEMISTRY AND ECODYNAMICS

Contents of VOLUME III

GLACIOLOGY AND CLIMATOLOGY

Part **A:**

HYDRODYNAMICS

RESEARCH CONTRACT A3/58/001

1

OIL SPILL MODELLING IN THE WEDDELL SEA

B. PETIT[1]

INSTITUTE OF HYGIENE AND EPIDEMIOLOGY
MANAGEMENT UNIT OF THE MATHEMATICAL MODEL (MUMM)
Gulledelle 100
B-1200 Brussels
Belgium

[1] Corresponding author E-mail : antarbp@camme.ac.be

Table of Contents

Oil Spill Modelling in the Weddell Sea

Abstract

This paper proposes a model of oil behaviour in ice-infested waters. It describes the interactions between oil and ice coupled with a sea ice formation model. The main features of oil spreading and dynamics in an ice pack are taken into account in the model which is tested in three different situations: at short term in cold waters and in the presence of ice, and at long term. The results show that the presence of ice completely modifies the classical spreading of an oil slick by increasing or shrinking the contaminated area, and by incorporating some oil in its structures. The model is used for the simulation of a possible spill in the Weddell Sea. The mean drift of oil follows the Weddell gyre, which takes the remaining contamination toward the circumpolar current. The part of the oil initially entrapped in the ice induces a second spill which cannot be qualified as accidental because the model may provide an answer to the basic questions: when, where, and how much?

Key words: ice, oil, Weddell Sea

1. Introduction

The consequences of oil pollution have been studied for several years in the Arctic Ocean. On the other hand, oil pollution in the Southern Ocean is rarely tackled because in the past, there was no oil extraction from the Antarctic continent and its continental shelf and since 1991, all industrial activities related to mineral resources are forbidden on the basis of the Madrid Protocol on Environmental Protection to the Antarctic Treaty.

Nevertheless, the oil pollution danger in the Antarctic exists and has been increasing proportionally to human presence and activities. Supply, scientific and tourist ships are cruising to and from Antarctic bases and cause or may cause problems to the Antarctic environment.

For instance, in the year 1989, two different ship accidents caused alarming pollution in the Antarctic coastal zone. On 28 January, the Argentine supply and tourist vessel "Bahia Paraiso" grounded at Palmer station, the United States research base on Anvers Island on the western side of the Antarctic Peninsula. Eight hundred tons of diesel and jet fuel were spilled. The spill spread in the Bismark Strait area and caused significant bird mortality. Inaccessibility of the polluted sites worsened the situation. One month later, on 27 February, the Peruvian research vessel "Humbold" grounded in Fildes Bay on King George Island at the northern end of the Peninsula. Thirty-five tons of diesel oil were spilled, this time fortunately causing little damage.

These accidents attracted considerable concern because they suddenly brought two facts to the attention of the public: the existence of a non-negligible risk of oil pollution in the Southern Ocean and the tremendous vulnerability of the Antarctic ecosystem. Efficient means should thus be available to obtain clear indications on the possible consequences of a spill and to react properly in case of emergency.

Adequate models exist to simulate the behaviour of oil spilled at sea and some of them consider its interactions with the Arctic ice but no reliable model is available for the specific Antarctic conditions. If it can be reasonably assumed that the behaviour of an oil slick is the same in Arctic and Antarctic oceans, the main difference is that the dynamics of the Antarctic ice pack is less constrained by the presence of coasts. It seems thus necessary to develop adequate tools able to predict the evolution of an oil slick in such a severe environment in order to assist in impact assessment studies.

The present paper describes a model that simulates interactions between ice and oil and that is coupled with a sea ice formation model (Demuth & van Ypersele 1989, Petit & Demuth 1992), reproducing the main features of the annual cycle of ice extent and thickness. The

evolution of an oil spill within the ice pack is based upon empirical methods developed by El-Tahan *et al.* (1988) for arctic ice-infested waters. The model is applied to a fictive spill in an area covering the Weddell Sea and the Drake Passage, which makes up a potential risk area because of the network of scientific stations on its coasts and the inherent traffic of supply vessels.

Mackay *et al.* (1980) have already indicated that an oil spill in open water is an extremely complex assembly of interacting processes so that the development of evolution models is certainly not an easy task. The introduction of ice, as a supplementary constraint on an oil spill, does not make the development of such a model easier. Nevertheless, the consideration of a limited number of phenomena can give good indications of the evolution of an oil spill in these conditions, with a certain degree of accuracy.

2. Sea ice modelling

The sea ice model, initially based on the "zero layer" model developed by Semtner (1976), computes the annual cycle of sea ice thickness and its spatial extent. This model is divided into two major parts dealing with the thermodynamical and dynamical processes which control the ice and determine its thickness and movement.

Its thermodynamical component computes the thickness and the temperature of the ice deduced from heat exchanged vertically through the ice-air and ice-ocean interfaces and horizontally through the leads.

The sea ice, assumed to be a uniform horizontal slab of ice, develops to balance the heat exchanges between the atmosphere and the ocean. Any imbalance leads to its formation or melting. The energy exchanged through the air-ice interface consists of the shortwave or solar radiation including the surface albedo, the non-solar heat flux gathering the longwave radiation from the atmosphere, the longwave radiation from the surface, the sensible and latent heat flux, and the conductive flux just below the surface. The thermal equilibrium at the surface gives the surface temperature. If its value exceeds the melting point (0°C for snow, -0.1°C for ice), the excess of energy is used to melt snow and/or ice.

At the base of the ice layer, the conductive flux within the ice is balanced by the vertical heat flux from the deep ocean. Any imbalance causes ice to grow or to melt at the bottom. In all calculations, the bottom temperature is supposed to be equal to the freezing temperature which depends on the mixed layer salinity.

Horizontally, the heat flux balance at the surface of the leads can modify the sea ice extent. The sea ice and the leads are connected to the deep ocean through a mixed layer model

proposed by Fichefet & Gaspar (1988), which gives the temperature, the salinity and the thickness of the mixed layer.

The dynamical component of the sea ice model provides the ice velocity as a linear function of the geostrophic wind and the upper ocean current, ensuring the horizontal redistribution of the amount of ice present at the ocean surface. In this process, the conservation of total ice mass per unit area m_{ice} is given by:

$$\frac{\partial m_{ice}}{\partial t} + \nabla \cdot (\mathbf{u}_{ice} m_{ice}) = 0 \tag{1}$$

The ice velocity $\mathbf{u}_{ice}$ is expressed by:

$$\mathbf{u}_{ice} = \mathbf{u}_{water} + \alpha_{ice} \mathbf{D}(\theta_{ice}) \mathbf{u}_{air} \tag{2}$$

where α_{ice} is the wind drift factor equal to 0.008; θ_{ice}, the deflection angle equal to 36° and $\mathbf{u}_{air}$, the wind velocity above sea level.

The surface water current $\mathbf{u}_{water}$ used for these simulations is obtained from a three-dimensional circulation model, which computes the hydrodynamic response of the ocean to the wind forcing (barotropic circulation). The numerical procedure based on the work of Paul & Lick (1981) and Jamart et al. (1982) is fully described in Petit & Demuth (1993). The wind stresses are computed from the climatological data compiled by Taljaard et al. (1969).

This sea ice formation model has been applied to a sector of the Southern Ocean, including the Weddell Sea and the Drake Passage and reproduces the main characteristics of the ice pack (ice thickness and extent, temperature, mixed-layer depth).

Figure 1 gives the seasonal cycle of sea ice area obtained by the model and observed by satellite between 1978 and 1987 (Gloersen *et al.* 1992). If one keeps in mind that the sea ice model is run with a set of monthly-averaged meteorological data for one typical year and is thus not able to reproduce all the time variations, the agreement between the results and the observations may be considered satisfactory.

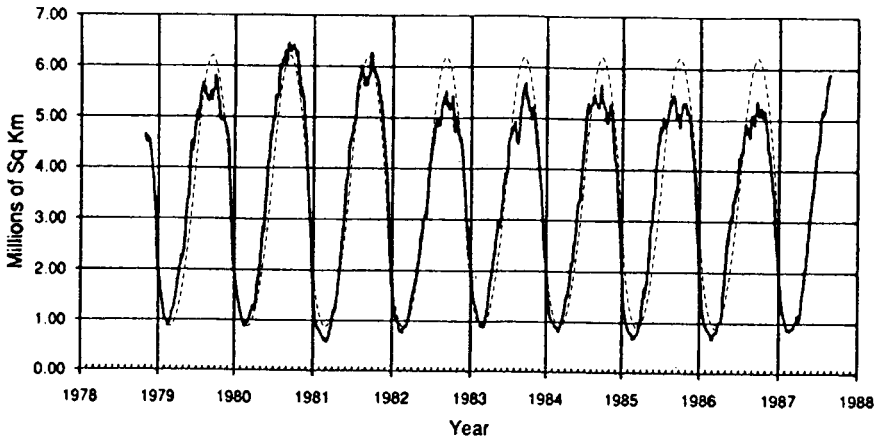

Figure 1. Sea ice area in the Weddell sea observed by satellite (solid line, from Gloersen *et al.* 1992) and computed (dashed line).

3. Oil spill evolution

The evolution of an oil spill in open sea is described by the general transport equation:

$$\frac{\partial c_{oil}}{\partial t} = -\mathbf{u}_{oil} \cdot \nabla c_{oil} + \nabla \cdot \left(K_h \nabla c_{oil} \right) + \phi \tag{3}$$

where c_{oil} is the mass concentration of oil usually expressed per unit area, $\mathbf{u}_{oil}$ is the net advecting speed, K_h is the horizontal dispersion coefficient representing the combined effects of turbulent dispersion and physical spreading due to surface tension, and ϕ indicates the various processes of oil degradation (Venkatesh & Murty 1988). The presence of ice completely modifies the behaviour of an oil spill (Schulze 1984) so that each term of equation 2 becomes dependent on the ice concentration. These modifications are fully described in the sections 4, 5, and 6.

It must however be noted as a preamble that the oil spill models are roughly divided into two types: a continuous and a "particle" approach. In the first one, the oil spreading is governed by different phases (Fay 1969): inertia/gravity, gravity/viscous and viscous/surface tension. In most of the cases, however, this method is used with Eulerian models and with some assumptions like radial symmetry. It provides a good evaluation of the surface of an oil slick and its mean thickness but fails to reproduce the shape of a slick. In the second approach, the oil spill is simulated by a large number of particles (Allen 1982, Ozer & Gong 1991). This

Lagrangian method allows a more efficient represention of the slick shape and a more direct introduction of some phenomena linked to horizontal and vertical turbulence like the injection of oil droplets in the water column and their recoalescence.

In fact, the total horizontal diffusion of an oil slick can be divided into three kinds of spreading according respectively to Fay's phases, turbulent diffusion and diffusion due to the convergence and divergence of the ice pack.

The presence of ice reinforces the spatial patchiness of the spill and multiplies the possible contacts between oil and ice, which is an argument in favour of the particle approach. At the same time, the diffusion due to convergence and divergence of the ice pack plays an important role by keeping a certain degree of continuity in the oil slick, which is an argument in favour of the continuous approach. The most appropriate approach to take into account the role of ice is thus a compromise between both methods: that is the reason why this model represents an oil release among the ice pack by a *certain* number of *continuous* oil slicks.

4. Oil drift in the presence of ice

The drift of oil in open waters is reasonably well understood. However, the presence of ice at sufficient concentration reduces the area available for oil, acts as a natural barrier, and alters consequently the normal evolution of the slick. In fact, oil does not simply move through the leads or the open areas in the ice pack because these zones are often obstructed by broken ice. Moreover, the closure of leads ejects an amount of oil onto the ice surface and under the ice layer (MacNeill & Goodman 1985). In other respects, the ice pack loses its confinement role during spring and summer when the break-up releases partly or totally the oil trapped among the ice floes or in the ice layer.

Observations during accidental oil spills and experiments (Deslauriers 1979, Reimer 1980, Allen 1984) reveal two regimes of oil drift in the presence of ice, the separation of which corresponds to a threshold value of the ice concentration c_{ice} (expressed as a percentage of ice surface per unit surface). The most commonly observed value of this threshold is about 30% although some observations give values up to 50%. Beneath this threshold value, the ice layer cannot easily trap oil and does not interfere with the general oil slick movement: oil and ice move separately.

In free open sea, one can accept that the wind stress and the ocean current are the main driving forces of the slick movement. Their equilibrium is expressed by:

$$\mathbf{u}_{oil} = \mathbf{u}_{water} + \alpha_{oil}\mathbf{D}(\theta_{oil})\mathbf{u}_{air} \tag{4}$$

where $\mathbf{u}_{oil}$ is the velocity of the centre of the slick, α_{oil} is the wind drift factor, $\mathbf{D}(\theta_{oil})$ is the transformation matrix. θ_{oil} is a deflection angle equal to $8\sqrt{|\mathbf{u}_{air}|}$ - 40° when $0 \leq |\mathbf{u}_{air}| \leq 25$m/s and to zero for wind speeds greater than 25m/s (Scory 1991).

Above the threshold value of 30%, the ice pack governs completely the oil movement so that both media move together, following the equation 2. This is confirmed by experimental oil spills monitored by Ross & Dickins (1987) on the Canadian Coast and by Vefsnmo & Johannessen (1994) in the marginal ice zone of the Barents Sea.

Both regimes should be continuously linked. A confinement function $f(c_{ice})$ is introduced to model the transition of oil drift from open sea to ice-infested water and vice versa. This confinement function is expressed by:

$$f(c_{ice}) = 0.5 + \pi^{-1}\text{atan}(c_{ice} - 30) \tag{5}$$

which varies rapidly from 0 to 1 in the vicinity of 30%. The general oil velocity can thus be expressed by:

$$\mathbf{u}_{oil} = \mathbf{u}_{water} + \left\{f(c_{ice})\alpha_{ice}\mathbf{D}(\theta_{ice}) + \left[1 - f(c_{ice})\right]\alpha_{oil}\mathbf{D}(\theta_{oil})\right\}\mathbf{u}_{air} \tag{6}$$

5. Oil spreading and diffusion in the presence of ice

During the first stages after the spillage, the physical spreading of oil is the result of an equilibrium between the different forces (gravity, surface tension, inertial force, viscous forces) acting on the continuous slick (Fay 1969). In the present model, it is computed by the spreading equation used by Scory (1991). This equation has been subsequently improved to take into account the modified net surface tension introduced by El-Tahan & Venkatesh (1994), which induces a strong reduction of the oil spill extent. After a given time, which is not precisely determined in previous oil spill studies, the turbulent diffusion exceeds this first spreading and becomes the predominant factor in the further evolution of the spill.

The presence of ice, namely by opening and closing free areas, hampers the evolution of the oil spreading that must thus be tuned appropriately as a function of ice concentration.

Within the ice pack, the oscillations of the ice blocks, their collisions, and the closure of the leads eject some oil *under* the ice or allow it to settle by splashes *on* the ice. The second phenomenon is apparently prevailing (MacNeill & Goodman 1985). The freezing of

contaminated water and the absorption of oil by snow accumulated on the ice layer lead to the incorporation of oil in the ice layer. Oil can thus be present on water but also in, under, or on the ice layer. These interactions between ice and oil affect certainly the thermodynamic equilibrium of the ice but this is not taken into account explicitly in the model, mainly due to the lack of reliable data on oil thermal conductivity and capacity.

Under ice, the oil fills the cavities and is simply maintained in this position by gravity forces, as long as the currents are not strong enough to flush it out. The under-ice storage capacity is far from negligible: in steady conditions, the equilibrium thickness of oil under flat ice is about 8mm (Schulze 1984). However, the ice is not always flat and some local features such as refrozen leads can offer larger free volume.

A steady position of an oil lens under the ice layer modifies the heat transfers through the ice layer. The difference of thermal conductivity between ice and oil is such that sea ice grows more slowly under oil and ice lips develop around the lens, entrapping oil under and progressively in the ice layer. During spring and summer, when the network of brine channels develops, the encapsulated oil migrates upwards, can reach the upper surface of the ice layer and collects in pools. Moreover, this oil present on the ice layer absorbs better the solar radiation and accelerates the ice melting.

The various processes which significantly affect the fate and behaviour of oil released in broken ice and their associated parameters have been identified by El-Tahan *et al.* (1988).

At low ice concentration, *i.e.* for c_{ice} 30%, as well as for the drift, oil is assumed to spread freely as in cold open water. This is, for instance, the case when the oil slick evolves in a wide opening in the ice pack like a polynya or when the oil slick leaves the ice pack for the open sea. The ice concentration affects only the extent of the oil-contaminated zone.

At high ice concentration, i.e. for $c_{ice} \geq 80\%$, Venkatesh *et al.* (1990) have deduced from geometrical considerations that the horizontal diffusion of oil is stopped. Actually, if the ice floes are assumed circular, they will be touching each other and the oil once trapped in the space between ice blocks will not be able to flow laterally. In these conditions, the thickness of the oil slick can thus be greater than that of a slick spreading in open sea. That was confirmed by experiments in real situations (Ross & Dickins 1987, Vefsnmo & Johannessen 1994). In some cases, more precisely if the oil thickness is greater than the threshold obtained by hydrostatic equilibrium, oil is allowed to flow over or even under the ice layer.

This reduction of oil diffusion has to be introduced in Equation (2) and the simplest way to express this relation is to multiply the horizontal diffusion coefficient K_h – which is proportional to the growing area occupied by the oil spill – by the fraction of free area and to set it to zero when ice is too concentrated. This relation is given by:

$$\begin{cases} K_h & for\ 0 \le c_{ice} < 0.3 \\ (1-c_{ice})K_h & for\ 0.3 \le c_{ice} < 0.8 \\ 0 & for\ c_{ice} \ge 0.8 \end{cases} \tag{7}$$

In addition to this classical diffusion, one has to consider another key component of the spreading: the oil flux between the sea surface and the lower surface of the ice layer, which is proportional to the under-ice storage volume. A limited number of field measurements are available to quantify this parameter. Comfort (1987) determined that the under-ice storage volume is a linear function of ice thickness for ice layers thicker than 0.5m. The storage volume per unit area is taken as 30% of the ice thickness standard deviation when the under-ice cavities are filled to the mean thickness level. The ice thickness standard deviation is found to vary from approximately 0.7% to 15.8% for the continuous ice sheets. Venkatesh et al. (1990) have chosen an ice thickness standard deviation of 7%, i.e. in the middle of the range observed by Comfort so that the under-ice storage volume per unit area T_{ui} can be written:

$$T_{ui} = 0.021 h_{ice} \tag{8}$$

where h_{ice} is the ice thickness.

It must be noted that the linear relation proposed by Comfort is, on the basis of his observations, valid for ice layers greater than 0.5m. Nevertheless, Equation (9) is also considered valid for thinner ice thickness, which seems reasonable because the under-ice storage volume must obviously tend to zero when ice disappears.

This oil flow becomes significant for ice concentration greater than 30% and in these conditions, the oil tends to occupy the free under-ice storage volume or to be ejected from there, at a rate proportional to the variation of its capacity. In the model, it is expressed by the following sink/source term $F_{oil,\ water \leftrightarrow ice}$ added in Equation (2):

$$F_{oil,\ water \leftrightarrow ice} = \frac{\partial}{\partial t} \rho_{oil}\ c_{ice} T_{ui} \tag{9}$$

where ρ_{oil} is the oil density.

6. Weathering

With time, not only the drift and the spreading of the oil spill change, but also its physical and chemical characteristics and associated processes, such as density, viscosity, pour point, surface tension, evaporation, emulsification, dispersion, and dissolution.

Due to the low temperatures and the presence of ice, most of these processes are slowed down. The ice tends to damp wave motion and thus reduces turbulence (MacNeill & Goodman 1985) so that the weathering processes induced by the mechanical energy available at the sea surface, *e.g.* emulsification and dispersion, are strongly reduced.

On the other hand, oil becomes more viscous due to the low temperatures. Although many authors point out the very weak influence of viscosity on oil spreading in temperate seas (*e.g.* van Oudenhoven *et al.* 1983), this parameter, which reveals a strong dependence on temperature, plays a more important role in cold conditions. On the basis of the limited available data in cold waters, El-Tahan *et al.* (1988) have expressed the equilibrium thickness of an oil slick as a linear function of oil viscosity. Moreover, Venkatesh *et al.* (1990) underline that the equilibrium thickness in broken ice is nearly 4 times that on cold water. In the extreme case, the oil can stop flowing because its temperature reaches its pour point.

The reduced emulsification and dispersion, the higher viscosity as well as the limited area free for spreading, as mentioned above, lead to an oil spill which is relatively thick and, at least, thicker than the equilibrium thickness. This, in its turn, reinforces the damping of the wave motion and constitutes a positive feedback attenuating more emulsification and dispersion.

These phenomena causing a strong reduction of the oil slick surface are also responsible for a strong reduction of evaporation. Finally, oil encapsulated in ice is almost unexposed to weathering and remains fresh.

The usual formulations of these processes described *e.g.* in Whiticar *et al.* (1993) allow to take explicitly into account the various effects of cold temperatures and are introduced in the present model.

7. Test cases: short term evolution

Ideally, the evaluation of a model needs several complete sets of data that cover most of the possible scenarios and conditions that the model is designed to handle. However, available quantitative field data on oil spills in broken ice are extremely limited. In these circumstances, the model described above has been tested for some kinds of possible evolution. The results presented here concern the short term evolution in cold waters and in the ice pack.

First, the equilibrium thicknesses of spills in cold waters compiled by El-Tahan & Venkatesh (1994) for some typically North American oils and those computed by the model are given in table I, which shows the capabilities of the model in reproducing the reduced spreading of oil in cold waters.

The discrepancies between results and observations are acceptable if one bears in mind that the processes concerned are very sensitive to the physical properties of oil. These are certainly not easy to measure and *e.g.*, Whiticar et al. (1993) give the dynamic viscosity of "Prudhoe Bay" oil at 0° as ranging from 19 to 577mPa.s.

Table I. Comparison between computed equilibrium thicknesses and observations (from El-Tahan & Venkatesh, 1994)

Oil type	Dynamic viscosity (mPa.s)	Density (kg/m^3)	Observed equilibrium thickness (mm)	Computed equilibrium thickness (mm)
Prudhoe Bay	500	915	3.03	3.79
Prudhoe Bay	570	915	7.30	6.27
ADGO	234	952	2.00	2.27
Prudhoe Bay	450	915	1.30	1.82

Secondly, the ability of the model to take into account the presence of ice in and around an oil slick in the first stages after a spill has been tested by simulating two spills observed by the Industry Task Group (1983). Both slicks concerned an oil volume of respectively 0.136 m^3 and 1.09 m^3 of Prudhoe Bay crude oil, which had a density of 914 kg/m^3 and a dynamic viscosity of 500 mPa.s. The oil was released in the presence of ice with a concentration varying between 38% and 62%. Figure 2 gives an estimation of the contaminated area provided by the model and compares it to the observations available for each spill. Even if there is only one observation for each of these spills, this figure shows that the model satisfactorily reproduces the initial oil spreading in these conditions. This figure also gives the

early spreading of oil in the absence of ice. The comparison between situations with and without ice indicates that the main influence of the ice is an increase of the spreading area as expressed by the formulation proposed by El-Tahan *et al.* (1988):

$$A_c = \frac{A_0}{1 - c_{ice}} \tag{10}$$

where A_c is the extent of the contaminated zone and A_0 is the extent of the same slick obtained in open water conditions.

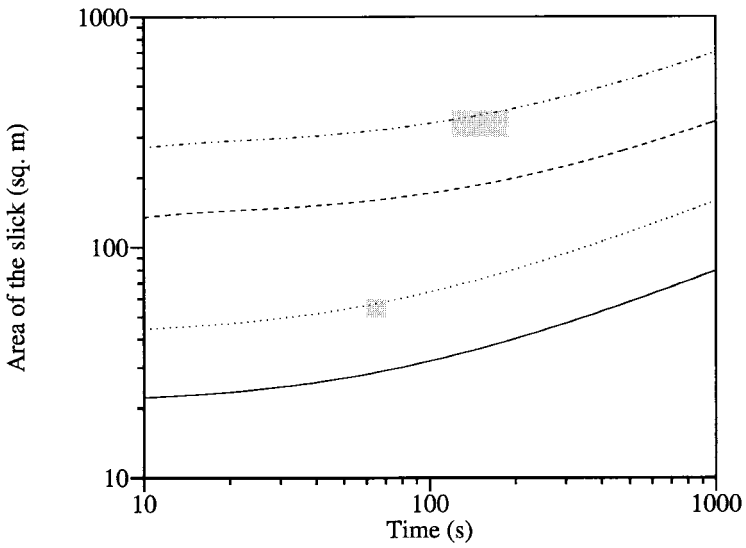

Figure 2. Early evolution of the contaminated area: released volume of 0.136m^3 without ice (solid line) and in the presence of ice (dotted line), released volume of 1.09m^3 without ice (dashed line) and in the presence of ice (dash-dot line), observations from Industry Task Group (1983) (grey rectangles).

8. Test cases: long term evolution

Some further scenarios have been designed to simulate the long term evolution of the oil behaviour under the influence of ice. These tests study the oil drift within the ice pack and evaluate the spreading and weathering of an oil slick. Due to the absence of relevant data in these extreme conditions, one has to bear in mind that the following results are only indicative.

In these scenarios, oil was released in the conditions given in table II.

Table II. Release conditions

Case	Position	Date	Initial ice concentration
#1	29°W, 73°S	Early January	53%
#2	48°W, 72°S	Early February	64%
#3	39°W, 72°S	Mid-February	54%

These positions and dates have been chosen in order to make possible the comparison of the results with the observations from Launiainen & Vihma (1994) who studied the drift of buoys deployed on ice floes. They also correspond to the minimum of the ice cover which allows a certain marine traffic with its associated risks of accident, this giving some realism to the scenarios.

Figures 3 (a, b, c) compare the trajectories of the buoys and those of the mass centre of the oil spill. This rough comparison is justified because the ice concentration is most of the time higher than 30% (as indicated *e.g.* in figure 4 giving the evolution of the ice concentration along the track corresponding to the case #3) and ice and oil tend thus to move together.

In the three cases, the oil trajectories are to some extent compatible with the drift of the buoys and clearly show the influence of the clockwise Weddell Gyre. One has to recall that the model runs with averaged meteorological inputs and is not able to reproduce all the details of reality. Moreover, the systematic delay in time might also be explained by the fact that the sea ice model computes the drift of the whole pack ice and does not take into account the small scale behaviour of the floes such as collisions and rotations. In case #1, the discrepancies between computed and observed drift are significant but, as described and explained by Vihma & Launiainen (1993), the floe on which the buoy was placed, has been submitted to strong inertial motions and has a more erratic behaviour than in the two other cases. In cases

#2 and #3, the behaviour of the floes was more steady and consequently, the agreement with the computed trajectories is more satisfactory.

The simulations confirm that, when the oil slick approaches 60°S, it is swept away by the Antarctic Circumpolar Current. However, for the case #2 (figure 3.b), the ice and oil trajectories begin to break away. It must be noted that this corresponds to a situation where the ice concentration is of the order of 30% and where oil and ice begin thus to have their own motion differently affected by the wind.

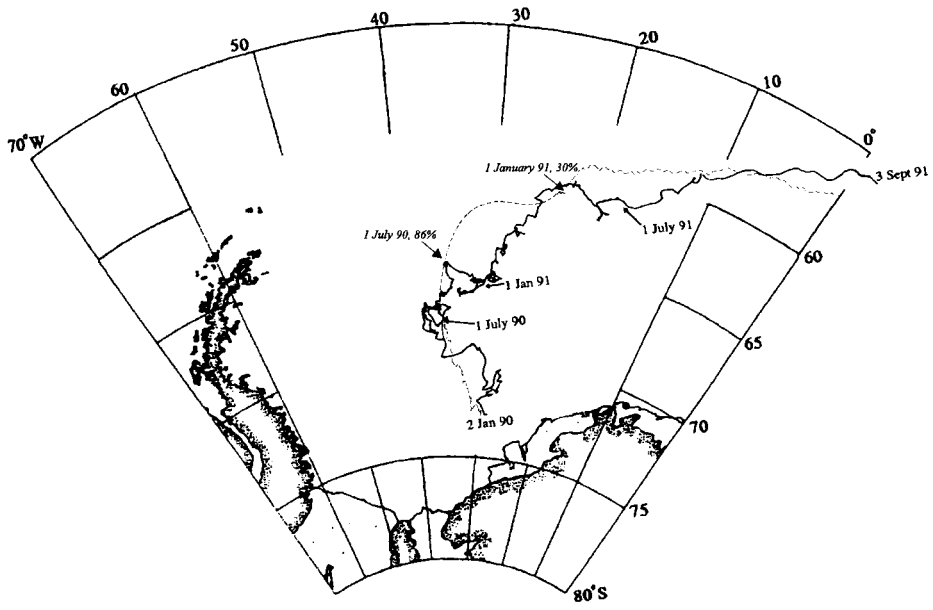

Figure 3.a Comparison between the computed trajectory of the mass centre of the oil slick (dashed line, some dates and ice concentrations being indicated in italics) and the observed trajectory of the buoy (solid line, some dates being indicated in roman, Launiainen & Vihma 1994) (case #1).

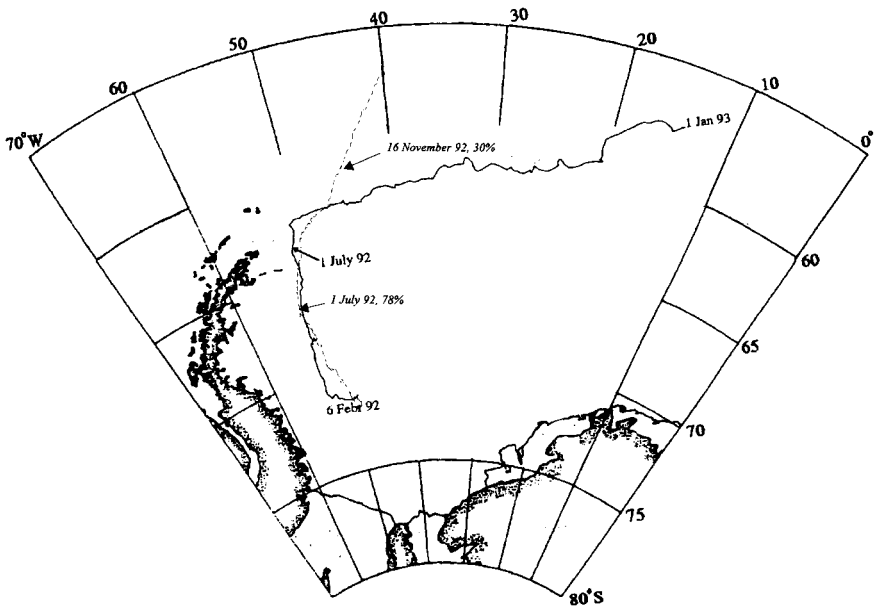

Figure 3.b Comparison between the computed trajectory of the mass centre of the oil slick (dashed line, some dates and ice concentrations being indicated in italics) and the observed trajectory of the buoy (solid line, some dates being indicated in roman, Launiainen & Vihma 1994) (case #2).

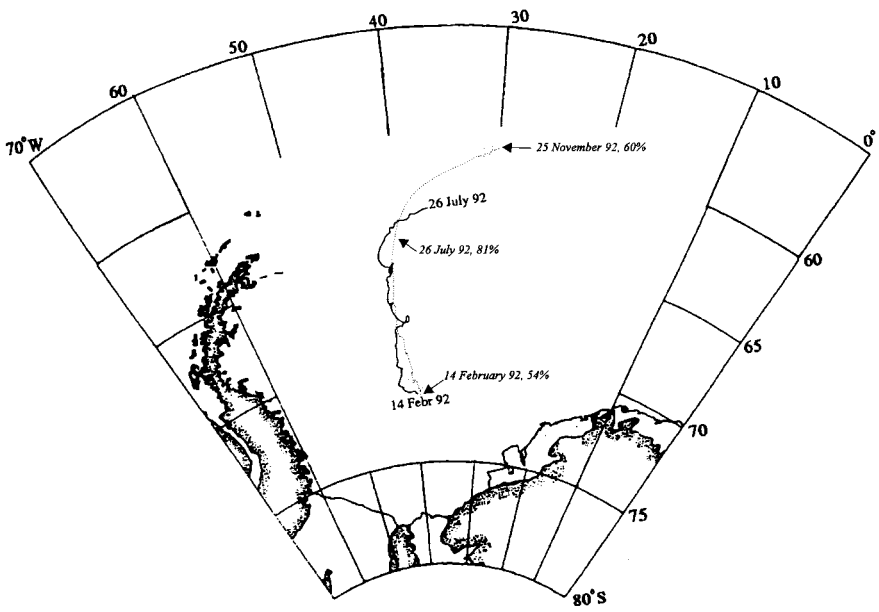

Figure 3.c Comparison between the computed trajectory of the mass centre of the oil slick (dashed line, some dates and ice concentrations being indicated in italics) and the observed trajectory of the buoy (solid line, some dates being indicated in roman, Launiainen & Vihma 1994) (case #3). The grey rectangles indicate the period during which pollution is visible.

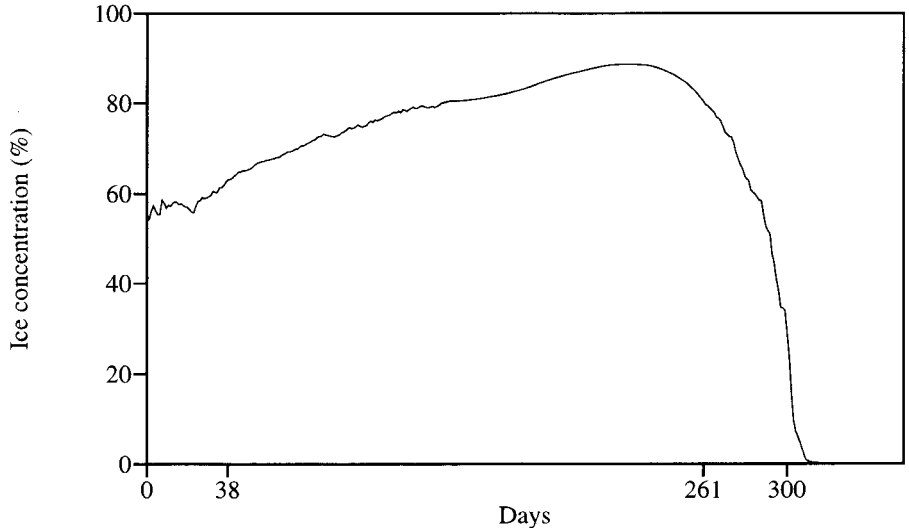

Figure 4. Evolution of the computed ice concentration along the track corresponding to the case #3 (Day 0 is 14 February).

Case #3 is then chosen to describe the oil spreading and weathering within the sea ice. With this aim, a release of $500m^3$ of Prudhoe Bay crude oil is simulated: it evolves along the trajectory described in figure 3.c and in the presence of ice at concentration given in figure 4. The Prudhoe Bay oil has been chosen for the simulations because we could gather sufficient information on this oil type but we have carried out simulations with marine gas oil for the British Antarctic Survey (Downie 1996).

Figure 5 illustrates the oil distribution among the different phases during the first two weeks after the release. The increase of total volume is due to the incorporation of sea water by emulsification. After this period, the oil present at the sea surface is completely weathered but about 20% of fresh oil remains stabilized under ice and will stay hidden until the break up.

The oil thickness (figure 6) begins to increase due to incorporation of sea water by emulsification, with some oscillations caused by transfers of oil between ice and water. When the dissolution becomes predominant, it continuously decreases and 38 days after the release, all trails of pollution seem to have disappeared from the sea surface. However, 260 days after the release, the fresh oil which was initially entrapped under ice causes a new contamination at the position (32°W, 61°S), which remains visible during almost 40 days.

Figure 7 describes the evolution of the pollution extent. The area of the first oil slick actually present at the sea surface reaches a steady value when oil transfers between ice and sea surface are stabilized. The contaminated area, which includes the ice in contact with oil, increases because, during this phase, the ice pack is growing as already indicated in figure 4. This figure also gives the extent of the delayed pollution and the second slick reveals a classical behaviour of oil in open cold waters.

Figure 8 describes the oil distribution among the different phases during the first two weeks after the appearance of the second spill. This distribution differs from the first one (figure 5) by the fact that, here, there is during several days a small but continuous release of fresh oil.

Finally, the particle approach gives the possibility of providing a realistic representation of the slick shape. Here, the $500m^3$ oil volume is divided into 50 particles of $10m^3$ and figure 9 describes, as an example, the slick shape after 7 days, which is characterized by its stretch along the average direction of the oil drift.

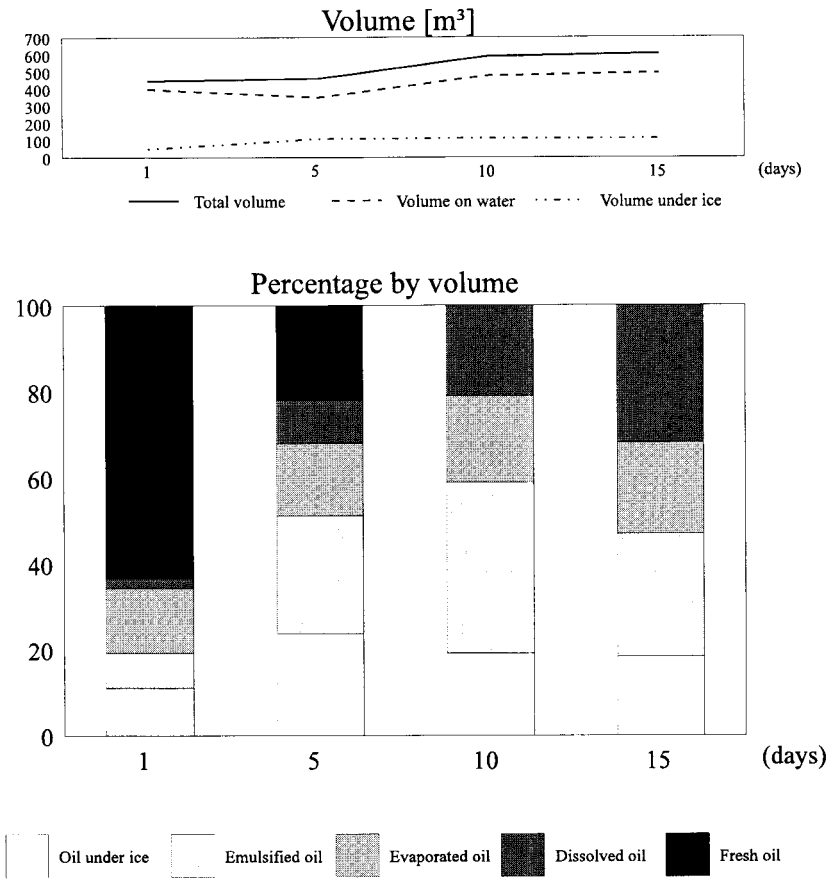

Figure 5. Evolution of the oil volume (above) and of the weathering (below) during the first two weeks (Day 0 is 14 February).

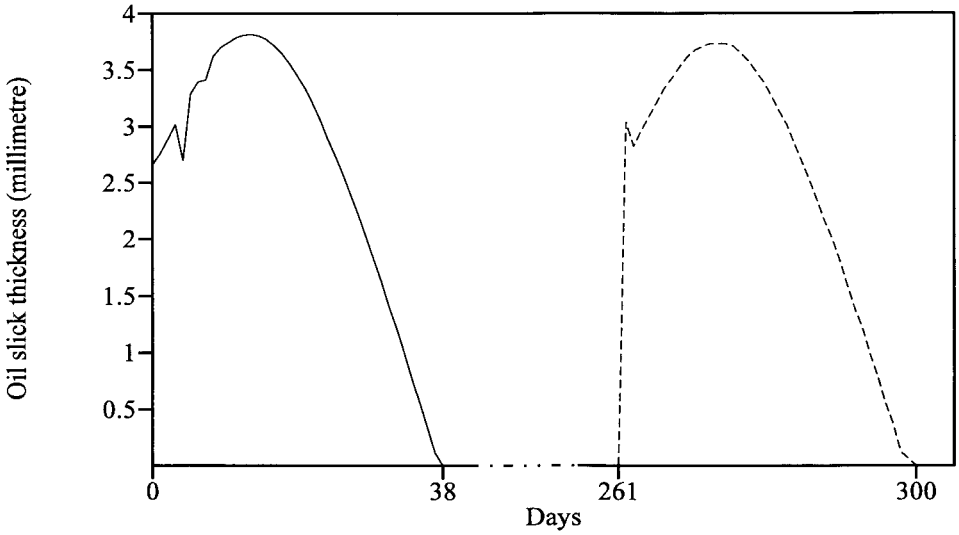

Figure 6. Evolution of the oil thickness: first (solid line) and delayed (dashed line) spill.

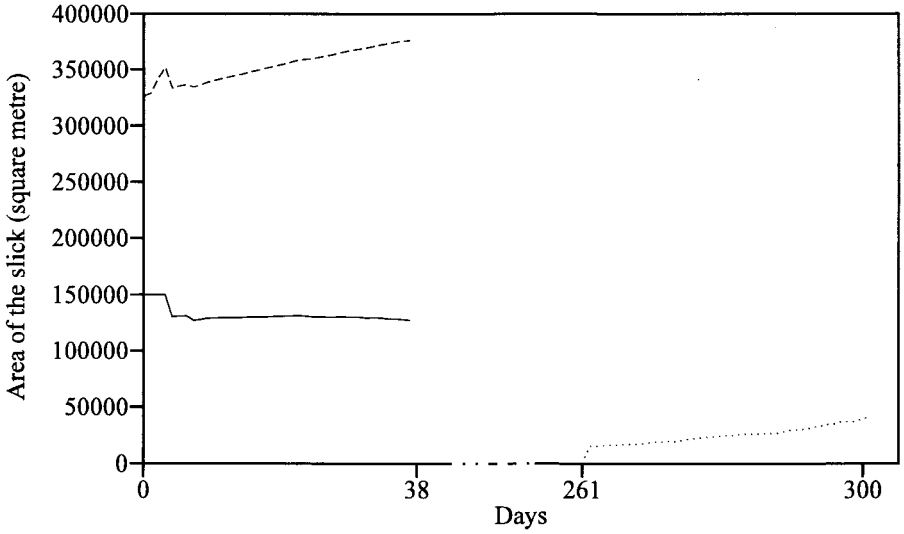

Figure 7. Evolution of the oil spill extent: oil on water (solid line) and total contaminated area (dashed line) for the first pollution, oil on water (dotted line) for the delayed pollution.

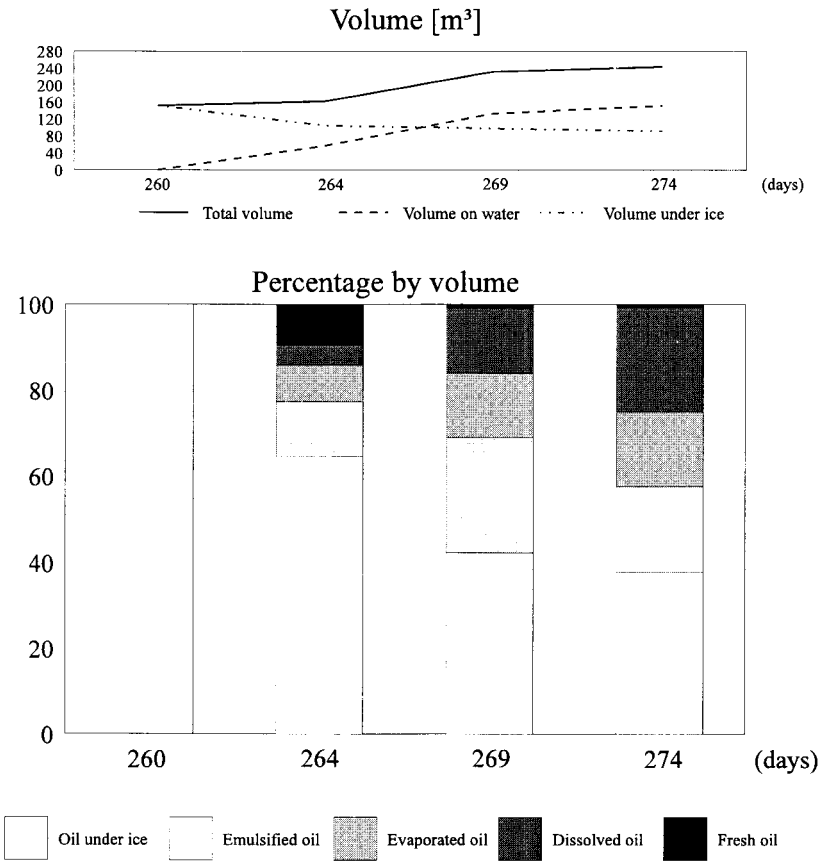

Figure 8. Evolution of the oil volume (above) and of the weathering (below) during the first two weeks for the delayed pollution.

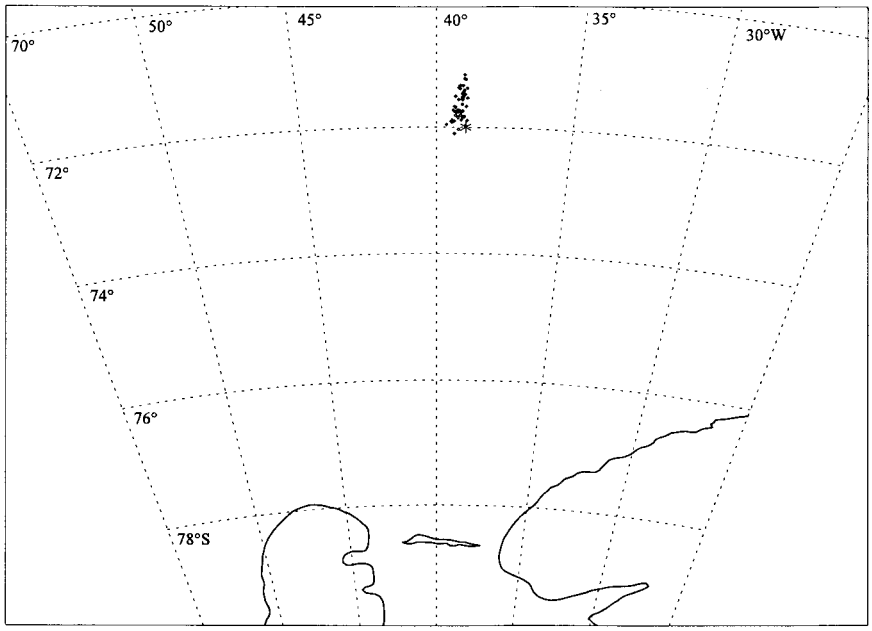

Figure 9. Evolution of the slick shape one week after the release. The asterisk indicates the release point.

9. Application to oil spill contingency plans in Antarctica

In 1996, the British Antarctic Survey (BAS) examined contingency planning for oil spill response in Antarctica and evaluated the capacities of Antarctic research stations and ships to react to pollution incidents. As part of this study, the BAS studied the use of oil spill simulation models as management tools to help in spill response. They made themselves acquainted with the modelling work done at MUMM during the XXth Antarctic Treaty Consultative Meeting held in Utrecht from 29 April to 10 May 1996.

Therefore, the MUMM and the BAS collaborated in running the model described in this paper for different scenarios designed by BAS to investigate the possible consequences of a major fuel spill. Data were supplied by BAS and Environment Canada. The scenarios involved the release of 163,000 litres of marine gas oil at different locations in the Weddell Sea. The results provided by MUMM consisted of oil slick trajectories and forecasts of the weathering of the fuel and pack ice conditions. They are presented in Downie (1996).

The joint study showed how useful computer models could be in spill response operations. Further development of this kind of model will benefit from close collaboration between

modellers and people with practical experience of working in the Antarctic and dealing with actual incidents.

Conclusions

On the basis of existing literature and observations, interactions between ice and oil are identified and introduced in a sea ice formation model to study the possible fate of oil pollution in the Weddell Sea. It appears clearly that the presence of ice pack completely modifies the evolution of an oil slick which acts as a moving boundary, controlling the spreading and the drift of an oil slick.

Some short term tests have been carried out with the model and have successfully reproduced the oil spreading on cold water and in the presence of ice.

One of the key results of the long term scenario is to show that almost 20% of the initially released oil cause later and further away a second pollution event. Since the evolution of the oil slick strongly depends on the way that oil and ice interact and since each accident has thus its own features, it is evident that, in other circumstances, a greater percentage or even all the oil could be blocked under ice provoking this kind of delayed pollution, which cannot be considered any more as "accidental". If one has to admit that logistical difficulties inherent to the Antarctic area hamper appropriate reactions in the very beginning of an accident, that is no more the case when one has in advance clear information on the time of an oil spill, its position, and the involved quantities, which is the case for this second spill. Without prejudice to complementary efforts concerning its validation, a major interest of the present model is to provide a tool able to deliver such information to authorities and intervention teams who would thus not be caught off their guard. This last point has been illustrated by the collaboration between BAS and MUMM on the contingency planning for oil spill response in Antarctica.

Acknowledgements

The author would like to thank Dr C. Demuth who developed the first version of the sea ice model, Dr G. Pichot for providing useful comments on the draft version of this paper, and the British Antarctic Survey for the collaboration on their contingency planning for oil spill response in Antarctica. This research is sponsored by the Belgian Program "Scientific research on the Antarctic" (Services of the Prime Minister – Federal Office for Scientific, Technical and Cultural Affairs, OSTC) under contract A3/58/001.

References

Allen, A.A. 1984. Oil Spill Demonstrations in Broken Ice, Prudhoe Bay, Alaska, 1983. Proc. Seventh Arctic Marine Oilspill Program Technical Seminar, 12-14 June 1984, Alberta, pp.342-354.

Allen, C.M. 1982. Numerical simulation of contaminant dispersion in estuary flows. Proc. R. Soc. Lond., Vol.A381, pp.179-194.

Comfort, G. 1987. Analytical modelling of oil and gas spreading under ice. Environmental Studies Revolving Fund rep. 077, Dep. of Energy Mines and Resources, Ottawa, Ont.

Demuth, C. & van Ypersele, J.-P. 1989. Simulations of the annual sea ice cover in the Weddell Sea. Belgian Scientific Research Programme on Antarctica. Scientific Results of Phase One (Oct.85-Jan.89). Volume III: glaciology and climatology. Services of the Prime Minister-Science Policy Office.

Deslauriers, P.C. 1979. Observations of Oil in Ice Floes and the 1977 *Ethel H.* Spill. Proc. Workshop on Oil, Ice and Gas, 10-11 October 1979, Toronto, Ont., Univ. Toronto, Inst. Environ. Studies, Publ. No.EE-14, pp.87-94.

Downie, R. 1996. Contingency Planning for Oil Spill Response in Antarctica. European postgraduate programme 1995/1996 in environmental management.

El-Tahan, H., Comfort, G. & Abdelnour, R. 1988. Development of a Methodology for Computing Oil Spill Motion in Ice-infested Waters. Rep. submitted by Fleet Technology Limited, Kanata, Ont., to Atmospheric Environment Service, Downsview, Ont., 85 pp.

El-Tahan, H. & Venkatesh S. 1994. Behaviour of Oil Spills in Cold and Ice-infested Waters-Analysis of Experimental Data on Oil Spreading. Proc. Seventeenth Arctic and Marine Oilspill Program Technical Seminar, 8-10 June 1994, Vancouver, British Columbia, pp.337-354.

Fay, J.A. 1969. The spread of oil slicks on a calm sea. In: *Oil on the Sea,* D.P. Hoult (Ed.), Plenum Press, pp. 53-63.

Fichefet, Th. & Gaspar, Ph. 1988. A model study of upper ocean-sea ice interactions. Journal of Physical Oceanography, 18, 181-195.

Gloersen, P., Campbell, W.J., Cavalieri, D.J., Comiso, J.C., Parkinson, C.L & Zwally, H.J. 1992. Arctic and Antarctic Sea Ice, 1978-1987: Satellite Passive-Microwave Observations and Analysis. Scientific and Technical Information Program, NASA SP-511, Washington D.C., pp.290.

Industry Task Group. 1983. Oil Spill Response in the Arctic. Part 2: Field demonstrations in broken ice. Shell Oil Company, Sohio, Alaska Petroleum Company, Exxon Company, U.S.A. and AMOCO Production Company, Anchorage, Alaska.

Jamart, B.M., Milliff, R., Lick, W. & Paul, J. 1982. Numerical studies of the wind driven circulation in the Santa Barbara Channel. Final Report to Exxon Production Research Company, 126 pp.

Launiainen, J. & Vihma, T. 1994. On the Surface Heat Fluxes in the Weddell Sea. The Polar Oceans and Their Role in shaping the Global Environment, Geophysical Monograph 85, AGU.

Mackay, D., Paterson, S. & Trudel, K. 1980. A Mathematical Model of Oil Spill Behaviour. A report submitted to the Environmental Impact Control Directorate, Environmental Protection Section, Ottawa, pp. 39.

MacNeill, M.R. & Goodman, R.H. 1985. Motion of Oil in Leads. Proc. Eighth Arctic Marine Oilspill Program Technical Seminar, 18-20 June 1985, Edmonton, Alberta, pp. 42-52.

Muench, R.D. & Gordon, A.L. 1995. Circulation and Transport of Water along the Western Weddell Sea Margin. Journal of Geophysical Research, Vol. 100, NO. C9, Pages 18,503-18,515.

Ozer, J. & Gong, C. 1991. PARCEL: a three-dimensional oil spill model. Oil Pollution Environmental Risk Assessment (OPERA), Proc. of the final workshop, Dalian, China, 9-10 December 1991, pp. 161-180.

Paul, J.F. & Lick, W.J. 1981. A numerical model for three-dimensional variable density hydrodynamics flows. U.S. Environmental Protection Agency Report, 150 pp.

Petit, B. & Demuth, C. 1993. Sea Ice Circulation in the Weddell Sea. Belgian Scientific Research Programme on the Antarctic. Scientific Results of Phase II (10/1988-05/1992). Volume III: glaciology and climatology. Belgian Science Policy Office.

Reimer, E. 1980. Oil in Pack Ice: The Kurdistan Spill. Proc. Third Arctic Marine Oilspill Program Technical Seminar, 3-5 June 1980, Edmonton, Alberta, pp.529-544.

Ross, S.L. & Dickins, D.F. 1987. Field research spills to investigate the physical and chemical fate of oil in ice pack. Environmental Studies Revolving Fund Rep. No. 062, Dep. of Energy mines and Resources, Ottawa, Ont., 118 pp.

Schulze, R. 1984. A field guide for Arctic oil spill behaviour. Arctec Inc., Columbia, Md.

Scory, S. 1991. The Mu-slick model. Management Unit of the North Sea and Scheldt estuary Mathematical Models, Report CAMME/91/03, 30 p.

Semtner, A.J. Jr. 1976. A model for the thermodynamics growth of sea ice in numerical investigations of climate. J. Phys. Oceanog., 6, 379-389.

Taljaard, J.J., van Loon, H., Crutcher, H.L. & Jenne, R.L. 1969. Climate of the Upper Air, I, Southern Hemisphere, Vol.1. Temperatures, Dew Points and Heights at Selected Pressure Levels. NAVAIR 50-1C-55, U.S. Naval Weather Service, Washington, D.C., 135 pp.

Van Oudenhoven, J.A.C.M., Drapers, V., Ebbon, G.P., Holmes, P.D. & Nooyen, J.L. 1983. Characteristics of Petroleum and its Behaviour at Sea. CONCAWE's Oil Spill Clean-up Technology, Special Task Force No. 8, Den Haag.

Vefsnmo, S. & Johannessen, B. O. 1994. Drift and Spread of Oil in Broken Ice Field Experiment. IAHR Symposium 1994, Trondheim, Norway.

Venkatesh, S., El-Tahan, H., Comfort, G. & Abdelnour R. 1990. Modelling the Behaviour of Oil Spills in Ice-infested Waters. Atmosphere-Ocean 28 (3), 303-329.

Venkatesh, S. & Murty, T. S. 1994. Numerical Simulation of the Movement of the 1991 Oil Spills in the Arabian Gulf. Water, Air, and Soil Pollution **74**: 211-234.

Vihma, T. & Launiainen, J. 1993. Ice Drift in the Weddell Sea in 1990-1991 as Tracked by a Satellite Buoy. Journal of Geophysical Research, Vol. 98, NO. C8, Pages 14,471-14,485.

Whiticar, S., Bobra, M., Fingas, M., Jokuty, P., Liuzzo, P., Callaghan, S., Ackerman, F. & Cao, J. 1993. A Catalogue of Crude Oil and Product Properties (1992 Edition). Publication No.EE-144, Environment Canada, Environmental Directorate, Environmental Technology Centre, Ottawa, Ont. Unpublished report.

Part **B:**

MARINE GEOPHYSICS

RESEARCH CONTRACT A3/02/002

BELANTOSTRAT BELGIAN CONTRIBUTION TO THE "ANTARCTIC OFFSHORE ACOUSTIC STRATIGRAPHY PROJECT (ANTOSTRAT)"

M. DE BATIST[1],
P.-J. BART
and K. VANNESTE

RENARD CENTRE OF MARINE GEOLOGY
UNIVERSITEIT GENT
Krijgslaan 281, s.8
B-9000 Gent
Belgium

In cooperation with :

MARINE GEOPHYSICS GROUP,
ALFRED WEGENER INSTITUT FÜR
POLAR- UND MEERESFORSCHUNG
(Bremerhaven, Germany)

and

GRQ MARINE GEOSCIENCES,
UNIVERSITAT DE BARCELONA
(Barcelona, Spain)

[1] Corresponding author E-mail : marc.debatist@rug.ac.be

TABLE OF CONTENTS

ABSTRACT

The scientific objective of ANTOSTRAT - the "Antarctic Offshore Acoustic Stratigraphy" Project - is to extract Antarctica's Cenozoic glacial history from the sediments of its continental margins, principally by using seismic stratigraphy, where possible calibrated by coring or borehole evidence. The present report summarises the Belgian research efforts and scientific contribution to ANTOSTRAT, with seismic-stratigraphic studies of various portions of the Antarctic continental margin:

- The Trinity Peninsula and South Shetland Islands margins of central Bransfield Basin, along the Antarctic Peninsula;
- The West-Antarctic continental margins of the Amundsen and Bellingshausen Seas;
- The East-Antarctic continental margin of the North-eastern Weddell Sea;

These areas are situated along portions of the Antarctic continental margin that exhibit different characteristics, such as different glacial regimes and glacial evolution (West-Antarctica as opposed to East-Antarctica), different depositional processes and environments (semi-enclosed basins, quasi-starved distal glacial-marine environments, deep-sea fan and drift environments, etc.), different preservation potential (subsiding shelf edge in Bransfield Basin as opposed to stable shelf edges in Weddell Sea or along the Amundsen-Bellingshausen margin), etc.

The Trinity Peninsula and South Shetland Islands margins of central Bransfield Basin

Swath bathymetry data acquired in central Bransfield Basin during the GEBRA-93 survey reveal new morphological features and trends that shed a light on the ongoing processes of back-arc basin formation and evolution. Basin compartmentalisation and progressive deepening towards the north-east via a series of bathymetrical steps suggests a progressive increase in basin maturity in that direction. The different shapes and sizes of large volcanic edifices dominating the basin-floor morphology can be interpreted in terms of successive evolutionary stages of incipient sea-floor spreading.

New high-resolution reflection seismic data indicate that the upper-slope deposits along the Trinity Peninsula margin contain resolvable records of at least three periods - since the Pliocene, beginning of the opening of Bransfield Basin - during which ice sheets advanced to the shelf edge for a significant amount of time. The record of glacial periods of lesser extent is probably not preserved in the upper-slope and shelf

deposits as suggested by the strong erosional unconformities.

Magnitude of slope progradation varies along the Trinity Peninsula margin and appears to be related to local sources of sediment supply associated with separate glacial troughs. Ice-stream activity within these troughs appears to have varied through time. A thick stack of prograding units is preserved at the mouth of Orleans Trough. Off the mouth of the Antarctic Sound, most of the correlative section has been removed by canyon incision at the Gebra Valley.

Development of basin-floor strata appears to be temporally distinct from the development of the prograding upper-slope wedges, the toes of which downlap the basin-floor strata. A drill hole - cf. recently submitted ANTOSTRAT-ODP Proposal - through this basin-floor section would provide an excellent opportunity to constrain the age of the glacial cycles associated with the progradational wedges.

The West-Antarctic continental margins of the Bellingshausen and Amundsen seas

A regionally-spaced reflection seismic data set has been acquired from the hitherto largely unexplored Bellingshausen and Amundsen Seas along the West Antarctic margin during the ANT XI/3 survey in 1994. These data show the large-scale stratigraphic architecture of the continental shelf, slope and rise, and contain a record of the long-term glacial history of the area. On all seismic profiles, the same variation of outer-shelf geometries is observed: (1) a lower unit of mainly aggradational sequences, (2) a middle unit of strongly prograding sequences, and (3) an upper unit exhibiting both progradation and aggradation. The lower aggradational sequences are thought to represent conditions before the onset of the major glacial advance of a grounded ice sheet, whereas the overlying sequences probably record several extended periods of ice-sheet grounding on the shelf since the Middle Miocene.

A prominent erosional surface defines the base of a prograding wedge occupying the continental slope along the margin. It is tentatively correlated with the transition from aggrading to prograding sequences on the outer shelf, and may thus reflect an intensification of the bottom-current regime in the lower parts of the palaeo-slope at response to the onset of glacial conditions on the continental shelf.

Sedimentation on the continental rise appears to have resulted in the construction of large sediment drifts that originate from the interaction of channelised

turbidity currents traversing the continental rise, and along-slope bottom currents. These drift deposits are believed to contain a good and easily recoverable record of glacial history of the adjacent continental shelf, and have been the main target of a recently submitted ANTOSTRAT-ODP proposal.

The East-Antarctic continental margin of the North-eastern Weddell Sea

Re-examination of high-resolution, analog seismic records in the vicinity of ODP Site 693 has allowed a number of fine-scale unconformities to be identified in addition to those defined previously. Three sub-sequences have been recognised within seismic units W6; two in seismic unit W7. They all occur within the seemingly homogeneous Pliocene strata at ODP Site 693, consisting of clayey mud, diatom mud and silty and clayey diatom-bearing mud. They coincide with stratigraphic horizons characterised by spikes in smectite percentage in an overall illite-dominant lithology.

Smectite spikes probably indicate a change in sediment source from the Antarctic continent where glacial activity produced illite in response to direct rock erosion, to the continental shelf where previously hydrolysed Cretaceous and Tertiary sediments were exposed. Eroded detritus could have been transported to the shelf edge by ice sheets. Sediment-laden melt water debauching from the ice-sheet grounding line may have created low-angle erosional unconformities in the middle-slope deposits and may have initiated mass flow that moved downslope towards Wegener Canyon across the mid-slope bench. The smectite-horizons found at ODP Site 693 would represent overbank deposition. The unconformities and sequence boundaries identified on seismic sections on the slope off Cape Norvegia - outside the immediate influence of the glacial prograding wedge deposits - are therefore probably directly related to processes of ice-sheet expansion.

INTRODUCTION

The cryospheric, palaeoceanographic and palaeoclimatic development of Antarctica are basic components of an understanding of the important role of this continent in the functioning of the world's climate system. Despite increased interest and strenuous efforts, however, our present knowledge of Antarctica's glacial history still suffers from sincere inconsistencies (e.g. Webb, 1990; Barker, 1995). Quite surprisingly, this knowledge is based mainly on low-latitude proxy data: oxygen isotope ratio measurements on deep-ocean sediments and records of eustatic sea-level changes from the world's continental margins. However, these inferences are ambiguous, and in disagreement. For example, there is still dispute over whether the principal increase in Antarctic ice volume, as interpreted from these low-latitude oxygen isotopic records, occurred at about 36 Ma, at 16-13 Ma or only after about 3 Ma. Within these various scenarios, assumptions have been made about the constancy of equatorial surface temperatures, or about the high-latitude surface origins and temperatures of intermediate to deep waters at low latitudes, that may be incorrect. Similarly, changes in continental ice volume provide the only generally-accepted, repeatable, rapid-acting cause for global eustatic sea-level change, yet the timing and amplitudes of sea-level change adduced from low-latitude margin sediments are disputed, and occur also at times when there is no independent evidence for the existence of substantial volumes of continental ice on Antarctica or elsewhere. Further, the isotopic and sea-level estimates of grounded ice volume disagree substantially with each other, at both long and short periods, throughout most of the Cenozoic. Onshore Antarctic evidence of glacial history is sparse, and is also presently controversial (e.g. Webb et al., 1984; Burckle & Potter, 1996): argument therefore continues as to when the Antarctic ice sheet came into existence, how and when it grew, and how stable it has been.

Ice cores through large continental ice sheets can help to resolve the problem, albeit only to a certain extent. Such ice cores (e.g. the GRIP and GISP2 cores in Greenland or the VOSTOK core in East Antarctica) have clearly demonstrated that snow accumulating continuously in large continental areas in high-latitudes can record changes of the climate system quite accurately (Lorius et al., 1985; Jouzel et al., 1987; GRIP Project Members, 1993; Dansgaard et al., 1993; Grootes, et al., 1993). These climate records can be determined from a number of proxy indicators: oxygen isotope ratios of enclosed air bubbles indicate continental ice volume variations, deuterium content indicates temperature variations, etc. The timing of these climate changes can be derived by various dating techniques (by extrapolating

precipitation models, magnetostratigraphic dating of dust particles,...), although most are far from absolute. But ice sheets are not simply passive piles of snow... under the pressure of the accumulating snow, the ice starts to deform and to flow in the direction of the margins of the continent. It takes about 150.000 to 200.000 years for the ice within the Greenland ice sheet to flow from the centre of the continent to the sea, and for the East Antarctic Ice Sheet (EAIS) estimates of 500.000 years or more have been advanced. This implies that the record of climate change to be extracted from such ice cores through the EAIS - i.e. the EPICA effort - can not extend far beyond that time period.

The sediments that have accumulated along the Antarctic continental margins and in the peri-Antarctic oceanic basins also contain a record that reveals details of the cryospheric development of the adjacent continent, and this record extends much further into time than the ice record does - often tens or even hundreds of million years. This marine geological record of climate change consists of two types of information:

1. ***Proxy data that are contained within the deep-sea sediments***, such as oxygen isotope ratios of benthic foraminifera indicating continental ice volume and temperature variations, down-core variations in ice-rafted debris (IRD) indicating variations in icebergs dynamics, specific clay mineral assemblages relating to the weathering processes acting on the continent, deep-sea hiatuses suggesting changes in bottom current activity, etc. Dating of these deep-sea sediment records can be achieved by using a combination of various classical techniques (biostratigraphy, magnetostratigraphy, etc.). The proxy data and the age information can, however, only be retrieved by means of high-resolution deep oceanic drilling (an endeavour requiring major logistic facilities), or by high-quality shallow coring (easier to perform, but providing a record that is very much limited in time, to usually not much more than one climatic cycle).
2. ***Direct data from the Antarctic margin sediments***. The sediments deposited on the outer shelves and slopes surrounding the Antarctic continent differ significantly in composition, texture and spatial organisation when deposited by glacially controlled processes from the sediments deposited under pre-, non- or interglacial conditions. These differences are explained and can be predicted by using glacial sediment transport and deposition models, although debate still continues as to which depositional processes can be read from the sedimentary record and as to in what extent they can be directly related to glacial processes: Anderson et al. (1983), King & Fader (1986), King et al. (1987), Alley et al. (1989), Larter & Barker (1989), Vorren et al. (1989), Boulton (1990), Bartek et

al. (1991), Cooper et al. (1991), Larter & Barker (1991), Kuvaas & Kristoffersen (1991), Anderson & Bartek (1992), Larter & Cunningham (1993), Eitreim et al. (1995), Vanneste (1995), Bart & Anderson (1996), etc. The required information can be retrieved - in a first approximation and in a qualitative way - by imaging these deposits using high-resolution seismic techniques, and - eventually, in a more quantitative approach - by drilling them at carefully selected sites, and by analysing composition, texture and age.

The principal scientific objective of ANTOSTRAT - the "Antarctic Offshore Acoustic Stratigraphy" Project, set up in 1989 by SCAR (Cooper & Webb, 1994) - is to extract Antarctica's Cenozoic glacial history from the sediments of its continental margins, principally by using seismic stratigraphy - where possible calibrated by coring or borehole evidence - and by applying the above-mentioned glacial and glacial-marine sedimentation models. The present report summarises the Belgian research efforts and scientific contribution to ANTOSTRAT, with seismic-stratigraphic studies of various portions of the Antarctic continental margin, and addressing also depositional environments (i.e. foot-of-slope and basin-floor systems) that are normally not included in the currently existing glacial sedimentation models. Four main study areas were addressed in the past years:

- The Trinity Peninsula and South Shetland Islands margins of central Bransfield Basin, along the Antarctic Peninsula;
- The West-Antarctic continental margins of the Amundsen and Bellingshausen Seas;
- The East-Antarctic continental margin of the North-eastern Weddell Sea;
- The East-Antarctic continental margin of the southern Weddell Sea (De Batist et al., 1993).

They are situated along portions of the Antarctic continental margin that exhibit different characteristics, such as different glacial regimes and glacial evolution (West-Antarctica as opposed to East-Antarctica), different depositional processes and environments (semi-enclosed basins, quasi-starved distal glacial-marine environments, deep-sea fan and turbidite environments, etc.), different preservation potential (subsiding shelf edge in Bransfield Basin as opposed to stable shelf edges in Weddell Sea or along the Amundsen-Bellingshausen margin), etc.

GLACIAL-INTERGLACIAL SEISMIC STRATIGRAPHY OF CENTRAL BRANSFIELD BASIN

1. INTRODUCTION

In 1987, a marine-geophysical expedition to the Antarctic Peninsula was jointly carried out by RCMG, AWI and the University of Kiel on board of F.S. POLARSTERN: the ANT VI/2 survey. Part of the seismic data of that survey was acquired in Bransfield Basin, a semi-confined back-arc basin at the northern tip of the Antarctic Peninsula. The results of this expedition have been published in a.o. Meissner et al. (1988), Henriet et al. (1989), GRAPE TEAM (1990) and Henriet et al. (1992).

In December 1993, RCMG returned to Bransfield Basin during the marine-geophysical GEBRA-93 survey (Canals et al., 1994), carried out in co-operation with the University of Barcelona, the Institute of Marine Sciences (Barcelona), the Spanish Institute of Oceanography (Madrid) and the University of Salamanca. Various types of data were collected in the central and eastern sub-basins : swath bathymetry and sea-floor imaging, seismic and parametric sub-bottom profiles and magnetic profiles.

This report focuses on the analysis of the reflection seismic and bathymetry data for the study of the basin's sedimentary infill as a record of its geodynamic evolution and of its Plio-Pleistocene glacial history. It is largely based on two of the papers that have emanated from the Belgian-Spanish co-operation during the GEBRA-93 survey (Gràcia et al., 1996; Prieto et al., in press) with additional insights from Vermeiren (1995).

2. GENERAL GEOLOGICAL SETTING

Bransfield Basin is a narrow and elongated, semi-confined back-arc basin at the northern tip of the Antarctic Peninsula, in a geodynamically complex setting of numerous microplates (Figure 1). It is located behind the subduction zone of the South Shetland Trench, and it is bounded by the South Shetland Islands to the North, Trinity Peninsula to the South, the prolongation of Hero Fracture Zone to the

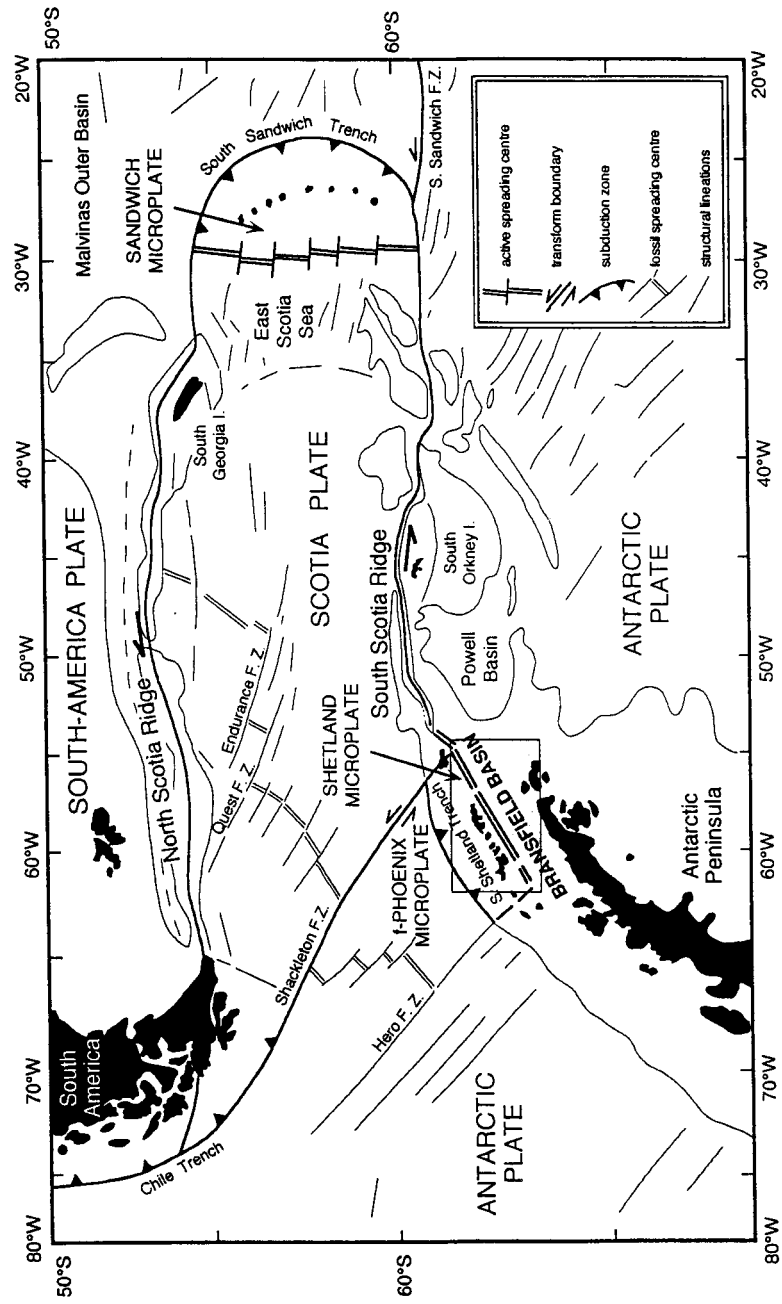

Figure 1. *Present-day tectonic setting of the Scotia Arc and the north-western Antarctic Peninsula regions, interpreted from GEOSAT satellite data. The GEBRA-93 study area is indicated by the shaded box.*

West, and the prolongation of Shackleton Fracture Zone to the East. The basin formed primarily by extensional thinning and rifting within the northern Antarctic Peninsula arc system, in response to the sinking of the Phoenix-Antarctic oceanic plate into the South Shetland Trench under the influence of its own weight (Roach, 1978). Previously, active subduction of the Phoenix Plate in the South Shetland Trench had been controlled by spreading on the Antarctic-Phoenix Ridge. This spreading ceased at 4.0 Ma (Barker, 1982; Barker & Dalziel, 1983). Cessation of spreading caused northwest migration of the trench (so-called "trench roll-back") and activated the associated intra-arc extension that created Bransfield Basin. Despite uncertainties regarding the timing of initial rifting, there is enough evidence (e.g. volcanic activity, seismicity, heat flow, magnetic anomalies, rock samples,...) to indicate that Bransfield Basin is a young and active rift basin (e.g. Keller et al., 1992).

Bransfield Basin, over 100 km wide and about 450 km long, is asymmetric with a deep axial zone juxtaposed to the South Shetland Islands (Jeffers & Anderson, 1991; Jeffers et al., 1991). The basin is subdivided into three sub-basins : the western, central and eastern sub-basins. Sub-basin boundaries appear to be aligned with the projection of fracture zones affecting the extinct Antarctic-Phoenix Ridge.

Gamboa & Maldonado (1991) and González-Ferrán (1991) presented evidence for numerous sub-aqueous volcanic centers intruding into and through thinned continental crust and forming a discontinuous chain within the rift's axis and on its western flank. A detailed morphostructural analysis of the volcanic edifices outcropping along this volcanic chain, correlated with petrological and geochemical data (Keller & Fisk, 1992), illustrates initial phases of back-arc sea-floor spreading (Gràcia et al., 1996). Intermittent eruptions of viscous volcanics and lava's eventually led to growth and subsequent sub-aerial exposure of Bridgeman and Deception Islands.

3. MATERIALS AND METHODS

A regional grid of 1100 km of single-channel reflection seismic profiles (16 profiles) was acquired in the central sub-basin of Bransfield Strait in December 1993 during the GEBRA-93 survey on board of B.I.O. HESPERIDES. The profiles - shot in dip and strike orientations with respect to the basin's main structural trend - cover the central basin floor and the outer shelf of the South Shetland and Trinity Peninsula margins (Figure 2). The seismic data were acquired using a 2.9 l BOLT 1500C

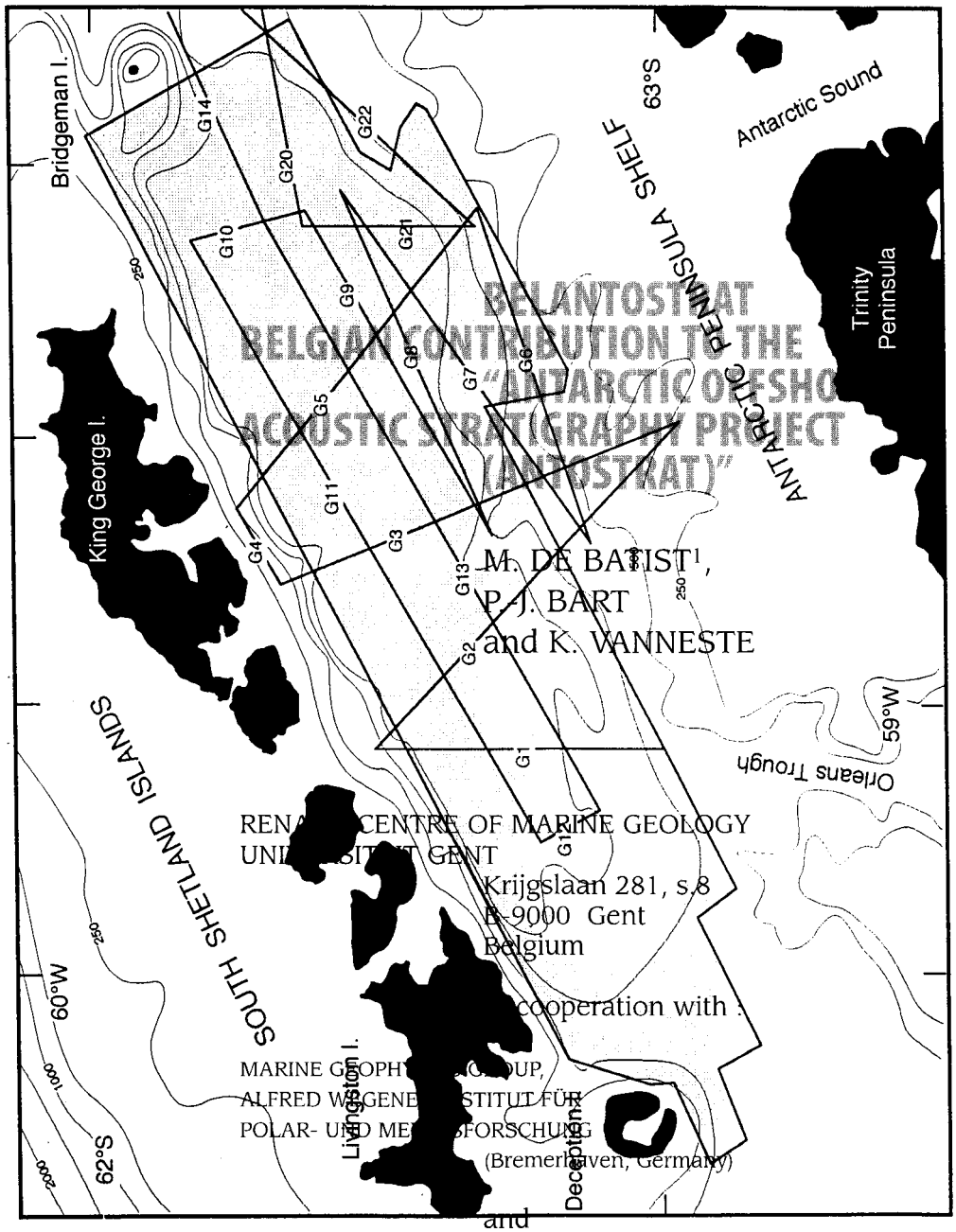

Figure 2. *Location map of the area surveyed with full swath bathymetry coverage and of the grid of high-resolution reflection seismic profiles recorded during the GEBRA-93 survey in the central sub-basin of Bransfield Strait.*

[1] Corresponding author E-mail : marc.debatist@rug.ac.be

airgun operated at 140 bar. Cable length of the SIG 120 streamer, used in a single-channel mode, was 150 m. The data were recorded digitally and processed on-line with RCMG's high-resolution ELICS DELPH2 seismic acquisition system. An EPC recorder provided analog paper records. Post-acquisition data processing, including bandpass- and deco-filtering, scaling, etc., was carried out at RCMG on both the DELPH2 and the PHOENIX VECTOR processing systems. This resulted in profiles with an excellent resolution (about 5 ms) and with a penetration in excess of 1.0 s TWT.

Swath bathymetry data were acquired over an area of 10.000 km^2 (Figure 2), between Bridgeman and Deception Island, using the combined SIMRAD EM12/EM1000 system of B.I.O. HESPERIDES. The survey completely covers the Trinity Peninsula margin from the upper slope down to the basin floor, and the slope of the South Shetland Islands margin. Post-processing of the swath bathymetry data was carried out at the Instituto de Ciencias del Mar (Barcelona).

4. SEA-FLOOR MORPHOLOGY

The swath bathymetry map (Gràcia et al., 1996) shows the main morphostructural characteristics of the surveyed area (Figure 3), and it reveals morphological features previously unknown or imprecisely known.

Central Bransfield Basin, from the South Shetland Islands slope to the Trinity Peninsula slope, is 230 km long, 60 km wide, and reaches a maximum depth of 1950 m in the King George Basin.

BAS (1985) and Jeffers & Anderson (1991) showed that the Trinity Peninsula continental margin is characterised by a broad shelf incised by several large-scale glacial troughs. The presence, position and morphology of these troughs could not be confirmed by these new data, because the coverage did not extend far enough onto the shelf.

The Trinity Peninsula continental margin is also characterised by a complex slope composed of several terraces at different bathymetric levels. The upper slope shows a main terrace, 700 to 800 m deep, with a slope break located at 800 m. Locally, a second terrace is present, which deepens gradually from 1000 to 1400 m. The average inclination measured from the upper terrace to the base of the slope

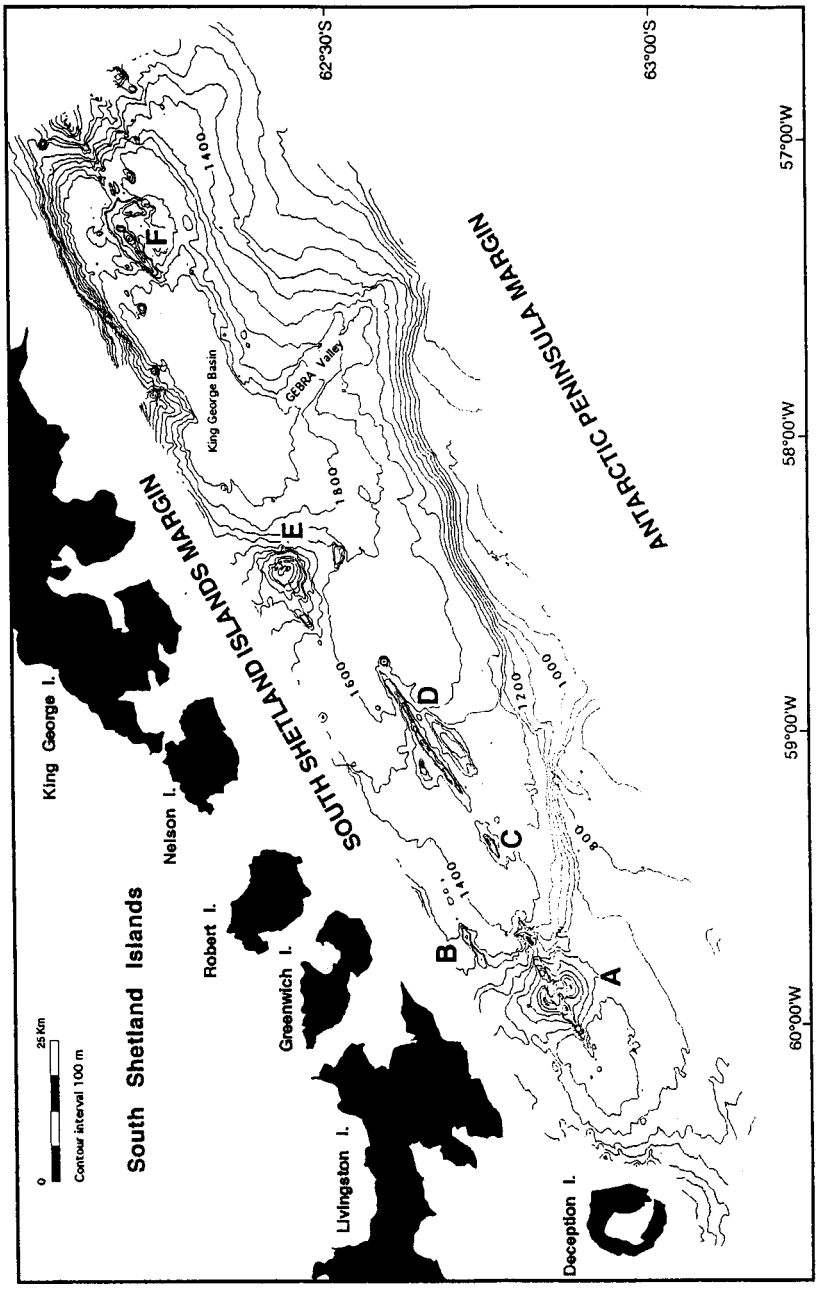

Figure 3. *Full-coverage swath bathymetry map of the central sub-basin of Bransfield Strait. Contour interval: 100 m. Labels A to F indicate the volcanic edifices rising above the basin floor.*

ranges from 8.5° in the central part, to 3.2° and 2.0° at the extremities of the Trinity Peninsula margin. Ice scours of about 40 m deep, produced by calved icebergs, are distinguished on the upper terrace to depths of up to 800 m.

A wide sub-marine valley has been found cutting into the slope, from the slope break at 800 m down to the basin floor. This valley, named Gebra Valley (Canals et al., 1994), has been mapped completely. It is 30 km long and is characterised by a 6 km wide, flat thalweg bordered by walls of up to 200 m high. Small isolated mounds and rises are distinguished within Gebra Valley, at the base of the slope.

Off the South Shetland Islands, only a narrow part of the margin has been surveyed with swath bathymetry. These data confirm that continental shelf adjacent to the islands is narrow, and that the slope is very steep. Very abrupt slope profiles of up to 14° were observed. In addition, the seismic lines show that the slope gradient becomes lower towards the southwest (e.g. 5.8° mean gradient on line G2). At some places, the slope presents a step-like morphology, facing the centre of the basin, and forming a small terrace at depths of about 750 m. Seismic lines also show that the narrow shelf at 300 m depth, is incised perpendicularly by troughs of up to 250 m deep.

The central part of the basin progressively deepens and widens towards the northeast. In a SW-NE direction, four bathymetric levels or terraces are distinguished (Gràcia et al., 1996). King George Basin constitutes the largest and deepest of these terraces, 20 km wide and 50 km long. Each terrace is bounded by NW-SE-trending morphological steps.

Linked to these morphological steps, the most striking features of the Central Bransfield Basin appear (Figure 3): six large volcanic edifices (labelled A to F) that rise above the sea floor and form a discontinuous lineament from Deception Island to Bridgeman Island (Gràcia et al., 1996). The shapes of these seamounts vary from circular to elongated. The largest circular and semi-circular seamounts (A and E) have basal diameters of more than 16 km and heights of about 550 m above the surrounding sea floor. The ridges (B, C and D) are 10 to 30 km long, 250 to 350 m high, and trend N55 to N60. In addition, numerous other small, isolated volcanic cones, 2.5 km wide and up to 400 m high, are scattered over the basin floor. All the volcanic edifices are concentrated in a narrow zone between the South Shetland Islands margin and the Deception/Bridgeman line. Gràcia et al. (1996) interpret the

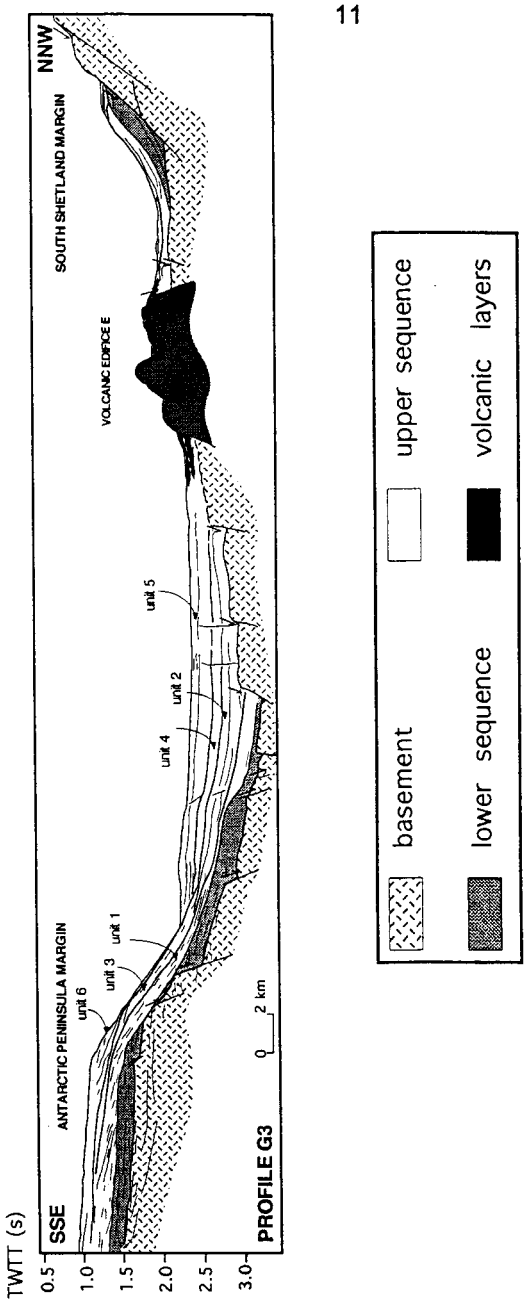

Figure 4. *Interpreted seismic profile G3, showing the acoustic basement, the lower sequence and the six sedimentary units that compose the upper sequence in the Trinity Peninsula margin. The graben-like structure between the margin and the volcanic edifice E allows the deposition of thick basin-floor units. The South Shetland Islands margin shows a step-like morphology, formed by seaward-facing faults, with a narrow hanging platform.*

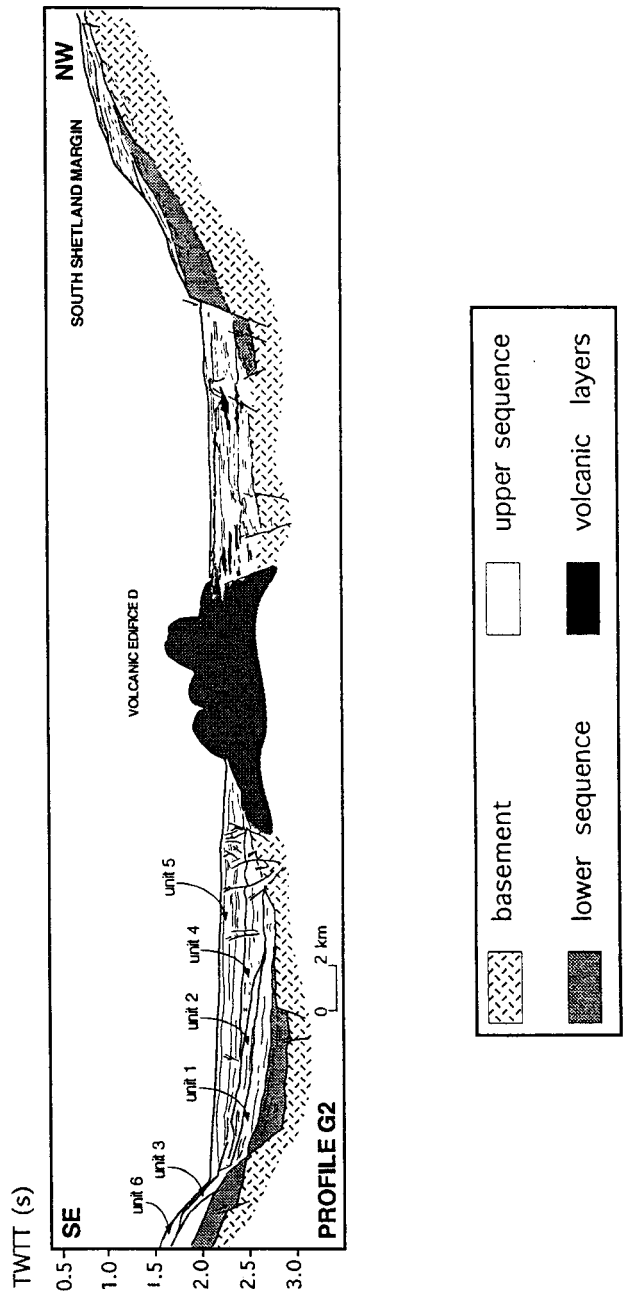

Figure 5. *Interpreted seismic profile G2, showing significant erosion surfaces in the Trinity Peninsula margin and within the basin-floor units. The South Shetland Islands margin deepens gently. Faults, interstratified lavas and laccoliths between the South Shetland Islands margin and the axial volcano disturb the original configuration of the sediments.*

different shapes and sizes of the large volcanic edifices in terms of successive evolutionary stages of incipient sea-floor spreading.

5. GENERAL SEISMIC STRATIGRAPHY

The seismic reflection data of the Trinity Peninsula margin, the South Shetland Islands margin and the central basin floor reveal the presence of an acoustic basement and a sedimentary cover (Figures 4 and 5). The sedimentary cover can be subdivided into two major sequences: a lower, faulted and folded sequence, and an upper sequence, only slightly affected by faulting and composed of six sedimentary units. The lateral continuity of these units in the basin centre is interrupted by the volcanic edifices. The main seismic characteristics of these different units are described in the following paragraphs.

Acoustic basement. Below the Trinity Peninsula margin, the seismic facies of the acoustic basement is made of high-amplitude, low-frequency, and medium- to poor-continuity reflections. Divergent stratified seismic facies configurations are indicative for a sedimentary nature. The top of the acoustic basement is a pronounced erosion surface. Basinward, the acoustic basement is separated from the laterally continuous, horizontal reflections above by a highly reflective surface. Below this surface, the basement shows a chaotic configuration with high-frequency, low-continuity reflections. These characteristics seem to indicate a crystalline nature.

Lower sequence. Over the basement, a strongly tectonised sedimentary sequence can be distinguished from the main platform to the basin floor. This unit shows stratified, semi-transparent seismic facies with reflections whose continuity and amplitude increase in basinward direction. The top of this sequence is a pronounced erosion surface.

Upper sequence. A complex upper sequence overlies this erosion surface. It is made up of six seismic units, that are numbered from 1 to 6 from base to top. This sequence is particularly well-developed along the Trinity Peninsula margin and on the central basin floor. The spatial position of each seismic unit within the basin, and its relationship with the surrounding units, allows two types of sedimentary units to be distinguished.

Upper-slope units. These units extend from the Trinity Peninsula main platform down to the base of the slope. They show a prograding to aggrading semi-

transparent seismic facies with high-frequency, low-continuity reflections.

Basin-floor units. These units are essentially confined to the central basin floor and pinch out (onlap) towards the foot of the slope. In the centre of the basin, they show a laterally continuous, stratified seismic facies with low-frequency, high-amplitude reflections. Landward and near the seamounts, they often change into a chaotic or semi-transparent seismic facies.

Volcanic edifices. The basin-floor seamounts are characterised by a chaotic seismic facies, with very low-continuity and high-energy reflections. Faulting has been observed in the vicinity of the volcanic edifices, as well as a number of short, flat or undulating high-amplitude reflections extending from the edifices into the surrounding basin fill (Figures 4 and 5). These could be interpreted as volcaniclastic layers (Carey & Sigurdsson, 1984) or inter-stratified lava flows. Locally, a number of buried, chaotic, mounded features have been observed. They are about 1 km long and 200 ms TWTT thick. Their upper boundaries are highly reflective surfaces. They are attributed to volcanic material (laccoliths) that did not extrude out onto the sea floor.

6. ARCHITECTURE OF THE TRINITY PENINSULA MARGIN

6.1 The upper-slope area

Acoustic basement. At some places in the main terrace, at about 700-800 m, outcropping acoustic basement forms slightly landward-dipping sub-terraces. Further downslope, the basement becomes progressively covered by the sedimentary wedge forming the Trinity Peninsula continental margin. Further into the basin, towards the basin centre, the basement deepens through a number of steep normal faults.

Lower sequence. The lower sequence extends over the basement from the upper slope, where it is generally thin (100 ms TWTT), to the centre of the basin, where it pinches out against the basement (Figures 4 and 5).

Upper sequence. The upper sequence forms a complex progradational package on the upper slope. It is composed of three sedimentary units (numbered 1, 3 and 6), that are bounded at the top by erosive surfaces (Figure 4). Unit 1 overlies the lower sequence from the upper slope to the centre of the basin. Further in the

basin centre, the underlying sequence pinches out and unit 1 directly covers the basement. Unit 3 is locally very thin or missing, a situation which appears to be related to the strong erosion at its top. Unit 6 forms the present-day sea floor, with a distinct slope break at about 800 m. These sedimentary units of the upper sequence form a nearly continuous cover along the entire upper slope, except in areas where they have been removed by erosion. Locally, a 75 m high mounded feature is distinguished between Units 3 and 6. The internal reflections in this mound are dipping in a landward direction.

6.2 The base-of-slope area

Lower sequence. The lower sequence reaches its maximum observed thickness of 400 ms TWTT in the area at the base of the slope. Laterally, it thins progressively towards both the northeast and the southwest, and finally disappears. It is partially affected by normal faulting and some internal unconformities can be distinguished within this sequence.

Upper sequence. Within the upper sequence, the upper-slope units (pinching out by downlap in basinward direction) meet the basin-floor units (pinching out by onlap in slopeward direction) at the base of the slope, thus forming a complex interfingering pattern.

At the base of the slope, the Gebra Valley clearly shows distinct asymmetric features. The eastern flank has a noticeable aggradational component with some internal erosional surfaces, whereas the western flank shows a 4 km wide levee and small distal lobes with heights not exceeding 75 m. Irregular, chaotic masses along the thalweg of Gebra Valley may indicate present-day slope instabilities.

6.3 The basin floor area

Acoustic basement. Between the base of the slope and the seamount chain in the centre of the basin, the basement deepens by normal faulting and develops into a narrow graben structure, trending parallel to the Trinity Peninsula margin (Figures 4 and 5). The basement also deepens in a direction parallel to the basin axis, from 2.6 s TWTT in the southwest to 3.3 s TWTT in the northeast. This along-axis deepening is related to the morphological steps observed in the sea-floor morphology.

Lower sequence. The thickness of the total sedimentary cover decreases from south0west to north0east, from about 750 ms TWTT to about 650 ms TWTT. The lower sequence, which is overlying the basement, is mostly made of seaward-dipping reflections, although locally, over tilted basement blocks, landward-dipping reflections can also be observed.

Upper sequence. Within the upper sequence, Unit 1 downlaps the underlying sequence and, more distally, the basement. Unit 2 and unit 4 extend from the base of the slope, where they onlap the toes of the upper slope units (Figure 4), to the volcanic edifices. Unit 5 overlies the former units. The Gebra Valley opens to a flat basin floor without any evidence of the large-scale deposits that would be expected at the mouth of such a major submarine valley. Near the volcanic edifices, a series of faults and fractures affect all basin floor units of the upper sequence.

7. ARCHITECTURE OF THE SOUTH SHETLAND ISLANDS MARGIN

7.1 The upper-slope area

Acoustic basement. The acoustic basement outcrops at the sea floor all along the South Shetland Islands margin, as it does in the Trinity Peninsula main terrace. Its seismic facies suggests a sedimentary nature.

The sedimentary cover along the South Shetland Islands upper slope is relatively thin (maximum observed thickness of 300 ms TWTT) and changes both in thickness and seismic facies character over short distances. These variations seem to be related to the fracturation of the margin, caused by the interplay of an along-margin normal fault and a svstem of other, normal faults joining and branching off along the margin.

Lower sequence. The lower sequence has a progradational character and pinches out (downlap) against the basement at the base of the slope.

Upper sequence. The upper sequence is continuous where the margin exhibits a step-like morphology and discontinuous where it deepens gradually towards the basin floor. This discontinuous character is attributed to erosion and margin fracturation. In front of King George Island, a flat narrow platform can be observed, with a 100 ms TWTT thick sedimentary cover characterised by an aggradational

pattern. This platform occurs at a depth of 750 m and has a width of around 1 km. It forms a hanging terrace and is limited by normal faults that have shaped this part of the margin into a step-like morphology (Figure 4). Towards the west, the slope develops into a gentler, but continuous feature deepening into the basin (Figure 5).

7.2 The base-of-slope area

The interfingering between upper-slope and basin-floor units, as observed along the Trinity Peninsula margin, has not been shown in the South Shetland Islands margin. Here, the lower sequence is onlapped by the basin-floor units of the upper sequence at the foot of the slope, where also some irregular mounded features, characterised by a chaotic seismic facies, indicate the abundant presence of slides, slumps and/or debris flow deposits.

7.3 The basin floor area

Scattered volcanism and faulting in the area between the axial seamounts and the South Shetland Islands margin impede seismic correlation of the sedimentary units along and across the basin. Nevertheless, what can be observed is that the basement deepens from 2.6 to 3.1 s TWTT in a SW-NE direction. The sedimentary cover is 0.5 s TWTT thick, and can be sub-divided into two parts. The lower part of the section is composed of high-frequency and high-amplitude reflections of medium continuity - characteristics that appear to be caused by the intrusion of sills and the presence of interbedded lava flows (Figure 5). The upper part of the section is characterised by a semi-transparent seismic facies, the uppermost portion of which is again well-stratified. Only this upper part of the section, with a total thickness of around 0.2 s TWTT, can be correlated to the youngest sedimentary unit associated with the Trinity Peninsula margin.

8. DISCUSSION

8.1 General seismic stratigraphy in relation to basin development

The geometry, distribution and architecture of the observed seismic-stratigraphic units allow us to attribute them to pre-rift, syn-rift and post-rift episodes

of the basin development.

- The acoustic basement of the Trinity Peninsula and South Shetland Islands margins, which appears to be of sedimentary nature, can be attributed to the pre-rift episode. It is probably composed of the meta-sediments of the Trinity Peninsula Group (Trinity Peninsula margin) and Myers Bluff Formation (South Shetland Islands margin), which are believed to be stratigraphically more or less correlative (Aitkenhead, 1975; Hyden & Tanner, 1981).
- The lower sedimentary sequence is characterised by internal unconformities and a local distribution. It is affected by normal faulting, and limited at the top by an unconformity of regional importance. Based on these observations, we attribute these strata to the syn-rift episode. As such, it is probably equivalent to the "rift" sequence identified by Gamboa & Maldonado (1991).
- The upper sedimentary sequence is characterised by wedge-shaped, progradational geometries on the slopes and by aggrading geometries on the basin floor, both generally less affected by faulting. These configurations have also been reported by e.g. Banfield & Anderson (1995). We attribute these deposits entirely to the post-rift episode, and as such they are probably equivalent to the "drift" sequence of Gamboa & Maldonado (1991).

Faulting and volcanism seem to exert an important influence on the distribution and seismic characteristics of the seismic-stratigraphic units as well as on their structural configuration, both in the Trinity Peninsula and South Shetland Islands margins. The along-basin trending (N55-N60) normal faults are responsible for determining the rift-like structure and the opening of the basin. The morphological steps that have been observed on the bathymetric data and that progressively deepen the sea floor towards the north-east have been interpreted from the seismic data as the surface expression of N145-trending normal faults. These faults also offset the acoustic basement, which deepens towards the north-east, from 2.6 s TWTT to 3.3 s TWTT in the King George Basin. Both sets of faults define the overall basin structure. The deepening and widening of the basin towards the north-east, which is expressed both by the surface morphology and the deep structure, may be explained as a progressive increase in basin maturity in that direction.

The volcanic edifices divide the basin floor into two separated depocentres. However, the role of the seamounts as a sedimentary barrier, as suggested previously by Jeffers & Anderson (1991), is only partial, as shown by the correlation of the youngest basin-floor unit (unit 5) from the Trinity Peninsula margin to the South Shetland Islands margin. A narrow band of deformation is observed close to

the volcanic edifices and interpreted as neotectonic features related to the present-day basin extension.

8.2 Seismic-stratigraphic record of glacial history

The shelf morphology. The overdeepened and irregular topography of the Trinity Peninsula and South Shetland platforms suggests that they were shaped by ice sheet erosion.

The shelf deposits. Banfield & Anderson (1995) report the presence of a mound- or ridge-like feature on the middle shelf of the Trinity Peninsula margin, and they interpret it as a grounding-zone deposit marking the seaward extent of the most recent glacial grounding event, for which they propose a minimum age of 13500 to 14500 years BP on basis of two radiocarbon ages (Figure 6). This would imply that during this most recent glacial grounding event (last glacial maximum ?) the ice sheets did not extend all the way to the shelf edge, but only reached the middle shelf area, which would confirm previously published hypotheses on the relatively limited extent and importance of the last glacial maximum (St.John & Sugden, 1971; Payne et al., 1989). The same feature - a 75 m high mound with landward-dipping internal reflections - is observed on the GEBRA-data. However, seismic-stratigraphic analysis suggests that this mound, which clearly overlies Unit 3, appears to be partly covered along its seaward side by deposits of Unit 6. The feature can therefore not be interpreted to represent the most recent glacial grounding event, but must be attributed to an older one. This raises questions about the preservation potential of such grounding-zone deposits during following and more drastic glacial phases. Nevertheless, the observation of the widespread glacial unconformities observed within the top part of the prograding upper-slope wedges suggests that the preservation potential of the shelf deposits is very limited, and that the record of glacial history contained within the shelf deposits may be only fragmentary.

The prograding upper-slope wedges. There is a general consensus that grounded ice sheets are - in one way or another - responsible for the deposition of prograding sequences along glaciated continental margins. This is thought to be true as well for the prograding sequences identified along the Trinity Peninsula and the South Shetland Islands margins.

The prograding upper-slope wedge along the Trinity Peninsula margin is composed on a regional scale of three sedimentary units (numbered 1, 3 and 6).

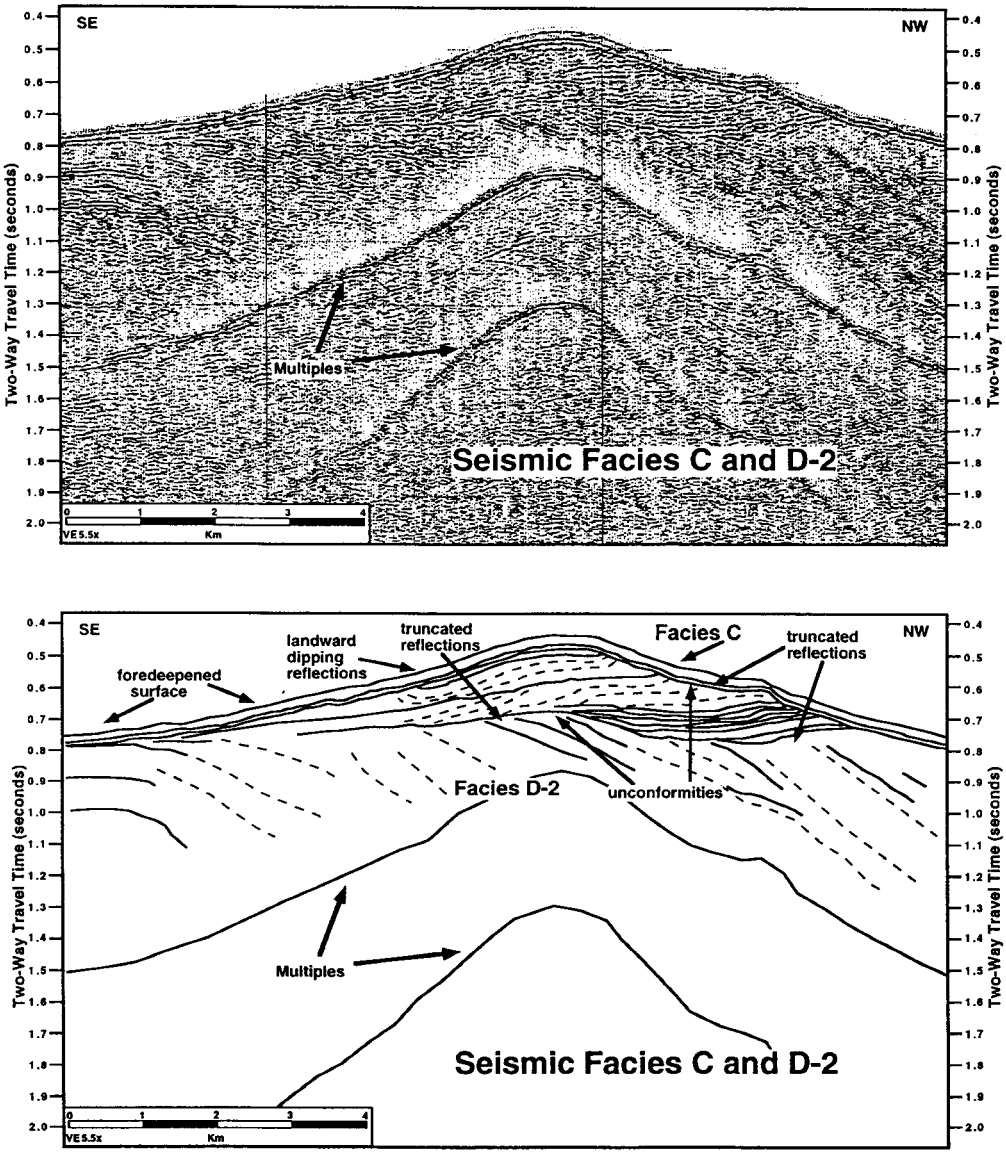

Figure 6. *Seismic profile showing a grounding-zone deposit on the Trinity Peninsula shelf. This ridge-shaped feature marks the seaward extent of a glacial grounding event (from Banfield & Anderson, 1995).*

Each prograding unit is truncated by an erosional unconformity, that has all the characteristics of a glacial unconformity (Bart & Anderson, 1995). The presence of these erosive surfaces, the pronounced prograding wedge shape and the confinement of the units to the upper-slope domain, all suggest that these deposits were formed during periods when ice-sheets had advanced all the way to the shelf edge. This hypothesis was recently also proposed by Banfield & Anderson (1995), who observed the same configurations and number of units on seismic data of comparable resolution. This implies that the investigated upper-slope deposits along the Trinity Peninsula margin contain resolvable records of at least three periods - since the Pliocene, beginning of the opening of Bransfield Basin - during which ice sheets advanced to the shelf edge for a significant amount of time.

Along the Trinity Peninsula margin, Unit 1 progrades down from the Trinity Peninsula upper slope and reaches the basin floor up to 12-15 km seaward from the upper terrace. In contrast, prograding units along the South Shetland Islands margin hardly reach the base of the slope. This observation can be interpreted in terms of volume of ice-sheets and size of the source areas delivering the terrigenous sediments to the prograding wedges: the Trinity Peninsula ice-sheets are much larger than the ice-caps of the South Shetland Islands. Perhaps most of the ice drainage from the South Shetland Islands and associated glacial sediments are captured within drainage systems that flow toward the Pacific Ocean rather than toward Bransfield Basin. Jeffers & Anderson (1991) show that the South Shetland's Pacific margin is quite broad and composed of at least four progradational units. However, the age of these units is not constrained to be post-Pliocene in age as are those of the Bransfield Basin.

Lateral changes in thickness of the upper-slope prograding wedges, as observed by Vermeiren (1995), suggest that in fact there is great lateral variability in the magnitude of slope progradation during a glacial period. On basis of conventional resolution seismic records, Larter & Barker (1989) concluded that slope progradation is a line source phenomenon on the Antarctic Peninsula's Pacific margin to the south of Hero Fracture Zone. This clearly does not apply to the high-resolution seismic data from Bransfield Basin, where the magnitude of slope progradation is apparently controlled by sediment supply associated with individual glacial troughs.

The basin-floor deposits. Banfield & Anderson (1995) show, using piston-core evidence, that during the present-day, interglacial stage little terrigenous sediment is transported off the continental shelf and slope, and that sedimentation occurs mainly

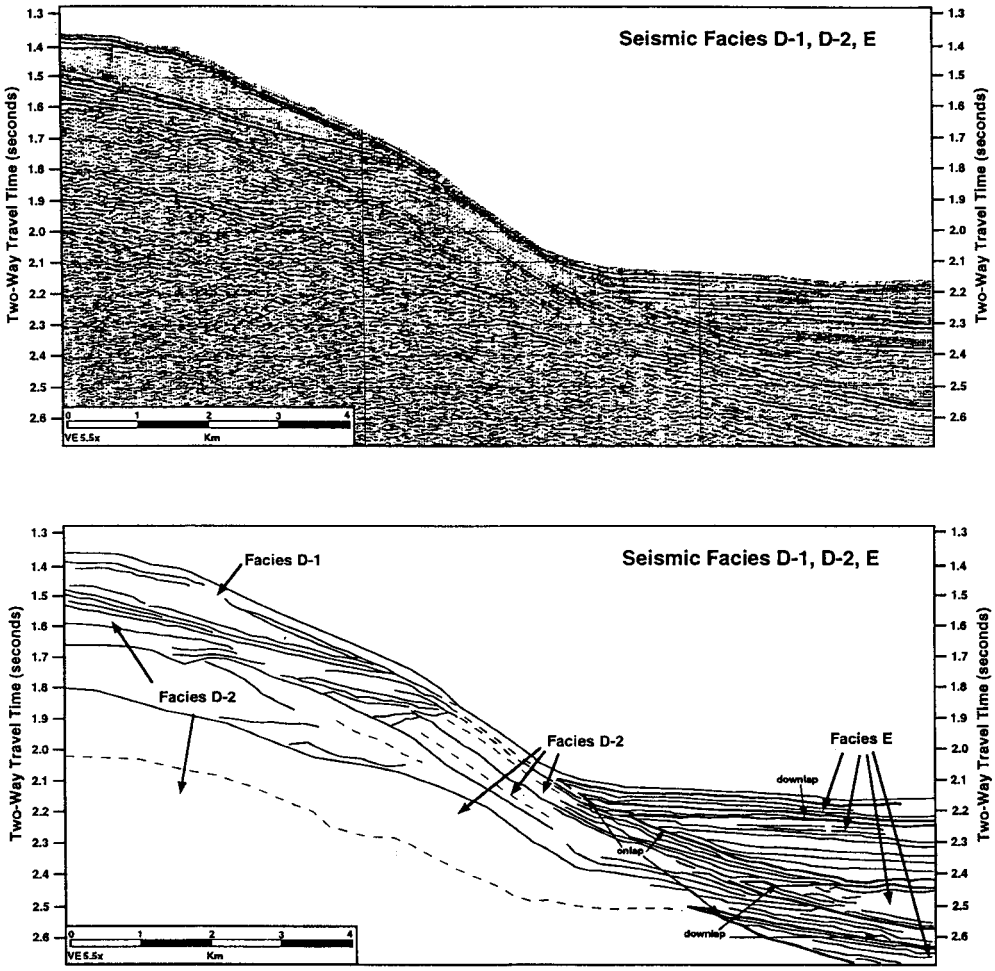

Figure 7. *Seismic profile showing the relationship between the slope and basinal deposits at the foot of the Trinity Peninsula slope (from Banfield & Anderson, 1995).*

by pelagic or hemipelagic processes forming thin drape deposits. They believe that the same applies also to older interglacial phases, although they find no seismic evidence in the basin-floor sedimentary record for drape deposits associated with such older interglacial phases. This is attributed to resolution constraints of the seismic technique. In the light of their observations, Banfield & Anderson (1995) propose that the basin-floor units have been deposited essentially during glacial episodes as distal equivalents of the prograding upper-slope wedge, and that they are composed of proglacial fan deposits formed by debris flow processes. The presence of debris-deposits and slope instability phenomena is suggested on the GEBRA-data by the irregular features with chaotic internal reflection configuration at the foot of the slope, by the physiography of the Gebra Valley and by the small mounded lobes.

Analysis of the GEBRA-data show that the seismic stratigraphy in the basin floor area is characterised by the basinward-directed downlap of the Trinity Peninsula slope units and by the onlap of the toes of these units by the basin-floor units, thus creating a typical interfingering "christmas-tree" configuration (Figures 4 and 5). This was also observed by Banfield & Anderson (1995), although they did not comment much on this observation (Figure 7). Nevertheless, it clearly suggests an out-of-phase relationship between deposition of the upper-slope wedges and deposition of the basin-floor units. This implies that sedimentation on the basin floor must either pre-date or post-date the glacial phase. This is in contradiction to the model proposed by Banfield & Anderson (1995).

As a general rule, the basin-fill deposits seem to be slightly thicker in front of the mouths of the troughs carved into the shelf of the Trinity Peninsula Margin. In these places the ice-stream activity would have been especially notable. This effect can be seen towards the south-west, in the vicinity of the Orleans Trough. Vermeiren (1995) has demonstrated that throughout the stratigraphic section these mini-depocentra are not always located off the same glacial through. This observation suggests that ice-stream activity may have been quite variable through time.

9. CONCLUSIONS

- The new swath bathymetry map reveals new morphological features and trends that shed new light on the ongoing processes of back-arc basin formation and evolution. Basin compartmentalisation and progressive deepening towards the

north-east via a series of bathymetrical steps suggests a progressive increase in basin maturity in that direction. The different shapes and sizes of large volcanic edifices dominating the basin-floor morphology can be interpreted in terms of successive evolutionary stages of incipient sea-floor spreading.

- The new high-resolution reflection seismic data indicate that the investigated upper-slope deposits along the Trinity Peninsula margin contain resolvable records of at least three periods - since the Pliocene, beginning of the opening of Bransfield Basin - during which ice sheets advanced to the shelf edge for a significant amount of time. The record of glacial periods of lesser extent is probably not preserved in the upper-slope and shelf deposits as suggested by the strong erosional unconformities.

- Magnitude of slope progradation varies along the Trinity Peninsula margin and appears to be related to local sources of sediment supply associated with separate glacial troughs. Ice-stream activity within these troughs appears to have varied through time. A thick stack of prograding units is preserved at the mouth of Orleans Trough. Off the mouth of the Antarctic Sound, most of the correlative section has been removed by canyon incision at the Gebra Valley. A new high-resolution seismic survey (GEBRA-96) is planned in order to examine the lateral continuity of the prograding slope strata and to determine the completeness of the stratigraphic record.

- Development of basin-floor strata appears to be temporally distinct from the development of the prograding upper-slope wedges, the toes of which downlap the basin-floor strata. A drill hole - cf. recently submitted ODP Proposal - through this basin-floor section in areas with seismic-stratigraphic evidence for the presence of volcaniclastic layers or inter-stratified lava flows would provide an excellent opportunity to radiometrically constrain the age of the glacial cycles associated with the progradational wedges.

GLACIALLY DEPOSITED SEQUENCES ALONG THE CONTINENTAL MARGIN OF THE BELLINGSHAUSEN AND AMUNDSEN SEAS

1. INTRODUCTION

Some segments of West-Antarctica's continental margin have been relatively well-studied. This is particularly the case for the Antarctic Peninsula sector. More westerly portions of this margin remain at this date, however, virtually unexplored. Only few surveys have ventured into the vast area of the Bellingshausen and Amundsen Seas and collected seismic data in the shelf region and on the continental rise (Hollister et al., 1976; Kimura, 1982; Cunningham et al., 1994). In addition, most of these studies - except the one reported by Cunningham et al. (1994) - surveyed the continental rise only in the area west of 78° W.

From January to March 1994, AWI and RCMG jointly carried out a marine-geophysical reconnaissance survey on board of F.S. POLARSTERN (survey ANT XI/3) with the aim to investigate the stratigraphic and tectonic setting of the shelf and slope region of the Bellingshausen and Amundsen Seas between 73° and 122° W.

This report focuses on the analysis of the reflection seismic data for the study of the margin's stratigraphy as a record of its geodynamic evolution and of its Cenozoic glacial history. It is largely based on two of the papers that have emanated from the Belgian-German co-operation during the ANT XI/3 survey (Nitsche et al., in press; Gohl et al., in press) with additional insights from Schoolmeester (1995).

2. GENERAL GEOLOGICAL SETTING

The tectonic history of the continental margin of the central and eastern Bellingshausen Sea is - just like the northern Antarctic Peninsula margin further to the east - dominated by the subduction of the oceanic Phoenix Plate under the Pacific margin of the continental Antarctic Plate. This subduction stopped after collision of the Antarctic-Phoenix Ridge with the Antarctic Plate. This collision occurred in successive steps and propagated from southwest (at about 20 Ma BP) to northeast (at about 4 Ma BP) as discussed by Larter & Barker (1991). The recent history of these parts of the margin resembles that of a young passive margin (Larter

& Barker, 1991). The former fore-arc slope has been buried by thick, mainly prograding sequences, attributed to the action of ice sheets grounded to the shelf edge at times of glacial maxima.

Bart & Anderson (1995) illustrate that the thermal-tectonic effect of the ridge-trench collision has exerted a major influence on the stratigraphic architecture of the north-western Antarctic Peninsula margin. Tucholke & Houtz (1976) and Larter & Barker (1991) postulate that sedimentation in the Bellingshausen Sea is also influenced by both tectonic and glacial history, but because the ridge-trench collision happened so much earlier in the Bellingshausen Sea area, tectonic processes may have played a less-influential role on the sedimentation during glacial times as compared to the Peninsula region.

The geological and tectonic setting in the western Bellingshausen Sea is presently still unknown, because of the sparse data available. The continental margin of the Amundsen Sea was formed as a passive rifted margin when New Zealand rifted away from West Antarctica about 90 Ma ago (Lawyer et al., 1992). Oceanic basement in the area becomes older towards the west, roughly from Miocene in the Antarctic Peninsula area to Cretaceous along the Amundsen Sea segment of the margin.

The glacial systems on western Palmer Land, northern Ellsworth Land and Marie Byrd Land drained mainly into the Bellingshausen and Amundsen Seas. Therefore, the continental margins along these seas are believed to contain a record of the glacial history of these drainage systems, and hence of part of the West-Antarctic ice sheet.

3. MATERIALS AND METHODS

About 3000 km of multi-channel reflection seismic data were acquired in those regions of the Bellingshausen and Amundsen Seas that were accessible in the period January-March 1994 (Figure 8). During the survey, the seismic system was used in various configurations, resulting in seismic data of low to intermediate resolution (10-150 Hz). Profiles 94002, 94003 and 94020 were shot with an array of eight 3.0 l PRAKLA-SEISMOS airguns, operated at 130 bar. The 96-channel SYNTRON streamer had a length of 2400 m. Because of damage to this streamer at the end of profile 94020, subsequent profiles were recorded with a shorter (600 m)

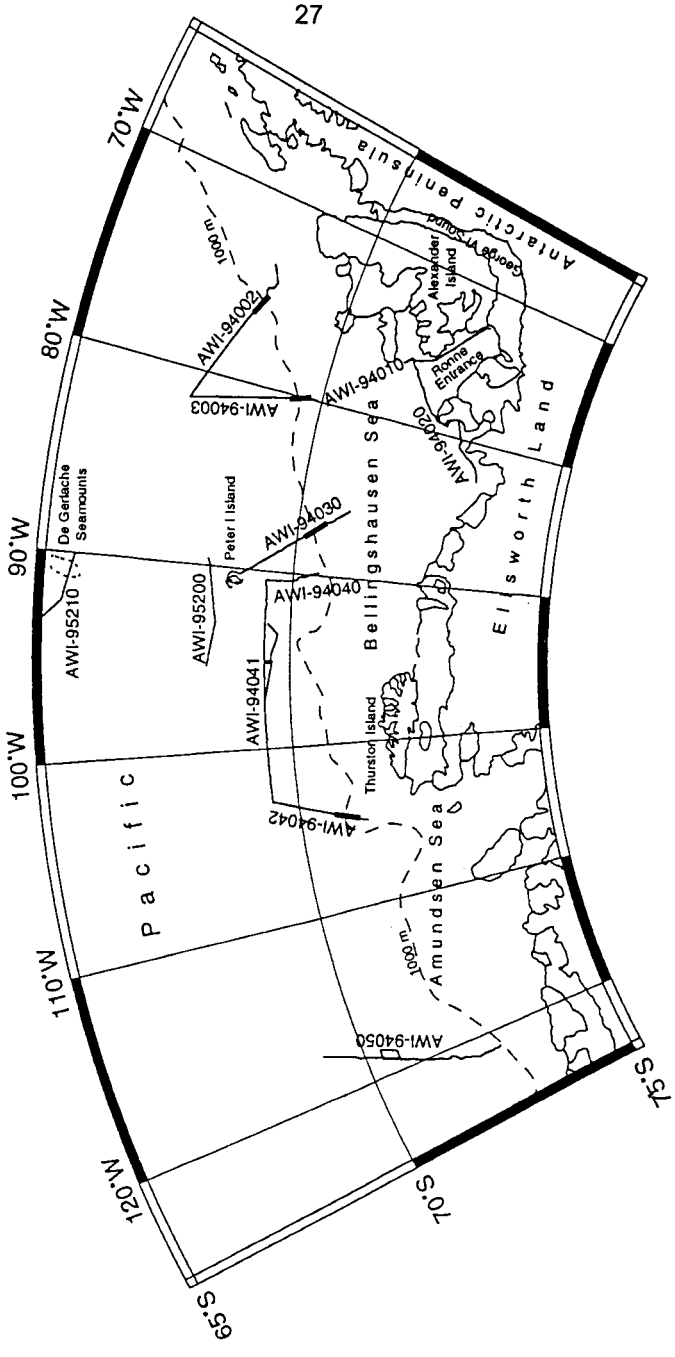

Figure 8. *Location map of the grid of multi-channel reflection seismic profiles recorded during the ANT XI/3 survey in the Bellingshausen and Amundsen Seas. The bold parts on some of the profiles mark the sections shown in this report. The shelf edge is approximated by the 1000 m contour.*

96-channel PRAKLA-SEISMOS streamer, but with the same airgun array. A cluster of three 4.5 l SODERA GI-guns was used for profile 94030. The airguns were towed at a depth of 5 m, while the streamer was towed at 10 m depth.

Data processing was partially carried out on board of F.S. POLARSTERN and partially at AWI, using the COGNISEIS DISCO 8.4 seismic processing system. These applied processing procedures included CDP sorting, NMO-correction, stacking and bandpass filtering. Velocity filtering was used to suppress sea-floor multiples beyond the shelves.

The acquired data (Figure 8) are clustered in four areas: (1) on the slope and rise off Alexander Island (lines 94002 and 94003), (2) within the Ronne Entrance (lines 94010 and 94020), (3) on the slope and rise of the Bellingshausen Sea south and south-west of Peter I Island (lines 94030, 94040, 94041 and 94043), and (4) in the east and central Amundsen Sea (lines 94042 and 94050/54).

(1) Profiles 94002 and 94003 (Figure 9) are the easternmost lines that were recorded. Both are long transects running from the outer shelf down the continental slope and onto the continental rise. They cross distinctly different domains of the West Antarctic continental margin, which are separated from each other by a change in margin strike direction. The continental slope crossed by line 94002 is extremely steep (~15°) and strikes SE-NW. Line 94003 crosses a more gentle slope (~30°), with a dip gradient and strike direction (WSW-ENE) that are more typical for most of the Bellingshausen Sea margin.

(2) Lines 94010 and 94020 are the southernmost profiles acquired in this region. They are located in the Ronne Entrance, a broad glacially eroded valley on the inner continental shelf extending from George VI Sound. Line 94010 was shot along the eastern rim of the Entrance, parallel to the south-eastern shore of Alexander Island. Line 94020 is a transverse profile across the Ronne Entrance.

(3) Five lines are located in the central and western Bellingshausen Sea. Line 94030 is a complete shelf-slope-rise transect, running from the outer shelf downslope towards Peter I Island. This volcanic island is located south of the De Gerlache Seamounts and rises more than 4000 m above the surrounding continental rise. Line 94040 is a shorter traverse section slightly more west. Line 94041 is a slope-parallel line extending from just south of Peter I Island towards the west. It was shot to investigate a remarkably large anomaly in the free-air gravity field of this area (McAdoo & Marks, 1992). Line 94043 represents an additional profile across this peculiar feature.

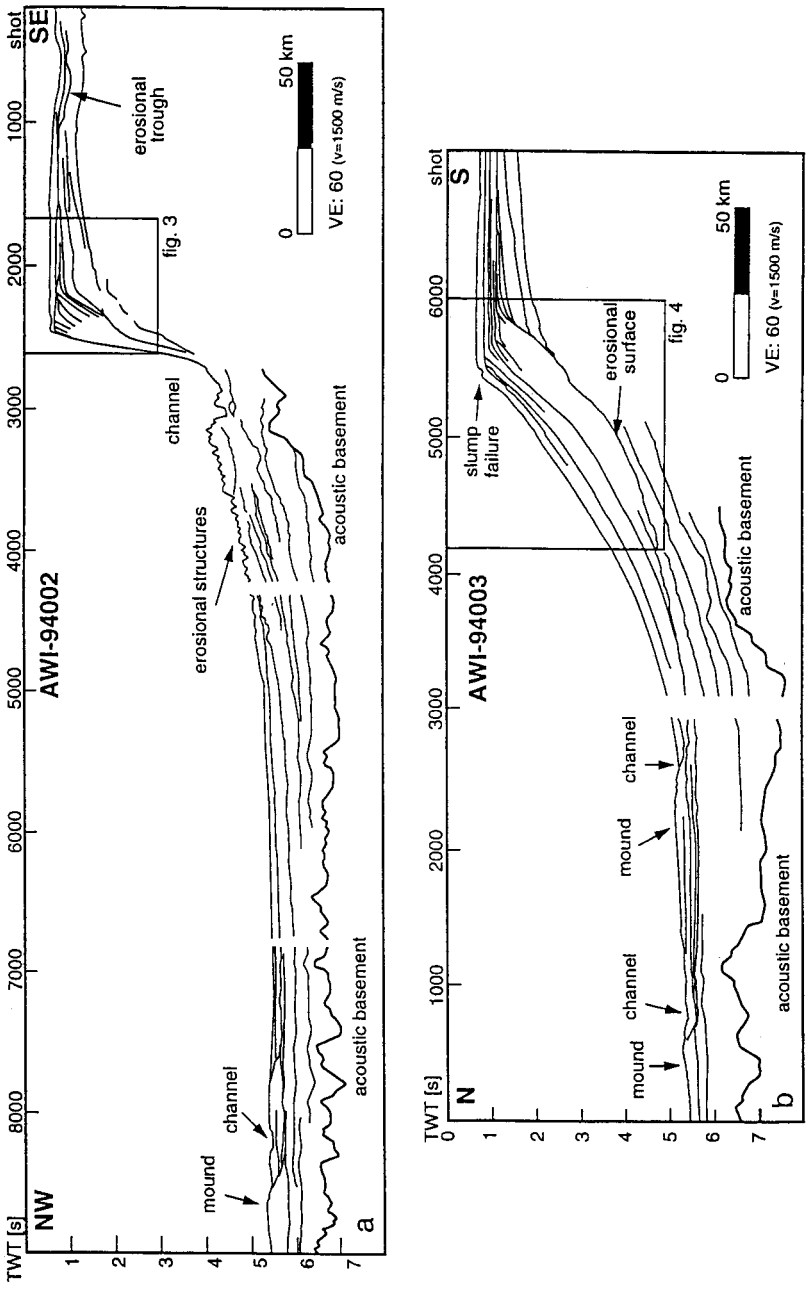

Figure 9. *Line-drawings of profiles 94002 and 94003. Profile 94002 runs parallel to the shelf edge until shotpoint 1500, at which it turns into a perpendicular direction. Both line-drawings are displayed at the same scale. The different slope gradient of both profiles is apparent. The mounded features at the northern end of both profiles belong to the same structure. Enlarged sections shown in Figures 10 and 11 are indicated by the boxes.*

4. The remaining lines are all located in the Amundsen Sea. Line 94042 crosses the continental margin near the boundary between the Bellingshausen and Amundsen Seas. Lines 94050 to 94054 form an incomplete transect in the central Amundsen Sea, in the vicinity of the Marie Byrd Seamounts. Unfortunately, heavy pack-ice conditions hindered a southward continuation of the line onto the upper slope and outer shelf.

4. SEISMIC STRATIGRAPHY OF THE CONTINENTAL SHELF, SLOPE AND RISE

Due to the inaccessibility of the inner shelf area, seismic work during the ANT XI/3 survey was concentrated on the outer continental shelf, slope and rise. Limited data are available, however, from the Ronne Entrance part of the inner shelf. These lines (94010 and 94020) reveal a generally overdeepened topography, indicative for glacial erosion by grounded ice sheets, with water depths of up to 900 m. Acoustic basement appears to be partly exposed at the sea floor.

The best way to discuss the seismic stratigraphy of the deposits that have accumulated along the investigated portions of the West-Antarctic continental margin is by means of the long shelf-to-rise transects that are oriented perpendicular to the shelf edge.

Below, the stratal geometry patterns will be discussed for four of such transects, proceeding from east to west along the margin.

4.1 Profile 94002

The easternmost part of the study area (profile 94002) is characterised by a steep and narrow continental slope, which falls app. 2550 m over a distance of barely 10 km, resulting in a gradient of ~15°. As a consequence, correlation of seismic horizons from the outer shelf to the foot of the slope is difficult (Figure 10).

The outer shelf, where the water depth is about 460 m, shows three distinct seismic-stratigraphic units (Figure 10):

- ***(Unit 1)*** a lower unit, composed of mainly aggradational and gently (< 10°) seaward-dipping strata, of which the associated foresets are not observed,
- ***(Unit 2)*** a middle unit, composed of purely progradational and, towards the top,

truncated sequences with no topset section preserved, and

- *(Unit 3)* an upper unit characterised by both progradation and aggradation, the latter becoming increasingly important towards the top.

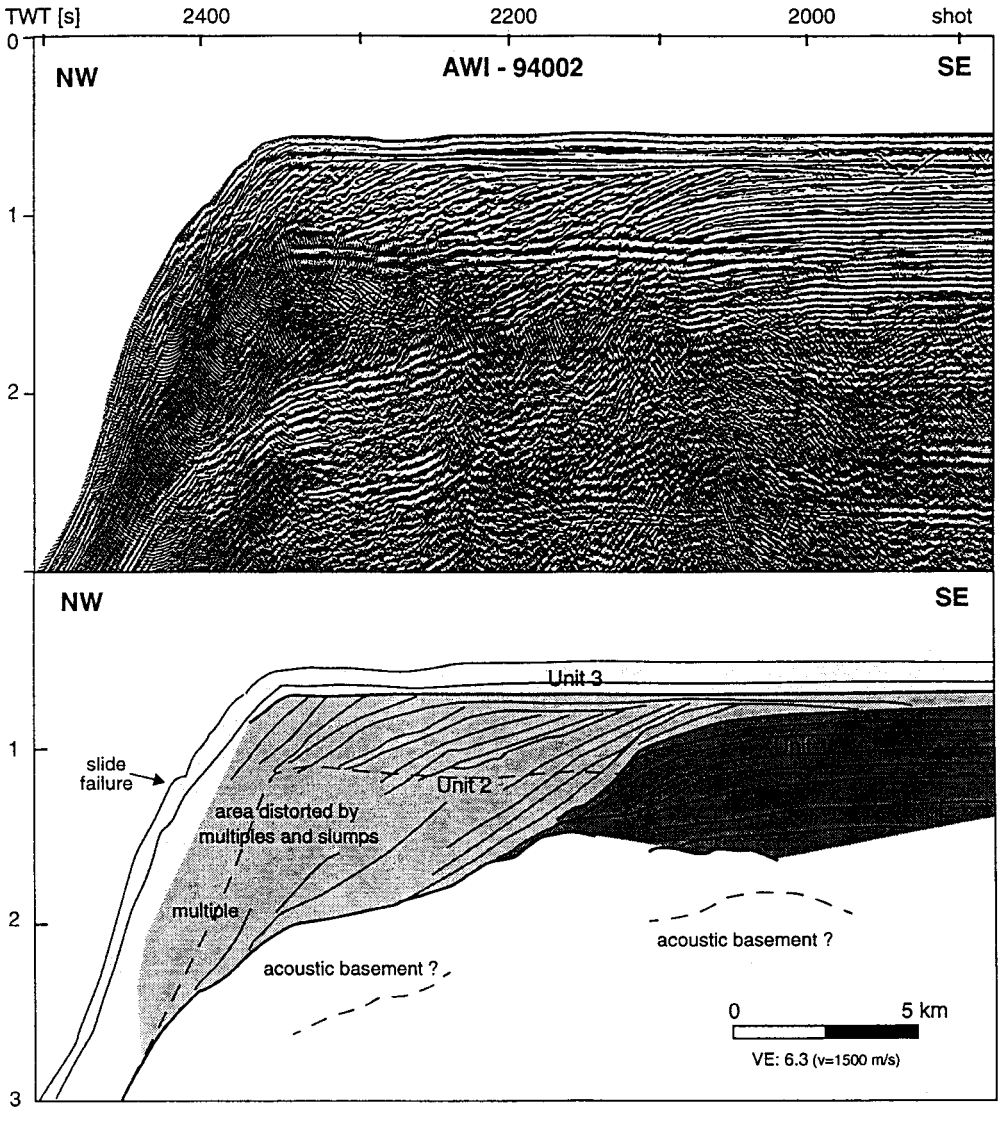

Figure 10. *Part of the outer shelf on profile 94002, shown as stacked seismic section and interpreted line-drawing.*

The important erosional surface truncating the steeply dipping foresets of the Unit 2 seems to have eroded landward into the gently dipping parallel strata of the lower unit as well. The topset sections of Unit 3 cover this unconformity, building an interval - up to 200 ms TWTT thick - of horizontally stratified sediments covering the shelf. Several indications of slump and slide structures are seen on the continental slope and, deeper into the section, on the palaeo-slope beyond the outer shelf. The total distance of progradation for the two upper units is 14 km.

Along the continental rise, the acoustic basement is overlain by a 2.0 s TWTT thick stack of sediments. These deposits seem to have accumulated locally into a mounded feature, exhibiting a chaotic seismic facies and a strikingly irregular surface morphology. The latter appears to be produced by several channel- or canyon-like erosional structures. The deepest canyon is located at the foot of the continental slope and exhibits a relief of about 200 m. The whole structure levels out gradually towards the deep sea, where it merges into a smooth and sub-horizontal sea floor.

4.2 Profile 94003

The depositional geometries and stratal patterns on profile 94003, located at about 80° W, are somewhat different from those of profile 94002. The slope is wider, and has a much more gentle gradient of 20° to 30°. This makes it easier to trace certain reflections from the outer shelf down the slope. Below the outer shelf, which is about 525 m deep, a similar three-fold succession of geometries is observed as on profile 94002. This is illustrated in the line-drawing of Figure 11. The lower unit (Unit 1) consists of parallel and gently seaward-dipping strata, showing at least 800 ms TWTT of aggradation. Above this lies a mainly progradational unit (Unit 2) whose upper boundary on the shelf is an erosional surface, truncating the underlying aggradational strata as well further landward. The upper unit (Unit 3) shows evidence of both modest progradation and upward increasing aggradation, resulting in a layer - 400 ms TWTT thick - of horizontally stratified sediments that cover the entire shelf. This is about twice the thickness of the corresponding unit on profile 94002. Total progradation of Unit 2 and Unit 3 is about 18 km.

A reflection that we interpret as acoustic basement is buried beneath 2.0-2.5 s TWTT of sediments on the continental slope and rise. Most prominent within this thick sedimentary section is an irregular, wavy-hummocky surface that clearly erodes underlying reflections in upslope direction. Overlying sediments form a wedge of prograding strata - up to 1.8 s TWTT thick - that downlap in a seaward direction onto

the erosional surface. As a result, the wedge rapidly thins to about 200 ms TWT on the lower slope. The prograding wedge is generally characterised by a well-stratified facies, which contrasts with the relatively transparent facies of the underlying units. One particular reflection stands out because of its higher amplitude and divides the wedge into two more or less equally thick intervals. An important observation is that this strong reflection seems to correspond to the transition from progradational to combined progradational-aggradational geometry identified on the outer shelf.

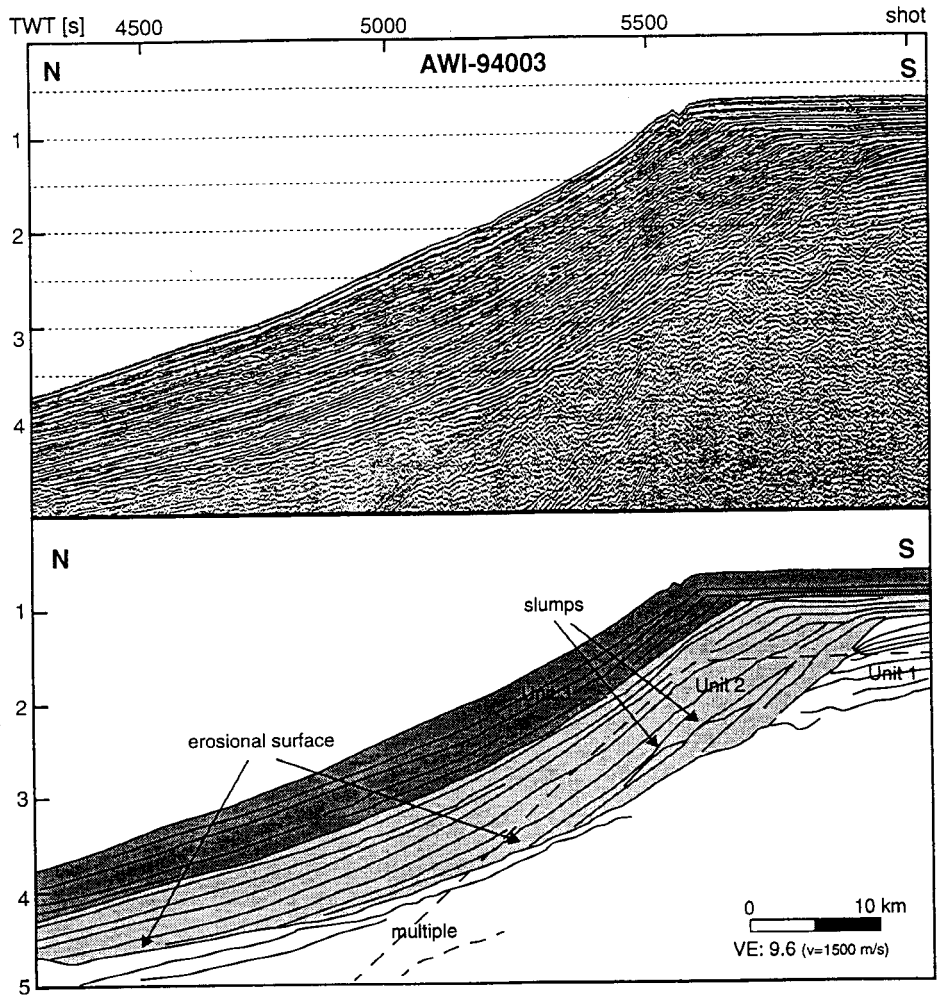

Figure 11. *Part of the outer shelf on profile 94003, shown as stacked seismic section and interpreted line-drawing.*

The erosional reflection defining the base of the wedge can be traced further downslope, towards the continental rise. Here, the overlying interval thickens again to form an up to 400 ms TWTT thick, transparent mound, which is locally associated with what appear to be sediment waves at the sea floor. This mounded feature was also observed on the adjacent extremity of line 94002, where it displays an asymmetric shape with a broad south-eastern and a narrower north-western shoulder, separated by a more than 50 m deep channel-like depression. It also appears to be perched against the eroded flank of an older but similar-looking transparent mass, about 500 m thick. The upper sediment mound might belong to a chain of large mounds that were reported recently by McGinnis & Hayes (1994) and by Rebesco et al. (1994) along the continental rise of the Antarctic Peninsula Pacific margin.

4.3 Profile 94030

The continental slope on profile 94030 dips more gently (10-20°) and is hence also much broader than on any of the other transects. The seismic-stratigraphic correlation from the outer shelf to the base-of-slope area is therefore easiest to establish on this profile (Figure 12). Also remarkable is the shelf-edge depth of about 700 m.

The outer-shelf sequence geometries (Figure 12) change from a lower unit of thick aggradational sequences (Unit 1), through a middle unit of mainly prograding sequences (Unit 2) into an upper unit of progradational-aggradational sequences (Unit 3). The topset deposits of the upper unit have a thickness of only 150 ms TWTT. The same stratal patterns are noted on a nearby seismic profile recorded by the British Antarctic Survey (Cunningham et al., 1994), although some differences in the detailed structure exist.

The present-day continental slope is underlain by a prograding wedge, delimited at its base by an horizon with characteristics very much like the base-wedge reflection observed on profile 94003. This horizon has a wavy-hummocky morphology, is clearly erosional in an upslope direction and defines a downlap surface for overlying strata. Its correlation with the stratigraphy on the outer shelf is hampered by strong sea-floor multiples, but it appears to correlate approximately with the transition between the lower aggradational and middle, purely progradational units. The limited thickness of the prograding wedge (1.0 s TWTT compared to 1.8 s WTT on the adjacent profiles) does not necessarily reflect a lower sediment supply,

but may be related to the broader and gentler slope. The total distance of progradation (32 km) is the largest observed on any part of the margin. As on profile

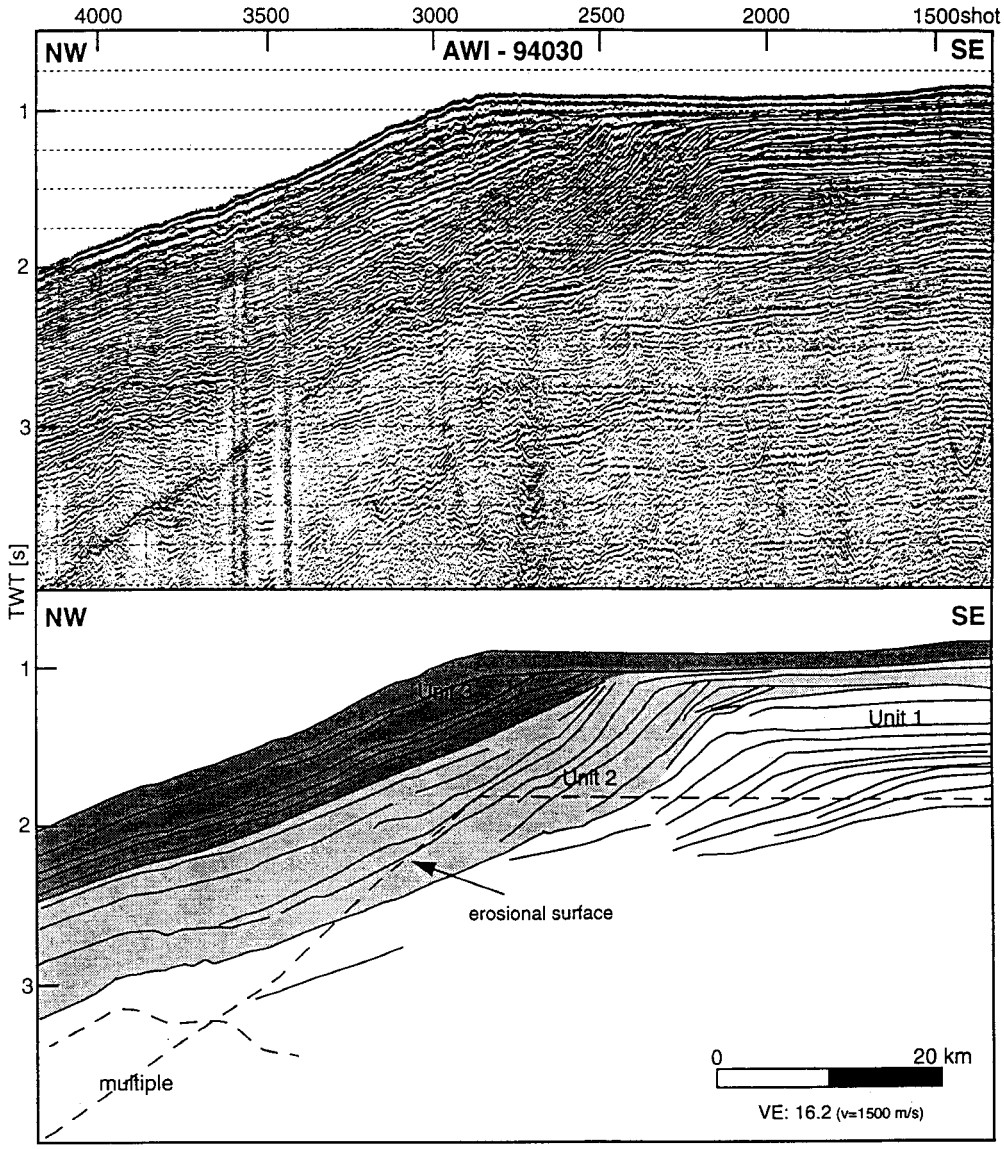

Figure 12. *Part of the outer shelf on profile 94030, shown as stacked seismic section and interpreted line-drawing.*

94003, the wedge is divided into two parts by a conspicuous, higher-amplitude reflection which can be correlated - unambiguously along this transect - with the transition from a purely prograding to prograding-aggrading geometry on the outer shelf.

4.4 Profile 94042

The westernmost transect, profile 94042 (Figure 13), shows a continental slope which is slightly steeper (3-4°) and thus narrower than on the two profiles discussed previously. The water depth at the shelf edge is approximately 540 m.

Two phases of outer shelf development are evident in this location: a phase of mainly progradation (Unit 2), followed by a phase of combined progradation and aggradation (Unit 3). The aggradational component of the latter accounts for a quite thick (400 ms TWTT) sediment cover over the continental shelf. Combined progradation of the two units amounts to about 24 km. Profile 94042 extends over only a small part of the continental shelf, but an older phase of aggradation, probably correlating with the lowermost outer shelf unit (Unit 1) recognised on the other profiles, can be identified near the landward end of the line.

Again a pronounced erosional surface, with characteristic wavy-hummocky morphology, defines the base of a prograding wedge on the continental slope. This wedge is up to 1.8 s TWTT thick. Due to the prominent downlap of internal strata onto its base, the wedge thins to a mere 100 ms TWTT at the foot of the slope. In the lower part of the wedge, a strongly reflecting horizon is recognised, which becomes less distinct towards the upper slope, but appears to correlate with the boundary separating progradational and progradational-aggradational sequences on the outer shelf. Below the wedge, at least 2.0 s TWTT of older sediments are evident, most of which are not recognised on the other profiles. It is likely that the continental slope here accommodates the oldest sedimentary succession encountered along the investigated margin.

On the continental rise, the interval overlying the erosional base-wedge reflector, thickens into a transparent mound - 300 ms TWTT thick - associated with sediment waves at the sea floor. This feature shows much resemblance with the mounded features observed on profiles 94002 and 94003.

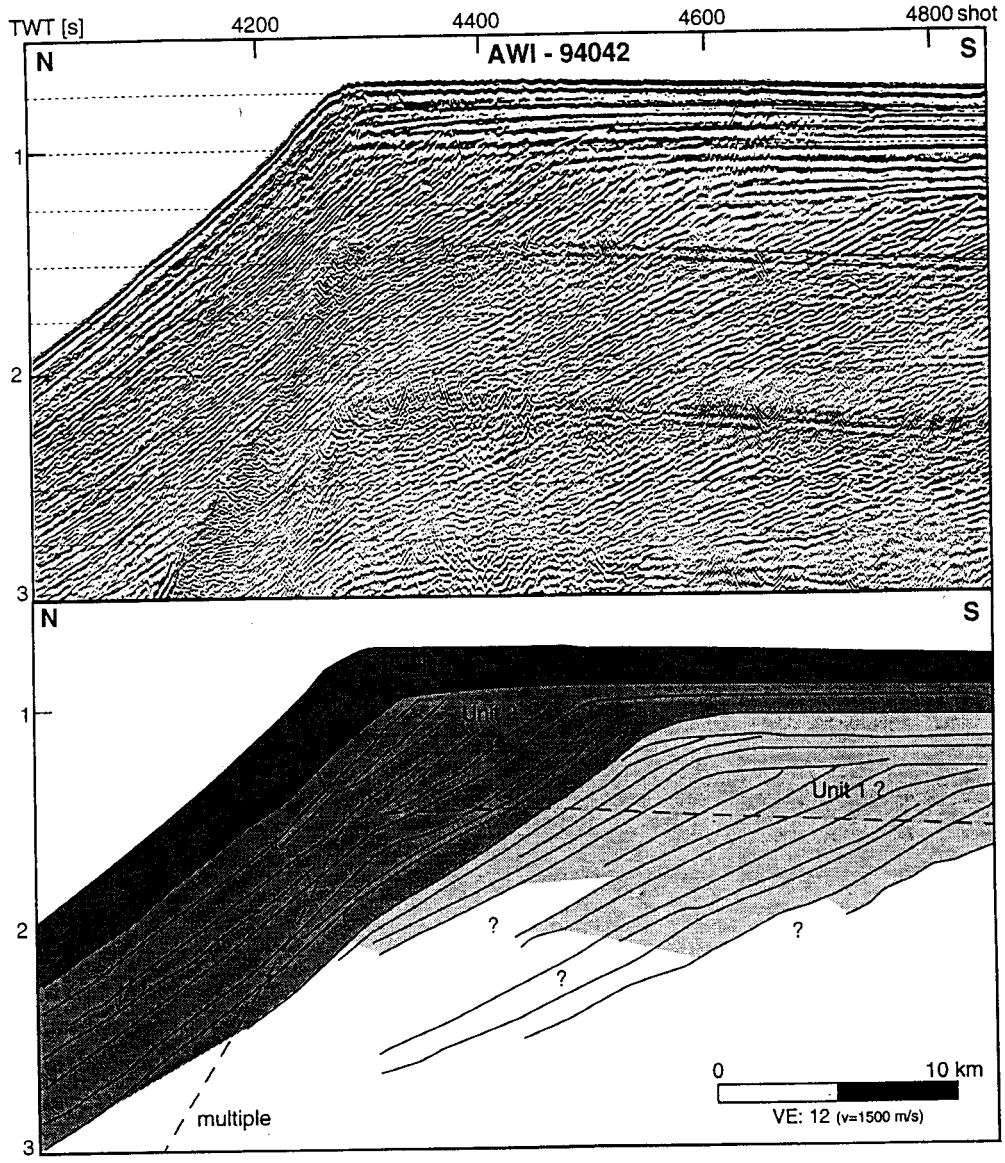

Figure 13. *Part of the outer shelf on profile 94042, shown as stacked seismic section and interpreted line-drawing.*

5. DISCUSSION

5.1 Seismic-stratigraphic record of glacial history

Firstly, it should be emphasised that the resolution obtained in the ANT XI/3 multi-channel seismic data is probably as much as an order of magnitude lower than that of the GEBRA-93 single-channel seismic data, discussed previously. The seismic-stratigraphic observations presented above should therefore not be compared to those from Bransfield Basin without taking this aspect duly into consideration. The importance of taking into account seismic resolution when studying the seismic-stratigraphic record of glacial history has been demonstrated very convincingly by Bart & Anderson (1995).

The outer-shelf and slope deposits. There are striking similarities found in the seismic stratigraphy and geometry of the outer shelf and the continental slope along the whole margin, although the spacing between the profiles and the lack of strike lines make it difficult to correlate reflections from profile to profile. Changes in the sedimentary pattern between the profiles are possible, but major differences are not likely. The profiles also show differences in slope gradient, depth of shelf and amount of progradation. This could be caused by differences in glacial drainage patterns, the nature of the source material being eroded, the transport path and other parameters. But it could also reflect the tectonic history and different stages of subsidence of the western Bellingshausen Sea and the Antarctic Peninsula (Tucholke & Houtz, 1976).

On the ANT XI/3 multi-channel seismic data from the Bellingshausen and Amundsen sea portions of the West Antarctic margin the same variation of outer shelf geometries is observed:
(1) a lower unit of mainly aggradational sequences,
(2) a middle unit of strongly prograding sequences, and
(3) an upper unit exhibiting both progradation and aggradation.
The older aggradational sequences closely resemble the "Type IIA"-sequences, as defined by Cooper et al. (1991) and found at various locations along the Antarctic continental margin. These sequences are thought to be generated during times prior to the onset of the major glacial advance of a grounded ice sheet, and are therefore often used as indicators for determining pre-glacial conditions.

The overlying sequences all show significant seaward migration of the palaeo-shelf edge, indicating a major change in depositional style. In analogy to

observations from other glaciated margins (e.g. Boulton, 1990; Bartek et al., 1991; Cooper et al., 1991; Kuvaas & Kristoffersen 1991; Larter & Barker, 1991; Vanneste et al., 1995), these sequences are interpreted as mainly glacial in origin. A glacial origin is also suggested by the identification on the southern end of profile 94002, where the line runs almost parallel to the shelf edge (up to shot 1500), of a number of broad erosional troughs in the shelf sediments correlative to the two upper progradational units.

The two upper units identified on the outer shelf would thus have been deposited during multiple glacial advances on the shelf, which caused deposition in an overall progradational style. Erosion was predominant on the inner shelf, while vertical aggradation of shelf strata was restricted on the outer shelf. Although Unit 2 shows only a slight aggradational component, this does not mean that there has been no aggradation. Such aggradational strata might have been eroded during later glacial phases when grounded ice re-advanced to the shelf edge. Even though it has been shown on the Antarctic Peninsula shelf further east that amounts of progradation and aggradation can vary strongly laterally within a given glacial sequence (Bart & Anderson, 1995; Larter & Cunningham, 1993), we believe that the widespread transition from progradational to both prograding and aggrading sequences is significant and reflects a broadly similar glacial development along the entire margin, at least in the long term. This does not imply, however, that the advancing ice sheet reached the outer shelf at the same time everywhere along the entire margin, or that these advances were of equal magnitude. Considering the great variations of shelf width and the position of the shelf ice of today, such a concurrent evolution is not likely. The grounded ice has to advance over a greater distance e.g. in the central Bellingshausen Sea than at the Antarctic Peninsula to reach the shelf edge. Also, it is unlikely that the velocity of the ice advance was the same along the entire margin. Investigations along the Antarctic Peninsula have shown that ice streams can cause lateral variations in the sediment deposition (Larter & Cunningham, 1993).

A remarkably comparable overall geometry has been observed by Bart & Anderson (1995) on the outer shelf area of the Antarctic Peninsula. They identify three major depositional packages, which they could further subdivide into 31 glacial units:

(1) Package 1, characterised mainly by aggradation and showing virtually no slope progradation;
(2) Package 2, characterised by significant slope progradation (up to 12 km);

(3) Package 3, characterised by aggradation and only a limited amount of slope progradation.

The onset of glaciation of the Antarctic Peninsula continental shelf is interpreted to occur within Package 1 (Bart & Anderson, 1995).

Age constraints for the onset of large-scale glaciation of the shelf are limited at present, and not entirely in agreement with each other. Results from deep-sea drilling suggest that, although local alpine glaciation on the continent may have started as early as Eocene (e.g. Birkenmajer, 1991), major West Antarctic glaciation probably began in Late Miocene times, as indicated by an increase in ice-rafted material found at DSDP sites of Leg 35 on the Bellingshausen continental rise. Further east along the Antarctic Peninsula margin, Larter & Barker (1991) correlate prograding sequences on the shelf with sediments on the continental rise that overlie young ocean floor. They estimated the age of this ocean floor by interpretation of marine magnetic anomalies to be 5.6 Ma. Due to the revision of the geomagnetic polarity time scale by Cande & Kent (1995) this age would be about 6.5 Ma. Bart & Anderson (1995) use the unconformities related to the successive ridge-trench collisions at different portions of the Antarctic Peninsula margin to obtain some age constraints on their seismic glacial stratigraphy. They postulate that the first evidence for glaciation on the continental shelf could be as old as early Middle Miocene. In fact, they identify three major phases in the glacial evolution:

(1) early Middle Miocene to the Miocene-Pliocene boundary: short-duration glacial phases producing essentially aggradation and no significant slope progradation;
(2) Miocene-Pliocene boundary to Pliocene-Pleistocene boundary: long-duration glacial phases producing significant slope progradation;
(3) Pliocene-Pleistocene boundary to Present: short duration glacial phases essentially aggradation and no significant slope progradation.

On most of the transects on the continental slope a conspicuous erosional surface is observed. It defines the base of a wedge of prograding and downlapping slope foresets. This erosional surface is interpreted to approximate the transition from "Type IIA"-sequences, as defined by Cooper et al. (1991), to characteristically prograding sequences on the outer shelf. This suggests that it is - in one way or another - related to the onset of large-scale glaciation of the West Antarctic shelf. However, caution is needed since there is no clear correlation of this surface from the slope to the shelf.

The continental rise deposits. Indications of slumps and slides on the

continental slope and large sediment mounds on the continental rise show that sediment reworking by gravity and currents plays an important role in the sedimentation history.

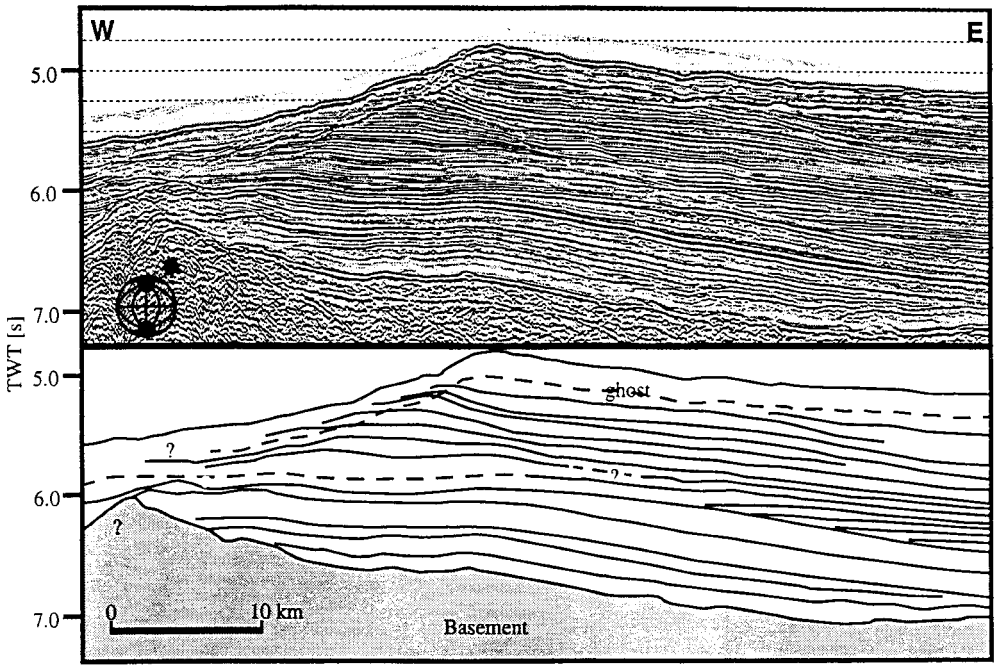

Figure 14. *Part of drift deposit on the continental rise on profile 94041, shown as stacked seismic section and interpreted line-drawing.*

On profiles 94002, 94003 and 94041 (Figure 14) to 94043 (Figure 15) a number of mound-shaped sedimentary bodies can be observed. The largest of these mounds - on profiles 94041 and 94043 - is about 700 m high and has a diameter of about 70 km. Its seismic facies consists of parallel reflectors of weak reflectivity. The dimensions and seismic appearance of these mounds are comparable to the mounded features on the continental rise along the Pacific margin of the Antarctic Peninsula and the eastern portion of the Bellingshausen Sea, reported by Rebesco et al. (1994) and McGinnis & Hayes (1994). These sedimentary bodies are inferred to have been deposited by a combination of channelised turbidity currents traversing the continental rise, and along-slope bottom currents (Rebesco et al., 1996]. They are termed giant sediment drifts. Detailed studies of the sedimentation pattern and deposition rates through time suggest that the sediment drifts along the Antarctic

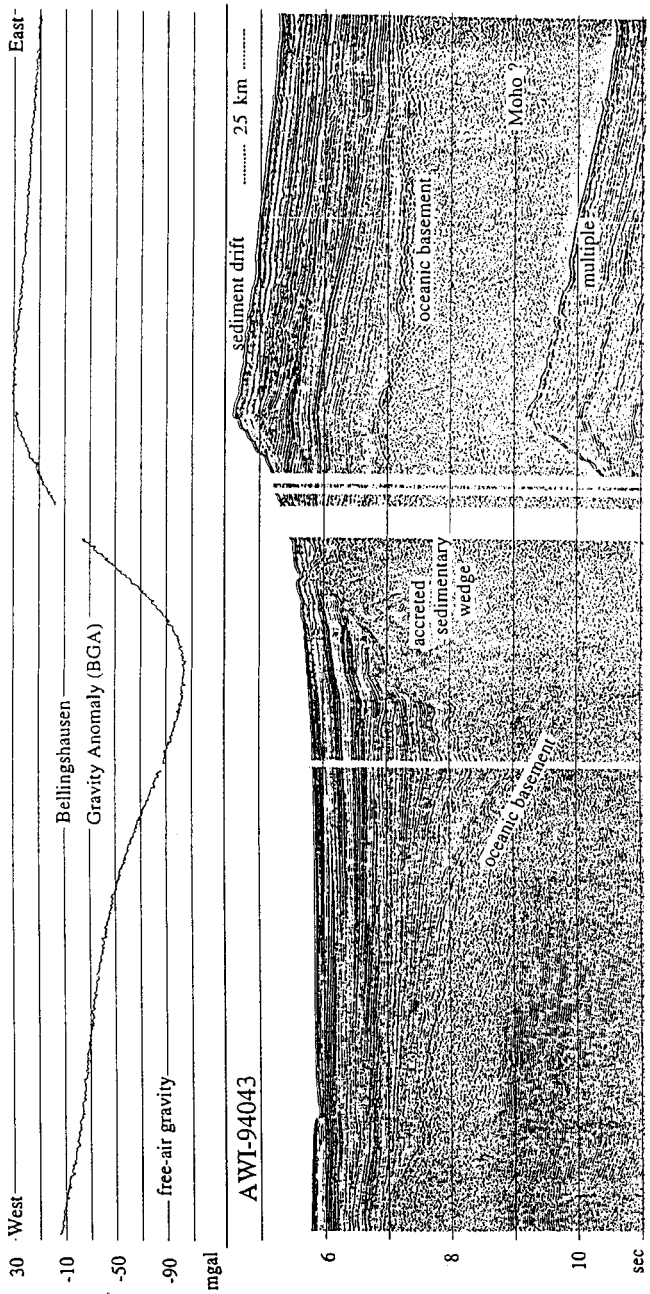

Figure 15. *Part of stacked seismic profile 94043 in conjunction with shipboard gravity data, across a sediment drift near Peter I Island.*

Peninsula margin may contain a record of variation of grounded ice-sheet cover on the continental shelf over the past 8 Ma or so. This record is complementary to that contained in the prograding and aggrading deposits on the continental slope and outer shelf, being more distal and less direct, subject to variation in bottom currents and slope stability, but being also probably more complete and in more easily recoverable lithologies (Rebesco et al., 1996; Barker, 1995).

Profiles 94041 (Figure 14) and 94043 (Figure 15) suggest that the location or - more accurately - the onset of drift deposition was initiated or controlled by an uplifted structure, affecting the oceanic basement and its overlying pre-drift sedimentary sequence. Satellite-derived gravity data (Sandwell & Smith, 1992) reveal large N-S-striking anomaly systems in the Bellingshausen Sea that are oriented obliquely to existing fracture zones and span from the shelf to an area north-west of Peter I Island across the De Gerlache seamounts to about 60° S. The ANT XI/3 seismic data (Figure 15) in conjunction with models of shipboard gravity data across the western anomaly (named Bellingshausen Gravity Anomaly) indicate the presence of a zone of possible intra-plate subduction with an eastward-dipping oceanic basement slab and an accretionary wedge on top (Gohl & Miller, 1997). This feature might be linked to the volcanism of Peter I Island at around 13 Ma (Bastien et al., 1976) which also places the onset of sediment drift nucleus at about the same age, assuming similar bottom current conditions since that time until present. Conversely, the drift deposits further east have been dated by Rebesco et al. (1996) to be probably younger than 8 Ma.

6. CONCLUSIONS

- A regionally-spaced reflection seismic data set has been acquired from the largely unexplored Bellingshausen and Amundsen Seas along the West Antarctic margin. Though limited in coverage, these data show the large-scale stratigraphic architecture of the continental shelf, slope and rise, and are believed to contain a record of the long-term glacial history of the area. On all seismic profiles, the same variation of outer-shelf geometries is observed:
  (1) a lower unit of mainly aggradational sequences,
  (2) a middle unit of strongly prograding sequences, and
  (3) an upper unit exhibiting both progradation and aggradation.
  The lower aggradational sequences are thought to represent conditions before the onset of the major glacial advance of a grounded ice sheet, whereas the overlying

sequences probably record several extended periods of ice-sheet grounding on the shelf since the Middle Miocene.

- A prominent erosional surface defines the base of a prograding wedge occupying the continental slope along the margin. It is tentatively correlated with the transition from aggrading to prograding sequences on the outer shelf, and may thus reflect an intensification of the bottom-current regime in the lower parts of the palaeo-slope at response to the onset of glacial conditions on the continental shelf.

- Sedimentation on the continental rise appears to have resulted in the construction of large sediment drifts that originate from the interaction of channelised turbidity currents traversing the continental rise, and along-slope bottom currents. These drift deposits are believed to contain a good and easily recoverable record of glacial history of the adjacent continental shelf, and have been the main target of a recently submitted ODP proposal.

FINE-SCALE SEISMIC STRATIGRAPHY AND CLAY MINERALOGY ON ODP SITE 693 : PALAEOCLIMATIC SIGNIFICANCE

1. INTRODUCTION

Since 1986, AWI and RCMG have undertaken three joint marine-geophysical expeditions to the eastern and north-eastern Weddell Sea on board of F.S. POLARSTERN: surveys ANT V/4, ANT VIII/5 and ANT X/2. Part of these surveys were conducted in the immediate vicinity - and in conjunction with the drilling operations of JOIDES RESOLUTION during Leg 113 - of ODP Sites 692 and 693, off Cape Norvegia. After integration of all these data with additional reflection seismic data available from BGR and NARE and with the borehole information from ODP Sites 692 and 693 (Barker et al., 1988; Barker et al., 1990), Miller et al. (1990) developed a detailed seismic stratigraphy for the eastern Weddell Sea. It has since been adopted by all researchers active in the area. The processed multi-channel seismic data used for this seismic-stratigraphic model did not allow to identify more than 4 seismic-stratigraphic units in the Oligocene to Present sedimentary section on ODP Site 693. It was however believed that the single-channel analog recordings of these data had much higher resolution potential, capable of resolving many more discrete seismic-stratigraphic events.

This report focuses on the refinement of Miller et al. (1990)'s seismic-stratigraphic model and on the investigation of the geologic and palaeoclimatic significance of the fine-scale seismic-stratigraphic features near ODP Leg 113 Site 693 through correlation with the published core data. It is largely based on the work of Wood (1993).

2. GENERAL GEOLOGICAL SETTING

ODP Site 693 (Barker et al., 1990) is located at a water depth of 2359 m on an app. 80 km wide mid-slope bench along the continental margin of the north-eastern Weddell Sea, off Cape Norvegia (Figure 16). The upper part of the continental slope - upslope of Site 693 - is very steep, up to 12-16° in places. It is made up of a well-developed prograding wedge (Figure 17). This wedge is part of the prograding wedge that characterises the entire eastern Weddell Sea continental margin (Kuvaas

& Kristoffersen, 1991) and is believed to be composed of glacial sediments and deposited by the action of ice sheets grounded at the continental shelf edge. This apparently continuous wedge overlies and downlaps an unconformity of regional importance. As this wedge virtually pinches out upslope of Site 693 (Figure 17), it is presently still uncertain as to how it correlates to the borehole information (Barker et al., 1990) and to the seismic stratigraphy at Site 693 (Miller et al., 1990).

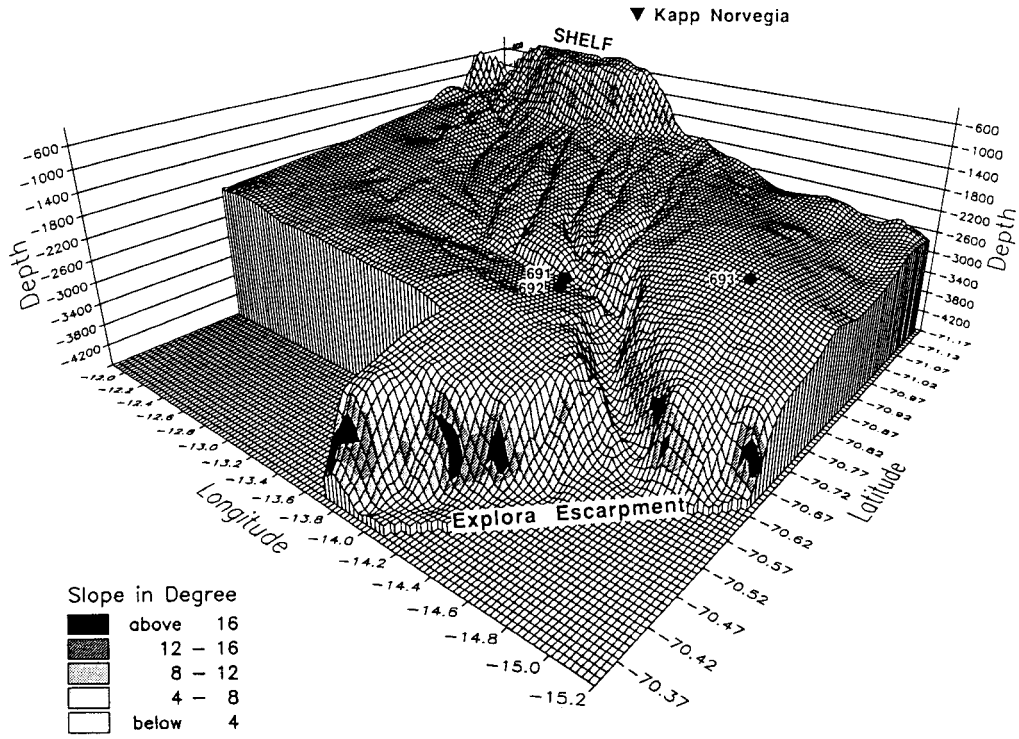

Figure 16. *Three-dimensional view of the Antarctic continental margin off Cape Norvegia from multi-beam bathymetric sounding, showing main morphologic aspects of the Wegener Canyon system and of ODP Sites 692-693 (from Fütterer et al., 1990).*

The lower part of the continental slope - downslope of Site 693 - is also very steep (Figure 17), and is represented by the Explora Escarpment (Hinz & Krause, 1982; Henriet & Miller, 1990). About 10 km north-east of Site 693, the Explora Escarpment is transected by the Wegener Canyon. In the centre of the mid-slope bench, the Wegener canyon branches into several morphologically less-prominent tributary valleys, and looses its deeply incised, steep-walled character (Fütterer et al., 1990).

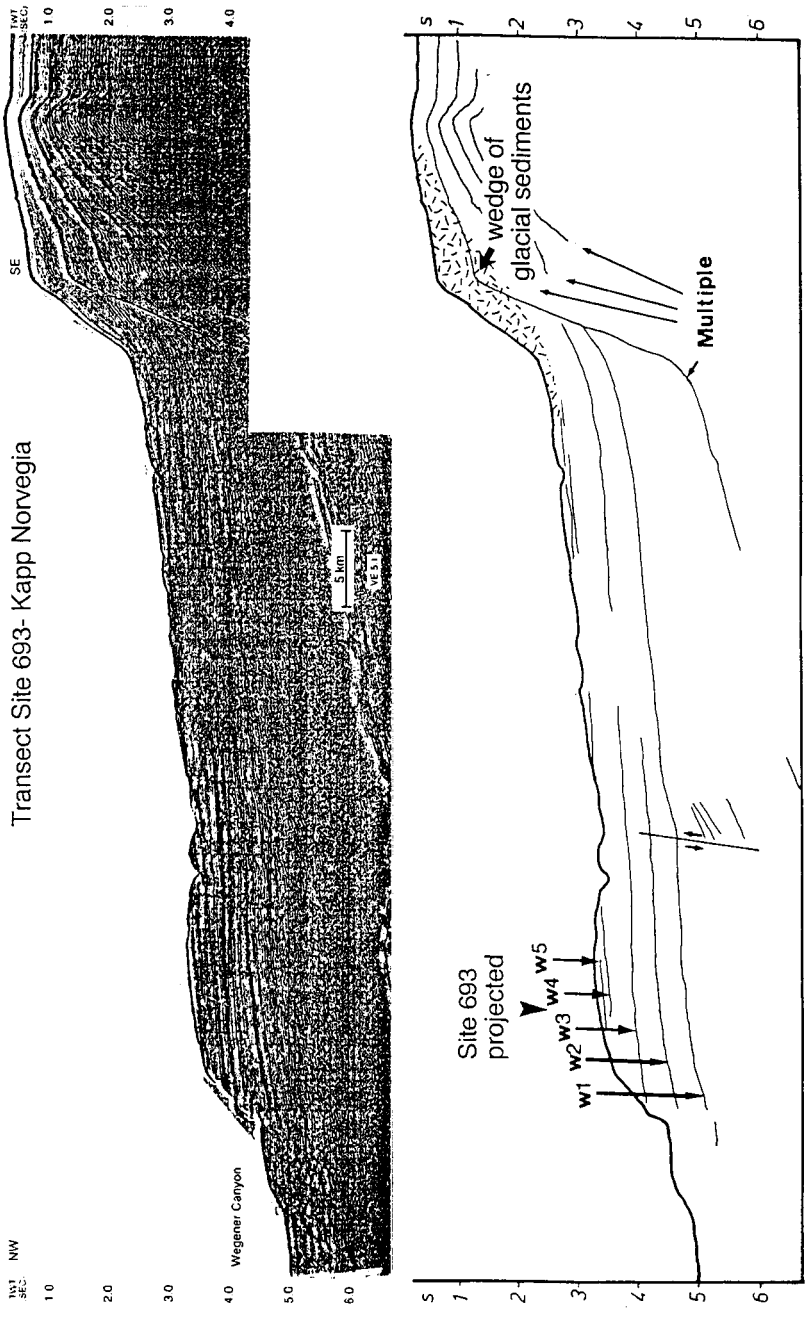

Figure 17. *Seismic profile 90110 (from Kaul, 1991) from Cape Norvegia to Explora Escarpment, through ODP Site 693.*

3. MATERIALS AND METHODS

Data used for this seismic-stratigraphic study included high-resolution seismic profiles acquired during survey ANT V/4 (1986-1987) and survey ANT VIII/5 (1989-1990) on board of F.S. POLARSTERN. Over 40 seismic airgun profiles resulted from these surveys, but this report focuses on four key profiles in the immediate vicinity of Site 693 (Figure 18).

Data were collected using a 24-channel PRAKLA-SEISMOS streamer of 600 m length and arrays of 3 BOLT airguns with volumes ranging from 1.2 to 2.5 l. The digital data acquisition system consisted of an EG&G GEOMETRICS ES 2420 seismograph. Analog monitor records of varied scales of were printed on two EPC recorders after band-pass filtering and time-variant gain amplification.

Seismic-stratigraphic interpretation of the analog monitor records included analysis of reflector configuration, amplitude, frequency and internal velocity. Seismic sequences and sub-sequences so identified were correlated with relevant ODP data (Barker et al., 1988) to place the observations within a coherent global geological framework.

4. PREVIOUS RESULTS ON SEISMIC STRATIGRAPHY AT ODP SITES 692-693

On multi-channel seismic profiles, seven major seismic-stratigraphic unconformities were recognised in the sedimentary strata overlying volcanic basement at ODP Site 693. They were named W1 to W7 from old to young and the seismic units overlying them w1 to w7 (Miller et al., 1990). The core itself drilled into sediments belonging to the top of seismic unit w3, which was proved to be Albian-Aptian of age (Barker et al., 1988), and tested section of all the overlying units. The digital seismic profiles show this portion of w3 to consist of chaotic discontinuous reflectors of varying intensity and configuration. Unit w3 is seismically noisy but despite this some onlap in a south-westerly direction can be identified.

All the units above W5 exhibit strong, regular and closely packed reflectors which are sub-parallel and continuous. These are only affected at the edges of the sediment lobes by incipient slumping. This change in seismic facies is proposed to indicate the increasing role played by glacial marine sedimentation in relation to

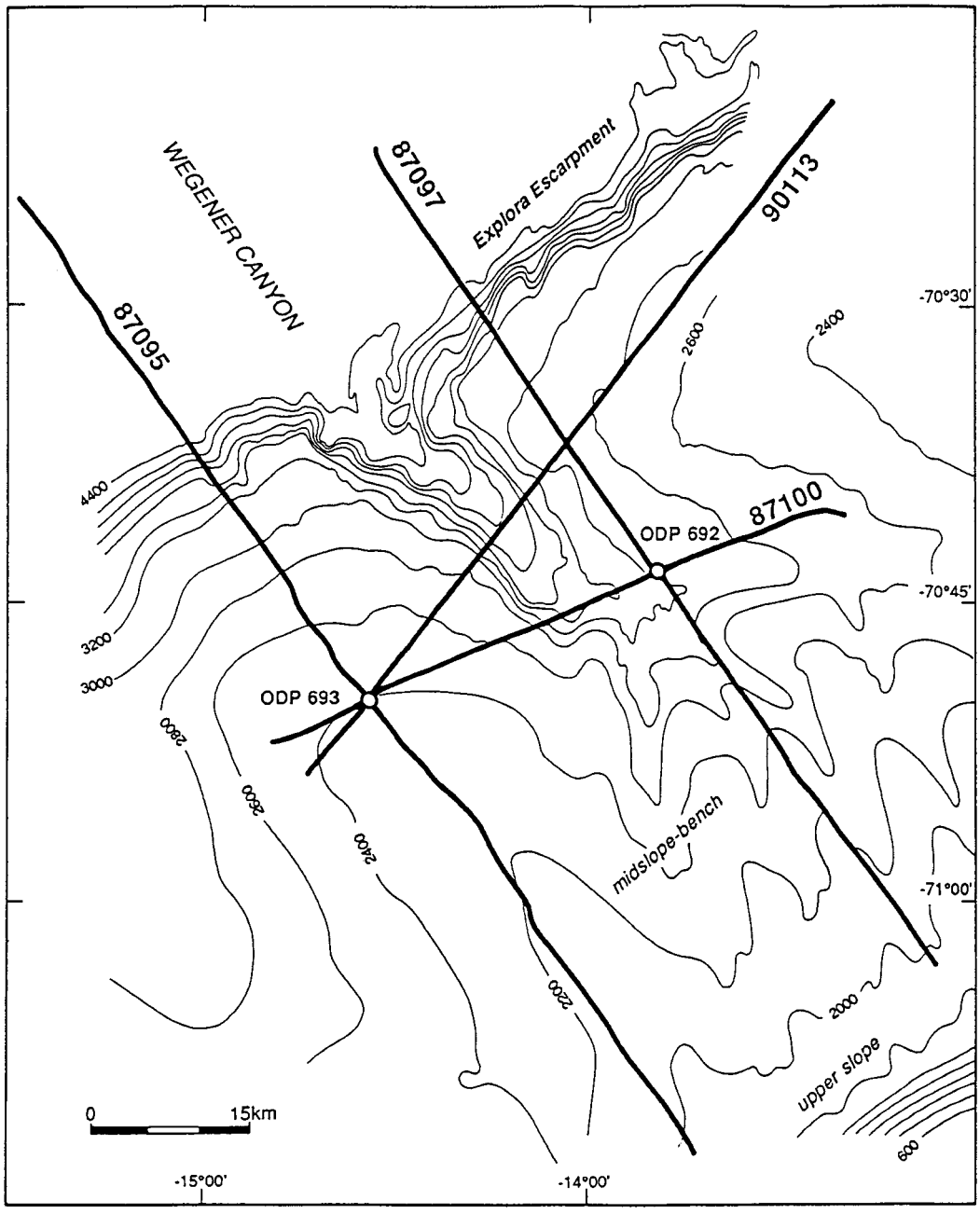

Figure 18. *Location map of ODP Sites 692-693 and of the seismic profiles used in this study.*

cooling and expansion of the East Antarctic ice sheets in mid-Miocene times (Henriet et al., 1989).

Unconformity W5 coincides with a very strong, continuous, locally wavy reflector. Diffraction hyperbola distinguish W5, and this maybe caused by a coarse lag of ice-rafted dropstones. It corresponds to a 5-7 Ma hiatus at Site 693 where most of the middle Miocene is missing. Seismic unit w5 is characterised by a new reflector configuration that is more rhythmic. It consists of strong continuous, sub-parallel events that wedge out to the north-west. It is disrupted by slumping at the edges of the sediment lobe to the south-west and north-east. The seismic unit is app. 50 ms TWTT thick and contains 5 to 8 traceable reflectors.

The uppermost reflectors of unit w5 are truncated by a strong erosional event, unconformity W6, at the edges of the sediment lobe and in a landward direction, giving a lensoid shape to w5. This unconformity is represented by a well-defined reflector, which has onlap in a landward direction. It does not coincide with any change in lithology. Seismic unit w6 is between 25 and 30 ms TWTT thick at the sediment lobe edges and thickens to 70 ms TWTT at Site 693 where 7-10 internal reflectors can be traced. These internal reflectors are sub-parallel and continuous but have a less strong intensity than those of the previous seismic units. Slumping also occurs in the southwest and in a landward direction. These sediment slumps appear to slide off well-defined slip planes.

The strong, low-amplitude, closely spaced reflectors of unit w6 are truncated by a strong, positive amplitude reflector, unconformity W7. Unit w7 exhibits the same reflector characteristics as w5 and w6. Internal reflectors in the lower part are widely spaced; overlying reflectors are more intense and closely spaced. Seismic unit w7 is between 50-80 ms TWTT thick at site 693 and contains 6-8 internal reflectors.

5. REFINED SEISMIC STRATIGRAPHY AT ODP SITE 693

ODP Site 693 core data suggest there is little change in lithology above unconformity W5 (Barker et al., 1988); this is also suggested by the homogeneous seismic facies on the processed multi-channel seismic data around Site 693. However, analog versions of these profiles clearly show that lithological unit IIIa (31.4-243.9 mbsf) can be sub-divided into smaller seismic-stratigraphic sequences, based on the identification of discrete, low-angle unconformities (Wood, 1993). The

initial division of the sequence from lithological units IIIa to I into seismic units w5, w6 and w7 could therefore be refined and four additional seismic units could be distinguished on the seismic data (Figure 19):

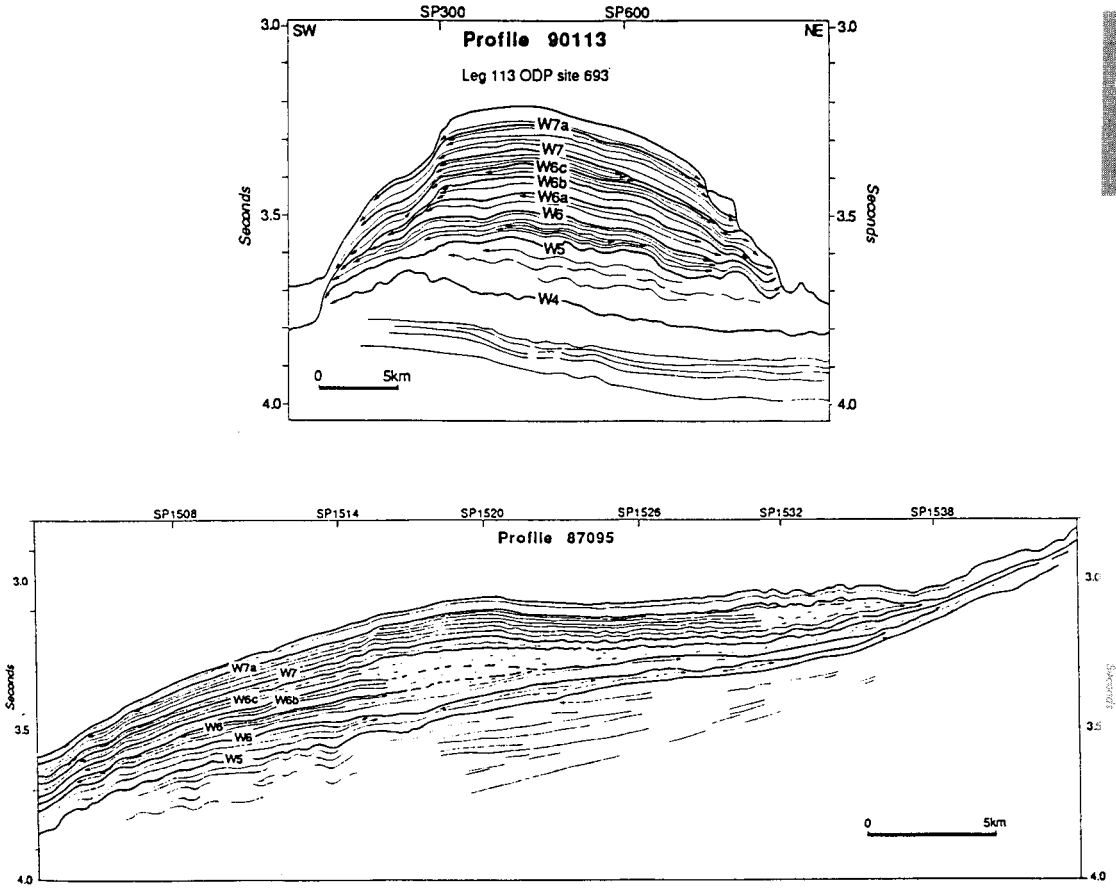

Figure 19. *Interpreted line-drawings of analog single-channel monitor records of profiles 90113 and 87095, showing the new fine-scale seismic-stratigraphic sub-division here presented.*

- ***Seismic unit w6a.*** Unconformity W6a is a strong event which truncates underlying reflectors within unit w6. It is overlain by seismic unit w6a, which is approximately 30 ms TWTT thick. It wedges out and is laterally correlative with a zone of slumps that are probably associated with listric faulting. It contains at least 8 traceable internal reflectors at Site 693 and thickens in landward direction.

- ***Seismic unit w6b.*** Unconformity W6b truncates several horizons within unit w6a. It is represented by a reflector with a higher frequency signature and it marks the lower boundary of a seismic unit (w6b) whose internal reflectors are well-defined. Unit w6b is approximately 25-30 ms TWTT thick and contains 6 strong reflector horizons that are affected by slumping at the edges of the lobate bathymetric mound on the mid-slope bench.
- ***Seismic unit w6c.*** Unconformity W6c is represented by a less strong reflector. It truncates reflector horizons within unit w6b. The seismic facies of unit w6c is almost transparent in places but weak sub-parallel, continuous reflectors can be traced throughout. Unit w6c is approximately 25 ms TWTT thick and contains 6 traceable reflector horizons that wedge out in a landward direction.
- ***Seismic units w7 and w7a.*** Seismic unit w7 has been sub-divided into two units (w7 and w7a) based on the recognition of marker reflector W7a, which truncates internal reflectors of unit w7. Most of the truncation occurs at the edges of the sediment lobe. Reflections within the overlying unit (w7a) are primarily masked by a large bubble effect on the ANT V/4 seismic profiles.

6. TIME/DEPTH CONVERSION AND CORRELATION TO ODP DATA

Depths of reflectors were calculated using the formula : Depth = Velocity x TWTT/2. This simplified depth calculation was applied as detailed velocity information from the digital data was poor. A mean velocity of 1550 m/s was used for the interval spanning the Cenozoic (Wood, 1993). This figure is based on the p-wave velocity calculations made by the Shipboard Scientific Party of Leg 113 (Barker et al., 1988) and sonobuoy refraction seismic data collected during the ANT V/4 and ANT VIII/5 surveys (Kaul, 1991). In Table 1, the calculated depths are listed of important reflectors or unconformities on seismic profiles at ODP Site 693 as well as their correlation to lithology and to specific events recorded with borehole measurements. The time-depth conversion shows that unconformities W7, W6c, W6b, W6a, and W6 all lie within litho-unit IIIA, which is seemingly lithologically homogeneous and consists of clayey mud, diatom mud and silty and clayey diatom-bearing mud.

The acquired physical property data at Sites 692-693 are of limited use (Barker et al., 1988). This is mainly due to the degree of drilling disturbance. Paul & Jobson (1987) have shown that minor changes in physical properties, especially bulk density and porosity related to water content, can produce seismic reflections. This may be the case for the ODP data set but the core has been greatly remoulded during drilling

which has rendered the physical property data set next to useless when trying to explain the occurrence of seismic reflectors.

Reflector	Depth	Stratigraphic position	Correlation to borehole information
W4	400 m	between units V/VI	increase in gamma-ray response decrease in resistivity decrease in sonic velocity decrease in smectite concentration
W5	255 m	Between units IIIB/C	*5 m above* decrease in gamma-ray response high resistivity spike high sonic velocity spike
W6	200 m	within IIIA	*5 m below* high sonic velocity spike
W6a	145 m	within IIIA	high sonic velocity spike
END OF WIRELINE LOGS			
W6b	125 m	within IIIA	
W6c	85 m	within IIIA	60% smectite concentration spike
W7	65 m	within IIIA	low smectite concentration
W7a	30 m	within II	low smectite concentration

Table 1. *Calculated depths of important unconformities at ODP Site 693 and their correlation to lithology and other specific events recorded with borehole measurements.*

7. CLAY MINERALOGY AT SITE 693

X-ray diffraction analysis was performed on 56 samples from ODP Site 693 in order to identify major palaeo-environmental changes. Clay mineral associations of chlorite, illite, smectite and kaolinite were examined. Four clay mineral units were thus identified, based on clay mineral abundances :

- UNIT C1, from sea floor to 165 mbsf (Lower Pliocene to Pleistocene): illite is the dominant mineral, smectite is less abundant and chlorite and kaolinite are rare.
- UNIT C2, from 260 mbsf (Upper Miocene to Lower Pliocene): very abundant illite.
- UNIT C3, from 260 to 398 mbsf (Upper Oligocene to Lower Miocene)
  - sub-unit C3a, from 260-240 mbsf: very abundant to exclusive illite with rare to common kaolinite and sporadic rare chlorite and smectite
  - sub-unit C3b, from 340 to 398 mbsf: very abundant illite with common kaolinite

- UNIT C4, from 398 to 484 mbsf (Aptian to Albian/Santonian)
  - sub-unit C4a, from 398 to 455 mbsf: exclusively smectite with sporadic to rare illite
  - sub-unit C4b, from 455 to 484 mbsf: very abundant smectite with rare illite and kaolinite

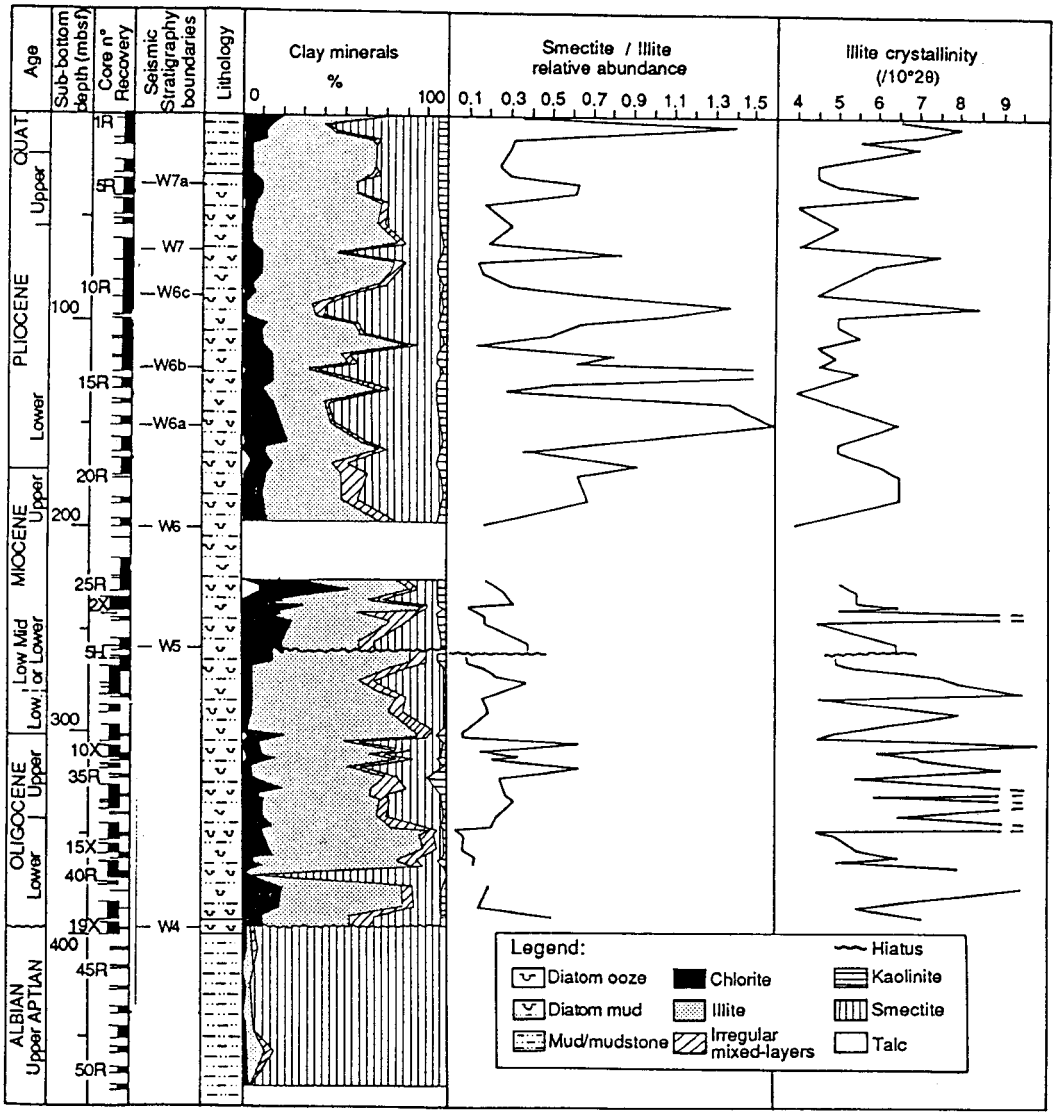

Figure 20. *Clay mineralogy, smectite/illite ratio and illite cristallinity observed at ODP Site 693 (after Robert & Maillot, 1990), plotted against the calculated position of important unconformity horizons on the same site.*

Figure 20 plots clay mineralogy as a percentage, smectite/illite ratios, illite crystallinity (Robert & Maillot, 1990) and shows the calculated position of important unconformity horizons. In the area off Dronning Maud Land smectite is the dominant clay mineral up to the W4 unconformity. Above W4 smectite decreases from 90 to 35 % and the dominance switches to illite, associated with sporadic smectite and chlorite. Smectite and chlorite increase at the expense of illite throughout unit w5. At the W6 unconformity, the data set is incomplete. No deductions can therefore be made on the origin of this event. A definite cyclical pattern starts above W6, within the upper Late Miocene to Pleistocene strata. Seven peaks in the smectite/illite relative abundance curve occur in this time span. These correlate with troughs in the illite crystallinity curve.

The major Cenozoic seismic markers correlate well - within errors of ± 5-10 m - with sharp rises in smectite abundance within the otherwise illite-dominant section. Associated to this also a decrease in the quality of illite crystallinity and an increase in the amount of detrital material can be observed. It should, however, be noted that recovery in this section at Site 693 was poor, and that therefore this correlation should be regarded with due reservation.

Unconformity W6a correlates with a large peak in smectite (55 %) and a substantial increase in detrital input (the D-index). Illite crystallinity is poor at $6.5^{10/20}$. Unconformity W6a would be of Messinian age and could be attributed to the well-known shift in the ^{13}C record. This period is marked by a drop in the $\delta^{18}O$-record of foraminifera from ODP Site 704 (Leg 114) on Meteor Ridge, and by an increase in IRD in sub-Antarctic waters (Robert, 1994, personal communication).

A similar pattern occurs with unconformity W6b. However, this event is associated with a low in the D-index. Smectite is abundant (60 %) and illite crystallinity appears to have been retained. Associated with these peaks are slight increases in chlorite abundance until midway through unit w6b. Unconformity W6b could correspond to the Miocene-Pliocene boundary, which is a period of glacial instability in West Antarctica and is hence attributed to a warming event (Robert, 1994, personal communication).

Unconformity W6c plots 5-10 m above the next peak in smectite. This maybe due to unprecise time-to-depth conversion, or to recovery effects. Associated with this peak is a large trough in illite crystallinity ($8.5^{10/20}$) and an increase in the D-

index. Sediments of unit w6c show a decline in smectite abundance, with fewer spikes which are less pronounced.

Unconformity W7 correlates with a short, sharp peak in smectite, accompanied by a drop in chlorite abundance. Illite crystallinity is poor ($7.5^{10/20}$) and the D-index remains high.

A similar pattern is found at reflector W7a, but in this case there is also a peak in chlorite. There is a final smectite peak which does not correlate with any significant reflector. This event may be masked by the bubble effect at the top of the seismic profiles.

8. IMPLICATIONS OF CHANGES IN CLAY MINERALOGY

The pattern of smectite/illite peaks correlating well with all the seismically defined unconformities suggests a clear causal relationship. As the composition of clay mineral assemblages is determined by source area, weathering/erosive processes, selective transportation, and deposition (Grobe et al., 1990), it is tempting to use clay mineralogy as a palaeo-environmental indicator.

Chlorite and illite are abundant throughout the Cenozoic at Site 693 and characterise source areas of steep relief where active mechanical erosion prevents soil development (Robert & Maillot, 1990; Robert & Chamley, 1992). Presence of smectite and kaolinite peaks suggests intermittent periods of warm, wet conditions where hydrolysis occurs or intermittent periods where previously hydrolysed sediments become reworked on the continental shelf.

Illite is a mica very similar to muscovite in construction. Best illite crystallinity is observed when the mineral forms under a cold arid environment during periods of weak hydrolysis (Robert & Maillot, 1990; Chamley, 1989; Robert & Chamley, 1992). In abundance, it reflects a decrease in hydrolytic processes and an increase in direct rock erosion under cold climatic conditions (Chamley, 1989). Illite is also abundant from source areas underlain by plutonic and high-grade metamorphic rocks such as those that constitute the East Antarctic Shield.

Smectite forms in a number of chemical environments, is prone to swelling and has weak bonding between the layers (Chamley, 1989). It originates in surficial soils

where substitution with other clay minerals occurs commonly. Smectite is associated with low latitudes but is not restricted to these areas. It forms under warm, wet climates or wherever hydrolysis is prominent (Chamley, 1989). Smectite present in marine sediments is more likely to have been derived from continental shelf sediments that have already undergone complex hydrolysis processes. They do not form easily in the marine environment (Chamley, 1989).

Cenozoic sediments commonly display a step-by-step increase in rock-derived minerals namely illite at the expense of smectite and kaolinite. "Accelerations and slackenings" of illite coincide with cooling and warming periods (Chamley, 1989; Robert & Chamley, 1992). The clay mineral change is attributed to the transition from glacial to interglacial conditions at the earth's surface. Evidence of increases in smectite, possibly originating from reworking of Late Cretaceous and Tertiary sediments cropping out on the continental shelf, within illite dominant lithology has been found in previous case studies (Chamley, 1988).

9. CONCLUSIONS

- Re-examination of high-resolution, analog seismic records in the vicinity of ODP Site 693 has allowed a number of fine-scale unconformities to be identified in addition to those previously defined by Miller et al. (1990). Three sub-sequences have been recognised within seismic units W6; two in seismic unit W7. They all occur within the seemingly homogeneous Pliocene strata at ODP Site 693, consisting of clayey mud, diatom mud and silty and clayey diatom-bearing mud. They coincide with stratigraphic horizons characterised by spikes in smectite percentage in an overall illite-dominant lithology.

- Smectite spikes probably indicate a change in sediment source from the Antarctic continent where glacial activity produced illite in response to direct rock erosion, to the continental shelf where previously hydrolysed Cretaceous and Tertiary sediments were exposed. Eroded detritus could have been transported to the shelf edge by ice sheets. Sediment-laden melt water debauching from the ice-sheet grounding line may have created low-angle erosional unconformities in the middle-slope deposits and may have initiated mass flow that moved downslope towards Wegener Canyon across the mid-slope bench. The smectite-horizons found at ODP Site 693 would represent overbank deposition. The unconformities and sequence boundaries identified on seismic sections on the slope off Cape

Norvegia - outside the immediate influence of the glacial prograding wedge deposits - are therefore probably directly related to processes of ice-sheet expansion.

GENERAL CONCLUSIONS

In the framework of the "Belgian Contribution to the Antarctic Offshore Acoustic Stratigraphy Project (BELANTOSTRAT)", RCMG has carried out a number of investigations along various portions of the Antarctic continental margin. These investigations focused on the study - mainly using medium- to high-resolution reflection seismic techniques - of the sedimentary palaeo-environments of these margins and on the analysis of the possible palaeoclimatic controls on the margin's build-up and evolution. The three sectors that were studied are:

I. the Central Bransfield Basin, with special emphasis on the Trinity Peninsula margin of this basin,
II. the continental margin of the Bellingshausen and Amundsen Seas, and
III. the continental margin of the northeastern Weddell Sea.

In each of these margin studies, the reflection seismic data have been analysed in detail, and seismic-stratigraphic concepts of glaciated margins have been used to attribute the observed seismic-stratigraphic features (glacial erosion surfaces, mid-shelf grounding-zone deposits, shelf-edge prograding wedges, basin-floor deposits, etc.) to specific stages in the evolution of the ice sheet on the adjacent continent.

Because of the qualitative differences in the available data (vertical resolution, 3-dimensional control within the grid, etc.), the detail and significance of the observed stratigraphic "signals" of ice-sheet dynamics vary distinctly from one study area to another:

- **Central Bransfield Basin**

  Sequence-stratigraphy of the Trinity Peninsula margin

  The investigated seismic profiles through the shelf and upper-slope deposits along the Trinity Peninsula margin yield new information about the formation and evolution of the Bransfield back-arc basin, about the tectonic and volcanic activity associated with it, and about the sedimentary processes responsible for the build-up of its margins.

  Sedimentary record of the glacial history of the Trinity Peninsula margin

  The seismic data illustrate that the Trinity Peninsula margin deposits contain resolvable records of at least three periods during which ice sheets advanced to the shelf edge for a significant amount of time. This record is represented by three distinct prograding shelf-edge wedges. Magnitude of slope progradation varies along the margin and appears to be related to local sources of sediment

supply associated with separate glacial troughs. Ice-stream activity within these troughs appears to have varied through time. In addition, the data show that the shelf deposits also contain a record of glacial periods of lesser extent, but this record is only erratically preserved due to strong glacial erosion. Up to present, no age information is available regarding these deposits.

Reconstruction of the glacial history of the Trinity Peninsula margin, and perspectives

The Trinity Peninsula margin has undergone at least three glacial periods during which the ice sheet extended out to the shelf edge for a significant amount of time. In addition, there are indications for glacial periods of lesser extent, although their record is only poorly preserved. Volume calculations and exact reconstructions of ice-sheet positions are impossible due to the large lateral variability of the glacial deposits. Estimation of age and duration of the glacial deposits is impossible due to the lack of reliable borehole age information.

⇒ A complete and reliable reconstruction of the glacial history of this margin will therefore only be possible after a detailed, 3-dimensional mapping of the complete record - including the sporadic and sparse remnants of glacial advances of lesser extent - contained within the entire upper-slope and shelf area. A new high-resolution seismic survey (GEBRA-96) is planned in order to examine the lateral continuity of the observed prograding slope strata and to determine the completeness of the stratigraphic record, with special emphasis on the potential of the shelf record.

⇒ The possibility of having deep-ocean drilling data from the basin-floor section in Bransfield Basin in areas with seismic-stratigraphic evidence for the presence of volcaniclastic layers or inter-stratified lava flows opens perspectives of radiometrically constraining the age of the glacial cycles associated with the progradational wedges, and hence to date the glacial periods observed on the seismic records. Such data may be acquired in the beginning of 1998.

- **Bellingshausen and Amundsen Seas**

Sequence-stratigraphy and sedimentary record of the glacial history of the Bellingshausen/ Amundsen Seas margin

A new, regionally-spaced reflection seismic data set has been acquired from the largely unexplored Bellingshausen and Amundsen Seas along the West Antarctic margin. Though limited in coverage, these data reveal for the first time the large-scale stratigraphic architecture of the continental shelf, slope and rise.

The stratigraphic architecture of the Bellingshausen/Amundsen Seas margin is interpreted in terms of the long-term glacial history of the area. All seismic profiles show the same variation of outer-shelf geometries. The lower, aggradational sequences represent conditions before the onset of the major glacial advance of a grounded ice sheet onto the shelf, whereas the overlying sequences record several extended periods of ice-sheet grounding on the shelf since the Middle Miocene.

An erosional surface defines the base of a prograding wedge on the continental slope all along the margin. It is correlated with the transition from aggrading to prograding sequences on the outer shelf, and may thus reflect a response to the onset of glacial conditions on the continental shelf, i.e. by an intensification of the bottom-current regime in the lower parts of the slope.

Large sediment drifts occur on the continental rise. They probably originate from the interaction of channelised turbidity currents and along-slope bottom currents, although the exact process of their formation is still matter of debate. It is, however, believed that these drift deposits contain a good and easily recoverable record of the glacial history of the adjacent continental shelf.

Reconstruction of the glacial history of the Bellingshausen/Amundsen Seas margin, and perspectives

The Bellingshausen/Amundsen Seas margin appears to have undergone a roughly comparable glacial evolution, as witnessed by its rather continuous and uniform large-scale architecture. A complete and reliable reconstruction of the glacial history of this margin - in high spatial and temporal resolution - is obviously impeded by the scarcity of the presently available seismic data (only regional coverage), by the limited resolution of the data, and by the total absence of borehole (age) information.

⇒ It is, however, believed that drilling of the drift deposits at the foot of the continental slope will yield an expanded and dateable record of the glacial history of the adjacent continental shelf. Such deep-ocean drilling information is expected in the first months of 1998.

- **Northeastern Weddell Sea**

Sequence-stratigraphy of the northern Weddell Sea margin

Re-examination of seismic records near ODP Site 693 has allowed a number of fine-scale unconformities to be identified in addition to those previously defined. Up to five additional sub-sequences have been recognised. They all occur within the seemingly homogeneous Pliocene strata at ODP Site 693, consisting of clayey mud, diatom mud and silty and clayey diatom-bearing mud.

Sedimentary record of the glacial history of the northern Weddell Sea margin, and perspectives

These unconformities coincide at ODP Site 693 with stratigraphic horizons characterised by spikes in smectite percentage in an overall illite-dominant lithology. Smectite spikes are interpreted to indicate a change in sediment source from the Antarctic continent where glacial activity produced illite in response to direct rock erosion, to the continental shelf where previously hydrolysed Cretaceous and Tertiary sediments were exposed. Eroded detritus could have been transported to the shelf edge by ice sheets. Sediment-laden melt water debauching from the ice-sheet grounding line may have created low-angle erosional unconformities in the middle-slope deposits and may have initiated downslope sediment transport across the mid-slope bench. The smectite-horizons found at ODP Site 693 would thus represent overbank deposits. The unconformities and sequence boundaries identified on seismic sections on the slope off Cape Norvegia - outside the immediate influence of the glacial prograding wedge deposits - are therefore probably directly related to processes of ice-sheet expansion.

⇒ This means that seismic-stratigraphic "signals" of glacial activity have been unambiguously correlated with the rock record, confirming their glaciogenic origin. This approach obviously will deserve further attention in future high-latitude deep-sea drilling legs.

ACKNOWLEDGEMENTS

This research was carried out with the support of the Belgian Science Policy Office (DPWB), within the framework of the Belgian Antarctic Research Programme, Phase 3, Project A3/02/002. Part of the study around Sites 692 and 693 (ODP Leg 113) has received additional support from the Belgian Fund for Joint Basic Research (FKFO). We also wish to acknowledge the Belgian National Fund for Scientific Research for granting a Post-Doctoral Fellowship (M. De Batist).

We thank the Marine Geophysics Group (H. Miller) of the Alfred-Wegener-Institut für Polar- und Meeresforschung (Bremerhaven, GER) and the Marine Geology Research Group (M. Canals) of the University of Barcelona (ESP) for the very pleasant and stimulating cooperation and for the hospitality and facilities offered to several members of our research team during the marine-geophysical cruises on board of F.S. POLARSTERN and B.I.O. HESPERIDES.

Thanks are also due to J.B. Anderson, J. Baraza, H. Chamley, G. Ercilla, C. Escutia, K. Gohl, E. Gracia, W. Jokat, B. Kuvaas, Y. Kristoffersen, F. Nitsche, L. Oszko, M.J. Prieto and C. Robert with whom we had the pleasure to discuss various aspects of this study. J.B. Anderson, B. Kuvaas and Y. Kristoffersen gave us access to some of their seismic data.

Part of the results here presented were obtained in the framework of the student research projects of T. Schoolmeester, J. Schatteman, E. Vermeiren and G. Wood.

REFERENCES

AITKENHEAD, N., 1975. The geology of Duse Bay - Larsen Inlet area, North-East Graham Land (with particular reference to the Trinity Peninsula Series). *British Antarctic Survey Scientific Reports*, **51**.

ALLEY, R.B., BLANKENSHIP, D.D., ROONEY, S.T. & BENTLEY, C.R., 1989. Sedimentation beneath ice shelves - The view from ice stream B. *Marine Geology*, **85**, 101-120.

ANDERSON, J.B., BRAKE, C., DOMACK, E., MYERS, N. & WRIGHT, R., 1983. Development of a polar glacial-marine sedimentation model from Antarctic Quaternary deposits and glaciological information. In : MOLNIA, B.F. (ed.) *Glacial-Marine Sedimentation*. Plenum Press, New York, 233-264.

ANDERSON, J.B. & BARTEK, L.R., 1992. Cenozoic glacial history of the Ross Sea revealed by intermediate resolution seismic reflection data combined with drill site information. In: KENNETT, J.P. & WARNKE, D.A. (eds.) The Antarctic paleoenvironment: A perspective on global change. *AGU Antarctic Research Series*, **56**, 231-263.

BANFIELD, L.A. & ANDERSON, J.B., 1995. Seismic facies investigation of the Late Quaternary glacial history of Bransfield Basin, Antarctica. In: COOPER, A.K., BARKER, P.F. & BRANCOLINI, G. (eds.) Geology and seismic stratigraphy of the Antarctic Margin. *AGU Antarctic Research Series*, **68**, 123-140.

BARKER, P.F., 1982. The Cenozoic subduction history of the Pacific margin of the Antarctic Peninsula: ridge crest-trench interactions. *Journal of the Geological Society of London*, **139**, 787-801.

BARKER, P.F., 1995. The proximal marine sediment record of Antarctic climate since the Late Miocene. In: COOPER, A.K., BARKER, P.F. & BRANCOLINI, G. (eds.) Geology and seismic stratigraphy of the Antarctic Margin. *AGU Antarctic Research Series*, **68**, 25-57.

BARKER, P.J. & DALZIEL, I.W.D., 1983. Progress in geodynamics in the Scotia Arc region. *AGU Geodynamic Series*, **9**, 137-170.

BARKER, P.F., KENNETT, J.P. et al., 1988. *Proceedings of the Ocean Drilling Program, Initial Reports. Vol 113.* College Station TX, 785 pp.

BARKER, P.F., KENNETT, J.P. et al., 1990. *Proceedings of the Ocean Drilling Program, Scientific Results. Vol 113.* College Station TX, 1032 pp.

BART, P.J. & ANDERSON, J.B., 1995. Seismic record of glacial events affecting the Pacific margin of the Northwestern Antarctic Peninsula. In: COOPER, A.K., BARKER, P.F. & BRANCOLINI, G. (eds.) Geology and seismic stratigraphy of the Antarctic Margin. *AGU Antarctic Research Series*, **68**, 75-95.

BART, P.J. & ANDERSON, J.B., 1996. Seismic expression of depositional sequences associated with expansion and contraction of ice sheets on the northwestern Antarctic Peninsula continental shelf. In: DE BATIST, M. & JACOBS, P. (eds.) Geology of siliciclastic shelf seas. *Geological Society Special Publication*, **117**, 171-186.

BARTEK, L.R., VAIL, P.R., ANDERSON, J.B., Emmet, P.A. & Wu, S., 1991. Effect of Cenozoic ice sheet fluctuations in Antarctica on the stratigraphic signature of the Neogene. *Journal of Geophysical Research*, **96**, 6753-6778.

BAS (BRITISH ANTARCTIC SURVEY), 1985. Tectonic map of the Scotia Arc. 1:3,000,000. British Antarctic Survey.

BASTIEN, T.W., LEHMANN, E.K. & CRADDOCK, C., 1976. The geology of Peter I Island. In: HOLLISTER, C.D., CRADDOCK, C., et al. (eds.) *Initial Reports of the Deep Sea Drilling Project. Vol 35.* US Government Printing Office, Washington, 341-357.

BIRKENMAJER, K., 1991. Tertiary glaciation in the South Shetland Islands, West Antarctica. In:

THOMSON, M.R.A., CRAME, J.A. & THOMSON, J.W. (eds.) *Geological evolution of Antarctica.* Cambridge University Press, 629-632.

BOULTON, G.S., 1990. Sedimentary and sea level changes during glacial cycles and their control on glacimarine facies architecture. In: DOWDESWELL, J.A. & SCOURSE, J.D. (eds.) Glacimarine environments: processes and sediments. *Geological Society Special Publication*, **53**, 15-52.

BURCKLE, L.H. & POTTER, N., 1996. Pliocene-Pleistocene diatoms in Paleozoic and Mesozoic sedimentary and igneous rocks from Antarctica: A Sirius problem solved. *Geology*, **24(3)**, 235-238.

CANALS, M., ACOSTA, J., BARAZA, J., BART, P., CALAFAT, A.M., CASAMOR, J.L., DE BATIST, M., ERCILLA, G., FARRAN, M., GRÀCIA, E., RAMOS, E., SANZ, J.L., SORRIBAS, J. & TASSONE, A., 1994. La Cuenca Central de Bransfield (NW de la Península Antárctica) : primeros resultados de la campaña GEBRA'93. *Geogaceta*, **16**, 132-135.

CANDE, S.C. & KENT, D.V., 1995. Revised calibration of geomagnetic polarity timescale for the Late Cretaceous and Cenozoic. *J. Geophys. Res.*, **100**, 6093-6095.

CAREY, S. & SIGURDSSON, H., 1984. A model of volcaniclastic sedimentation in marginal basins. In : KOKELAAR, P.B. & HOWELLS, M.F. (eds.) Marginal Basin Geology: Volcanic and Associated Sedimentary and Tectonic Processes in Modern and Ancient Marginal Basins. *Geological Society Special Publication*, 16, 37-58.

CHAMLEY, H., 1989. Clay sedimentology. Springer Verlag, Berlin, 623 pp.

COOPER, A.K., BARRETT, P.J., HINZ, K., TRAUBE, V., LEITCHENKOV, G. & STAGG, H.M.J., 1991. Cenozoic prograding sequences of the Antarctic continental margin: a record of glacio-eustatic and tectonic events. *Marine Geology*, **102**, 175-213.

COOPER, A.K. & WEBB, P.N., 1994. The ANTOSTRAT Project - An international effort to investigate Cenozoic Antarctic glacial history, climates, and sea-level changes. *Terra Antartica*, **1(2)**, 239-243.

CUNNINGHAM, A.P., LARTER, R.D. & BARKER, P.F., 1994. Glacially prograded sequences on the Bellingshausen Sea continental margin near 90°W. *Terra Antartica*, **1(2)**, 267-268.

DANSGAARD, W., JOHNSEN, S.J., CLAUSEN, H.B., DAHL-JENSEN, D., GUNDESTRUP, N.S., HAMMER, C.U., HVIDBERG, C.S., STEFFENSEN, J.P., SVELNBJÖRNSDOTTIR, A.E., JOUZEL, J. & BOND, G., 1993. Evidence for general instability of past climate from a 250-kyr ice-core record. *Nature*, **364**, 218-220.

DE BATIST, M., HENRIET, J.P., MILLER, H., MOONS, A., DENNIELOU, B., KAUL, N., MAES, E., JOKAT, W., SCHULZE, B., UENZELMANN-NEBEN, G., VERSTEEG, W. & THE GRAPE TEAM, 1993. High-resolution seismic investigation of the evolution (stratigraphy and structure) of the continental margins of the eastern Weddell Sea and of the Antarctic Peninsula. In : CASCHETTO, S. (ed.) *Belgian Scientific Research Programme on the Antarctic.* Scientific Results of Phase Two (Oct 88-Mai 92), Belgian Scientific Research Programme on Antarctica. Vol 2 : Marine Geophysics, 66 pp.

EITTREIM, S.L., COOPER, A.K. & WANNESON, J., 1995. Seismic stratigraphic evidence of ice-sheet advances on the Wilkes Land margin of Antarctica. *Sedimentary Geology*, **96**, 131-156.

FÜTTERER, D.K., KUHN, G. & SCHENKE, H.W., 1990. Wegener canyon bathymetry and results from rock dredging near ODP Sites 691-693, Eastern Weddell Sea, Antarctica. In : BARKER, P.F., KENNETT, J.P. et al. (eds.) *Proceedings of the Ocean Drilling Program, Scientific Results. Vol 113.* College Station TX, 39-48.

GAMBOA, L.A.P. & MALDONADO, P.R., 1991. Geophysical investigations in the Bransfield Strait and in the Bellingshausen Sea - Antarctica. In : ST.JOHN, B. (ed.) Antarctica as an Exploration Frontier. *AAPG Studies in Geology*, **31**, 127-141.

GOHL, K. & MILLER, H., 1997. Seismic and gravity data reveal Tertiary intraplate subduction in the

Bellingshausen Sea, Southeast Pacific. *Geology*, **25(4)**, 371-374.

GOHL, K., NITSCHE, F.O., VANNESTE, K., MILLER, H., FECHNER, N., OSZKO, L., HÜBSCHER, C., WEIGELT, E. & LAMBRECHT, A., (in press). Tectonic and sedimentary architecture of the Bellingshausen and Amundsen Sea Basins, SE Pacific, by seismic profiling. In: *Proceedings of the VII International Symposium on Antarctic Earth Sciences.*

GONZÁLEZ-FERRÁN, O., 1991. The Bransfield rift and its active volcanism. In : THOMSON, M.R.A., CRAME, J.A. & THOMSON, J.W. (eds.) *Geological evolution of Antarctica*. Cambridge University Press, 505-509.

GRÀCIA, E., CANALS, M., FARRAN, M., PRIETO, M.J., SORRIBAS, J. & GEBRA TEAM, 1996. Morphostructure and evolution of the Bransfield back-arc basin (NW Antarctic Peninsula). *Marine Geophysical Researches*, **18(2-4)**, 429-448.

GRAPE TEAM, 1990. Preliminary results of seismic reflection investigations and associated geophysical studies in the area of the Antarctic Peninsula. *Antarctic Science,* **2(3)**, 223-234.

GRIP PROJECT MEMBERS, 1993. Climatic instability during the last interglacial period recorded in the GRIP ice core. *Nature*, **364**, 203-207.

GROBE, H., FÜTTERER, D.K., SPIEß, V., 1990. Oligocene to Quaternary sedimentation processes on the Antarctic continental margin, ODP Leg 113, Site 693. In : BARKER, P.F., KENNETT, J.P. et al. (eds.). *Proceedings of the Ocean Drilling Program, Scientific Results, Vol 113.* College Station TX, 121-130.

GROOTES, P.M., STUIVER, M., WHITE, J.W.C., JOHNSEN, S.J. & JOUZEL, J., 1993. Comparison of the oxygen isotope records from the GISP2 and GRIP Greenland ice cores. *Nature*, **366**, 552-554.

HENRIET, J.P., MEISSNER, R., MILLER, H. & THE GRAPE TEAM, 1992. Active margin processes along the Antarctic Peninsula. In : SHIMAMURA, H., HIRN, A. & MAKRIS, J. (eds.) Detailed Structure and Processes of Active Margins. *Tectonophysics,* **201**, 229-253.

HENRIET, J.P. & MILLER, H., 1990. Some speculations regarding the nature of the Explora-Andenes Escarpment. In : BLEIL, U. & THIEDE, J. (eds.) *Geologic History of the Polar Oceans : Arctic versus Antarctic*. Kluwer Acad. Publ., Netherlands, 161-169.

HENRIET, J.P., MILLER, H., MOONS, A., MEISSNER, R., VAN HEUVERSWYN, E., JOKAT, W., VERSTEEG, W., KAUL, N., HUWS, D. & THE GRAPE TEAM, 1989. Reflection seismic investigations in the Weddell Sea and along the Antarctic Peninsula. In : CASCHETTO, S. (ed.) *Antarctica.* Scientific Results of Phase One (Oct 85-Jan 89), Belgian Scientific Research Programme on Antarctica. Vol 2 : Marine Geophysics, part B, 1-79.

HINZ, K. & KRAUSE, W., 1982. The continental margin of Queen Maud Land, Antarctica: seismic sequences, structural elements and geological development. *Geol. Jahrb.*, **23(E)**, 17-41.

HOLLISTER, C.D., CRADDOCK, C., et al., 1976. *Initial Reports of the Deep Sea Drilling Project. Vol 35.* US Government Printing Office, Washington, 929 pp.

HYDEN, G. & TANNER, W.G., 1981. Late Paleozoic-Early Mesozoic fore-arc basin sedimentary rocks at the Pacific Margin in Western Antarctica. *Geologische Rundschau*, **70**, 529-541.

JEFFERS, J.D. & ANDERSON, J.B., 1991. Sequence stratigraphy of the Bransfield Basin, Antarctica: Implications for tectonic history and hydrocarbon potential. In: ST.JOHN, B. (ed.) Antarctica as an exploration frontier - hydrocarbon potential, geology, and hazards. *AAPG Studies in Geology*, **31**, 13-30.

JEFFERS, J.D., ANDERSON, J.B. & LAWVER, L.A., 1991. Evolution of the Bransfield basin, Antarctic Peninsula. In : THOMSON, M.R.A., CRAME, J.A. & THOMSON, J.W. (eds.) *Geological evolution of Antarctica*. Cambridge University Press, 481-485.

JOUZEL, J., LORIUS, C., PETIT, J.R., GENTHON, C., BARKOV, N.I., KOTLYAKOV, V.M. & PETROV, V.M., 1987. Vostok ice core: a continuous isotope temperature record over the last climatic cycle (160,000 years). *Nature*, **329**, 403-407.

KAUL, N., 1991. Detaillierte seismische Untersuchungen am östlichen Kontinentalrand des Weddell-Meeres vor Kapp Norvegia, Antarktis. *Berichte zur Polarforschung*, 89, 120 pp.

KELLER, R. & FISK, M.R., 1992. Quaternary marginal basin volcanism in the Bransfield Strait as a modern analogue of the southern Chilean ophiolites. In: Parson, L.M., Murton, B.J. & Browning, P. (eds.) Ophiolites and their modern oceanic analogues. *Geological Society Special Publication*, **60**, 155-169.

KELLER, R., FISK, M.R., WHITE, W.M. & BIRKENMAJER, K., 1992. Isotopic and trace elements constraints on mixing and melting models of marginal basin volcanism, Bransfield Strait, Antarctica. *Earth and Planetary Science Letters*, **111**, 287-303.

KIMURA, K., 1982. Geological and geophysical survey in the Bellingshausen Basin, off Antarctica. *Antarctic Record*, **75**, 12-24.

KING, L.H. & FADER, G., 1986. Wisconsinan glaciation of the continental shelf: Southeast Atlantic Canada. *Geological Society of Canada Bulletin*, **363**, 72 pp.

KING, L.H., ROKOENGEN, K. & GUNLEIKSRUD, T., 1987. Quaternary seismostratigraphy of the Mid Norwegian shelf, 65°-67°30' N: A till tongue stratigraphy. *Continental Shelf and Petroleum Technology Research Institute IKU, Publication*, **114**, 58 pp.

KUVAAS, B. & KRISTOFFERSEN, Y., 1991. The Crary Fan : A trough-mouth fan on the Weddell Sea continental margin, Antarctica. *Marine Geology*, **97**, 345-362.

LARTER, R.D. & BARKER, P.F., 1989. Seismic stratigraphy of the Antarctic Peninsula Pacific margin : a record of Pliocene-Pleistocene ice volume and paleoclimate. *Geology*, **17**, 731-734.

LARTER, R.D. & BARKER, P.F., 1991. Neogene interaction of tectonic and glacial processes at the Pacific margin of the Antarctic Peninsula. In: MCDONALD, D.I.M. (ed.) Sedimentation, tectonics and eustasy: Sea-level changes at active margins. *International Association of Sedimentologists Special Publication*, **12**, 165-186.

LARTER, R.D. & CUNNINGHAM, A.P., 1993. The depositional pattern and distribution of glacial-interglacial sequences on the Antarctic Peninsula Pacific margin. *Marine Geology*, **109**, 203-219.

LAWYER, L.A., GAHAGAN, L.M. & COFFIN, M.F., 1992. The development of paleoseaways around Antarctica. In: KENNETT, J.P. & WARNKE, D.A. (eds.) The Antarctic paleoenvironment: A perspective on global change. *AGU Antarctic Research Series*, **56**, 7-30.

LORIUS, C., JOUZEL, J., RITZ, C., MERLIVAT, L., BARKOV, N.I., KOROTKEVICH, Y.S. & KOTLYAKOV, V.M., 1985. A 150,000-year climatic record from Antarctic ice. *Nature*, **316**, 591-595.

MCADOO, D. & MARKS, K., 1992. Gravity fields of the southern oceans from Geosat data. *J. Geophys. Res.*, **97(B3)**, 3247-3260.

MCGINNIS, J.P. & HAYES, D.E., 1994. Sediment drift formation along the Antarctic Peninsula. *Terra Antartica*, **1(2)**, 275-276.

MEISSNER, R., HENRIET, J.P. & the GRAPE TEAM, 1988. Tectonic features northwest of the Antarctic Peninsula : new evidence from magnetic and seismic studies. *Ser. Cient. INACH*, **38**, 89-105.

MILLER, H., HENRIET, J.P., KAUL, N. & MOONS, A., 1990. A fine-scale seismic stratigraphy of the eastern margin of the Weddell Sea. In : BLEIL, U. & THIEDE, J. (eds.) *Geologic History of the Polar Oceans : Arctic versus Antarctic*. Kluwer Acad. Publ., Netherlands, 131-161.

NITSCHE, F.O., GOHL, K., VANNESTE, K. & MILLER, H., (in press). Indication of glacially deposited sequences in the Bellingshausen and Amundsen Seas, West Antarctica: First results of a regional

seismic survey. In: Geology and seismic stratigraphy of the Antarctic Margin II. *AGU Antarctic Research Series.*

PAUL, M.A. & JOBSON, L.M., 1987. Acoustic and geotechnical properties of soft sediments from the Witch Ground Basin, Central North Sea. Unpublished report, Heriot Watt University.

PAYNE, A.J., SUGDEN, D.E. & CLAPPERTON, C.M., 1989. Modeling the growth and decay of the Antarctic Peninsula Ice Sheet. *Quaternary Research*, **31**, 119-134.

PRIETO, M.J., GRÀCIA, E., CANALS, M., ERCILLA, G. & DE BATIST, M., (in press). Sedimentary history of the Central Bransfield Basin (NW Antarctic Peninsula). In: *Proceedings of the VII International Symposium on Antarctic Earth Sciences.*

REBESCO, M., LARTER, R.D., BARKER, P.F., CAMERLENGHI, A. & VANNESTE, L.E., 1994. The history of sedimentation on the continental rise West of the Antarctic Peninsula. *Terra Antartica*, **1(2)**, 277-279.

REBESCO, M., LARTER, R.D., CAMERLENGHI, A. & BARKER, P.F., 1996. Giant sediment drifts on the continental rise west of the Antarctic Peninsula. *Geo-Marine Letters*, **16**, 65-75.

ROACH, P.J., 1978. The nature of back-arc extension in Bransfield Strait. *Journal of Geophysical Research*, **53**, 165.

ROBERT, C. & CHAMLEY, H., 1992. Late Eocene-Early Oligocene evolution of climate and marine circulation : deep sea clay mineral evidence. *AGU Antarctic Research Series*, 56, 97-117.

ROBERT, C. & MAILLOT, H., 1990. Palaeoenvironments in the Weddell Sea area and Antarctic climates as deduced from clay mineralogy associations and geochemical data. In : BARKER, P.F., KENNETT, J.P. et al. (eds.) *Proceedings of the Ocean Drilling Program, Scientific Results, Vol 113.* College Station TX, 51-65.

SANDWELL, D.T. & SMITH, W.H.F., 1992. Global marine gravity from ERS-1, Geosat and Seasat reveals new tectonic fabric. *EOS Transactions*, **73**, 133.

SCHOOLMEESTER, T., 1995. Reflectie-seismische studie van de glaciaire erosie en sedimentatie in de Bellingshausen en Amundsen Zee, Antarctica. Unpublished M.Sc. Thesis, University of Gent, 81 pp.

ST.JOHN, B. & SUGDEN, D.E., 1971. Raised marine features and phases of glaciation in the South Shetland Islands. *British Antarctic Survey Bulletin*, **24**, 45-111.

TUCHOLKE, B.E. & HOUTZ, R.E., 1976. Sedimentary framework of the Bellingshausen Basin from seismic profiler data. In: HOLLISTER, C.D., CRADDOCK, C., et al. (eds.) *Initial Reports of the Deep Sea Drilling Project. Vol 35.* US Government Printing Office, Washington, 197-227.

VANNESTE, K., 1995. A comparative seismic stratigraphic study of major Plio-Pleistocene glaciogenic depocentres along the polar North Atlantic margins. Unpublished Ph.D. Thesis, University of Gent, 291 pp.

VANNESTE, K., UENZELMANN-NEBEN, G. & MILLER, H., 1995. Seismic evidence for the long-term history of glaciation on the central East Greenland shelf south of Scoresby Sund. *Geo-Marine Letters*, **15**, 63-70.

VERMEIREN, E., 1995. Reflectieseismische studie van het Bransfield Bekken, Antarctica. Unpublished M.Sc. Thesis, University of Gent, 69 pp.

VORREN, T.O., LEBESBYE, E., ANDREASSEN, K. & LARSEN, K.B., 1989. Glacigenic sediments on a passive continental margin as exemplified by the Barents Sea. In: POWELL, R.D. & ELVERHØI, A. (eds.) Modern glacimarine environments: Glacial and marine controls of modern lithofacies and biofacies. *Marine Geology*, **85**, 251-272.

WEBB, P.N., 1990. The Cenozoic history of Antarctica and its global impact. *Antarctic Science*, **2(1)**, 3-

21.

WEBB, P.N., HARWOOD, D.M., MCKELVEY, B.C., MERCER, J.H. & STOTT, L.D., 1984. Cenozoic marine sedimentation and ice-volume variation on the East Antarctic craton. *Geology*, **12**, 287-291.

WOOD, G., 1993. *A fine-scale seismic stratigraphy of the Cenozoic sediments around ODP Sites 691/693, Leg 113, off Kapp Norvegia, Antarctica*. M.Sc thesis, UCNW-RUG. CEC Erasmus Project "Mercator" in marine geosciences, 153 pp.

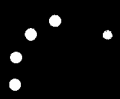

FEDERAL OFFICE FOR SCIENTIFIC,
TECHNICAL AND CULTURAL AFFAIRS
Rue de la Science 8
Wetenschapsstraat 8
B-1000 Brussels
Tel: +32/2/238 34 11 – Fax: +32/2/230 59 12